THE NICOTINIC ACETYLCHOLINE RECEPTOR: GENE EXPRESSION AND ION CHANNEL FUNCTION

Thesis by

Lei Yu

In Partial Fulfillment of the Requirements

for the Degree of

Doctor of Philosophy

California Institute of Technology

Pasadena, California

1987

(Submitted April 15, 1987)

To my parents,

whose love and support

made this possible.

Stumble and learn;

Compare and learn;

Live and learn.

------ Inspired by three Chinese proverbs.

ACKNOWLEDGMENTS

My graduate career at Caltech has been an invaluable and a most rewarding experience for me, both scientifically and personally. This is thanks to the many people I have been fortunate enough to know and to be associated with at Caltech.

To a naive young lad, Norman Davidson's group was like a big family. People were always willing to help, and I cannot imagine where I would be without the helpful suggestions from Dave Hershey, Chuck Rozek, Sue Celniker, Lenny Garfinkel, Nevis Fregein, Al Goldin, Terry Snutch, Hermann Lubbert, and everyone else in the group. Marie Krempin did an excellent job running the tissue culture facility, for which I thank her. The labmates in 04 Church, Sandy Sharp, Bev Bond Matthews, and Bob LaPolla, provided much needed inspiration on a daily basis and tolerated my occasional oversights, which caused inconvenience for them. Sandy and Bev were very generous in offering advice, both scientific and linguistic. Bob shared the night shift with me and was the initiator not only on the mouse AChR project which eventually got me into "receptology", but also on the "background music" war with the rest of us in the room. I still savor my "victory" when he asked me not to turn off the radio one day --- the music was Bizet's *Carmen*. The graduate students in the lab, Vann Parker, Mike Snyder, Kath Mixter Mayne, Bev, Arthur Roach, Bill Mattox, and Mickey Hu, not only provided peer support and encouragement in times of (scientific) sickness and health, but were also great company when I was working in the lab late at night and on weekends. In the past year especially, Bev and Bill helped me a great deal in going through the emotional highs and lows typical of a finishing graduate student as they themselves were also struggling to "get out." It is gratifying that I am finishing just in time to be able to attend the graduation ceremony together with them, a celebration I have longed for.

But most important to my "subbasement development" was Norman. He was very understanding of my initial naiveté in science, patient with my slow learning, enthusiastic in providing valuable advice whenever asked, and jubilant with every bit of progress I made along the way (including those in tennis matches against *him*). I am particularly grateful to Norman for the academic freedom he provided, which enabled me to grow as a scientist.

A logical extension of the research on the AChR molecular biology was its electrophysiology. I am very grateful to Henry Lester for allowing me the opportunity to pursue this endeavor. Henry was not only a superb advisor in giving direction as the project unfolded and installing in me the sense of "instant gratification" of electrophysiology, but he was also a patient teacher in providing hands-on instructions in every facet of the technology, from setting up equipment to analyzing data. The atmosphere in Henry's lab is like that in a classroom: People were eager to share information and experiences, and the lunch-time gathering in the conference room always sparkled with reviews of interesting literature, discussion and evaluation of each other's new results, and plans for the next exploration. Kiyonori Yoshii, who got me started with the AChR electrophysiology and recording techniques, was a great friend and collaborator. Our conversations were often spiced with references to our similar cultural backgrounds, and writing down Chinese/Japanese characters often came in handy when one of us could not find an appropriate English word to express a thought. The addition of Reid Leonard to the lab opened a new chapter for the AChR project. His expertise in single-channel recording enabled me to complete my thesis work, and his cheerful personality made bearable the long grueling hours in front of the oscilloscope. As collaborators, it was reassuring to know that we were always in tune, whether working or singing. I would also like to thank many people in and outside the lab for their helpful suggestions and encouragement:

Cesar Labarca, Doug Krafte, Ben Curtis, and Jonathan Pollock, among many others. The lab would run into difficulties without the efficient management of Moira Fearey, and I am thankful to her for the things she has done. I am also thankful to Floyd Shon for his much-needed help in modifying and improving the computer programs used in this work.

The members of my thesis committee, David Anderson, Mary Kennedy, David Van Essen, and Barbara Wold, in addition to Norman and Henry, have provided invaluable guidance during my thesis work, and I would like to express my sincere gratitude to them. I am indebted to Reid for his help during the preparation of this thesis, and I know how much extra work this added to his already demanding research load and his just as important domestic responsibilities. I therefore want to thank his wife Debbie, and their baby Ryan, for being understanding and supportive.

My and many others' graduate lives in Biology at Caltech would have been much more complicated if it weren't for the efficient administrative management efforts of Charles Brokaw and Nancy Gill, and I would like to thank them for the work they have done for us graduate students. Support for my graduate study at Caltech was provided by a California Foundation for Biochemical Research Fellowship, for which I am grateful. My special thanks go to James Bonner, without whose early encouragement and enthusiastic recommendation I would not have been able to come to Caltech.

Coming from a faraway country with a very different culture, I benefited enormously from the help of many friends in adjusting to the new environment. First of all, I would like to thank Boning Gao, who helped me a great deal from the very beginning (starting at LAX), both in and outside the lab. I have always admired her conscientiousness and diligence in science, her modesty, and her consideration for others, and I value our friendship very much.

And there is the Prufrock House. Having lived there for five years, I have learned a lot from my housemates old and new. Sharing the bathroom with Kath was quite an experience for me, and she would have cured me completely of my inability to keep a room meticulously clean had she stayed a few more months. Bev, Greg Matthews, Tina Kramer, and Mike Garyantes offered unsolicited but much-needed (and much-appreciated) distractions away from work, such as hiking, camping trips to the desert and mountains, ping-pong, tennis, badminton, and volleyball, in addition to keeping me entertained every day with provocative and interesting conversations. The Eating Group (also known as the J. Alfred Prufrock Society of Culinary Philosophy) provided a unique chance for me to get to know American culture and people, albeit with a very biased group of samples. The members in the Eating Group were very eager to teach me new words, and consequently my vocabulary has been expanded to include words of all ratings. It is the help and support from all these friends and colleagues that has made my graduate tenure at Caltech most enjoyable and enriching.

Finally, I would like to thank the people who brought me to this wonderful world --- my parents. Being scientists themselves and fully aware of the effort it takes to achieve any goal, they offered me this maxim when I left them to go to college ten years ago: "千里之行,始于足下。"* Well, Mom and Dad, here I have taken another step.

* English translation: "A long journey is made up of many small steps."

ABSTRACT

The nicotinic acetylcholine receptor (AChR) is a complex protein, which functions as a ligand-gated ion channel on the postsynaptic membrane at the neuromuscular junction and mediates signal transmission from neuron to muscle. Research on the AChR has had a long history and has benefited from the endeavors of scientists from many disciplines. The intensive, multidisciplinary studies have yielded valuable knowledge about this molecule, which serves as a model for the understanding of many fundamental questions in biological sciences. Chapter 1 presents a review of the AChR.

As a tissue-specific and developmental stage-specific molecule, AChR is under temporal and spatial control for its synthesis. Chapter 2 reports a qualitative and quantitative study of AChR gene activity during muscle cell differentiation, using a cDNA clone isolated from a murine muscle cell line, which codes for the γ subunit of the mouse AChR. The results indicate that the regulation of mRNA accumulation levels is a major mechanism in the differential synthesis of the AChR.

The marriage between AChR and molecular biology resulted in many cDNA clones which, after being introduced to African frogs, produced the next generation ---- *Xenopus* oocytes with exotic AChRs on them. Chapter 3 describes the attempt to localize "determinants" that specify species subunit identity in the AChR by constructing chimeric cDNA clones composed of fragments from different origins, taking advantage of the *Xenopus* oocyte expression system. The results from surface toxin-binding assay and two-electrode voltage-clamp recording suggested that while the species specificity can be dictated by certain subunits, the determination of subunit identity does not reside at a defined locus in the fragments tested.

Does the complex composition of multisubunits in the AChR bear any functional significance? Chapter 4 addresses this question through the study of mouse-*Torpedo* AChR hybrids. The complete substitution of AChR subunits between mouse and *Torpedo* receptors generated all 16 combinations, and a systematic analysis of these hybrids revealed an interesting pattern with respect to the voltage sensitivity in the ACh-induced response: The identity of the β subunit determines, while the interaction between the β and δ subunits modulates, the AChR voltage sensitivity. The results, therefore, suggest that different subunits of AChR may play a central role in different functional properties.

Patch-clamp technique has offered an opportunity for analyzing transmembrane current flow with the high resolution of single-channel recording. Chapter 5 describes such a study on homologous and hybrid AChRs. Voltage influence on the three parameters were evaluated, and the results indicate that the single channel conductance is independent of membrane potential and that the channel closing and opening rates together constitute the basis for the voltage sensitivity in whole-cell recording with the closing rate making the major contribution. Also investigated were the subunit roles in species specificity of channel-open duration and voltage dependence. The results are in agreement with those reported on channel duration and support the conclusions of our previous work on the subunit involvement in determining the voltage sensitivity of the AChR response.

TABLE OF CONTENTS

Page

CHAPTER 1

The biology of the nicotinic acetylcholine receptor

INTRODUCTION

As I am writing down these very words, the pen in my hand is moved across the paper at my will, via the exquisitely coordinated movements of the skeletal muscles on my hand and arm. The muscle movements, in turn, are controlled by the motor neurons, and central to the signal delivery from neuron to muscle is the chemical synaptic transmission process ---- the interaction of acetylcholine (ACh) and its receptor (AChR). Upon binding of ACh released from the nerve terminal, the AChR acts as a pore to allow a transient ion flow across the cell membrane, which gives rise to muscle contraction. Such is the mechanism for nerve-muscle communication in me, a (-) typical human being, and it is also the mechanism in other vertebrates.

The study of the AChR has gone a long way. At present, the AChR is the most thoroughly studied membrane receptor involved in cell-cell communication (reviewed by Fambrough, 1979; Karlin, 1980; Conti-Tronconi and Raftery, 1982; Anderson, 1983; Popot and Changeux, 1984; Stroud and Finer-Moore, 1985; McCarthy *et al.*, 1986). This intensive research on the AChR is due to four factors.

The first and foremost is the attractiveness of the AChR as a model system for many fundamental questions in biology: gene structure and evolution, regulation of gene activity during animal development, coordination of the synthesis of complex protein components, protein modification during and after polypeptide translation, multisubunit protein assembly, membrane protein transport and localization, metabolic modulation of protein lifetime in the membrane, cell-cell signaling via transmitter-receptor interaction, biophysical properties of the membrane channel such as ion selectivity and channel conductivity, and the structural basis for these properties.

The second factor is the rich sources of the AChR in the electric organs of certain fish, *Torpedo californica* and *Torpedo marmorato* (marine elesmobranch fish) and *Electrophorus electricus* (fresh-water electric eel). The AChR protein can be readily extracted for biochemical study and protein sequencing, which provided crucial information leading to the eventual isolation of the AChR genes and their transcription products.

The third factor for the prosperity in the AChR study is the existence of neurotoxins obtained from the venom of poisonous snakes, for example, the elapid *Bungarus multicinctus*. These toxins bind to the AChR with high specificity, and can be used for assaying receptor distribution, for affinity purification of the AChR, and for the quantitation of the receptor molecules.

The fourth factor that has contributed to the understanding of the AChR is the high receptor density at the endplate of the neuromuscular junction in many amphibian and mammalian muscles. Historically, in fact, this was the prime reason that attracted intensive investigations of the AChR physiological properties since the study by Fatt and Katz (1951). Because of the accessibility of muscles, the high density made possible detailed electrophysiological studies of AChR.

In the following sections, a review is presented of the major properties of the AChR.

STRUCTURE

Biochemical characterization

Molecular characterization of the AChR was initiated by receptor purification through biochemical fractionation of the electric tissues from a variety of fish (reviewed by Heidmann and Changeux, 1978). Gram quantities of AChR protein could be so obtained in high purity (specific activity greater than 4μ moles α-bungarotoxin sites/gram protein, Claudio and Raftery, 1977; Sobel *et al.*, 1977). This purification made possible the detailed biochemical characterization. SDS-polyacrylamide gel electrophoresis of the purified receptor showed that it consisted of four components, α, β, γ, and δ subunits, with estimated molecular weights of 40, 50, 60, and 65 kd, respectively (Claudio and Raftery, 1977). Reynolds and Karlin (1978) and Lindstrom *et al.* (1979) deduced the subunit stoichiometry as $\alpha_2\beta\gamma\delta$, and this was verified by quantitative sequencing of the affinity-purified AChR protein (Raftery *et al.*, 1980). The AChR pentamer is often copurified with a protein fraction of 43kd molecular weight (sometimes called ν proteins), which can be dissociated from the AChR at high pH (Neubig *et al.*, 1979). These 43kd proteins may be involved in AChR-cytoskeleton anchoring rather than being an active component of the receptor, since oocyte-expressed AChRs were functional without them (Mishina *et al.*, 1984; White *et al.*, 1985).

Molecular cloning

Our understanding of the primary structures of the AChR polypeptides has been greatly advanced in the past few years by the cloning of genomic and cDNA sequences coding for the AChR subunits from various species. The initial isolation of complete or partial subunit-coding cDNAs were from *Torpedo californica*. Two

approaches were employed either by oligonucleotide hybridization based on the partial amino acid sequence data (Noda *et al.*, 1982, 1983a, b) or by differential hybridization with electric organ RNA (Ballivet *et al.*, 1982; Claudio *et al.*, 1983; Hershey *et al.*, 1983). Using these sequences as hybridization probes, many more AChR clones were isolated from a variety of species (tabulated by Stroud and Finer-Moore, 1985; and Kubo *et al.*, 1985; Takai *et al.*, 1985; Boulter *et al.*, 1985, 1986; Isenberg *et al.*, 1986; Buonanno *et al.*, 1986; Beeson *et al.*, 1986; Hermans-Borgmeyer *et al.*, 1986; Yu *et al.*, 1986, and this thesis). A comparison of the sequences unveiled an interesting pattern: While all the AChR subunits share some homology with one another, a given subunit more resembles its equivalent from another species than a different subunit of the same species (Stroud and Finer-Moore, 1985). This suggests that the heterologous composition of the AChR evolved prior to the divergence of these species and that the subunit identities have been preserved through evolutionary history, presumably because they carry distinct functional roles (Conti-Tronconi *et al.*, 1982). This view is supported by the finding from subunit substitution studies that the homologous from different species could replace each other to give highly functional receptors, whereas different subunits from the same species could not (White *et al.*, 1985; Sakmann *et al.*, 1985).

Structural features

The structure of the AChR complex has been extensively studied by a variety of methods, including electron microscopy, small angle X-ray diffraction, neutron scattering, circular dichroism, resonance Raman spectroscopy, immunoelectronmicroscopy, chemical modification, and proteolytic cleavage analysis (reviewed by Stroud and Finer-Moore, 1985; McCarthy *et al.*, 1986). The overall picture generated from these studies is that the subunits are aligned next

to each other in the plasma membrane to form a funnel-shaped cylinder, with the long axis of the receptor perpendicular to the plane of the membrane. This "funnel" has a quasi-fivefold symmetry and protrudes from the lipid bilayer on both sides of the membrane. The inside wall of the subunits forms a central hole, which presumably constitutes the ion channel. The arrangement of the individual subunits in the receptor is still an unsettled question; what is known is that the two α subunits are separated by one other subunit, which is not δ (Holtzman *et al.*, 1982), leaving two possible ways of arrangement ---- αγαβδ (Wise *et al.*, 1981) or αβαγδ (Kistler *et al.*, 1982; Zingsheim *et al.*, 1982).

It has been established that the α subunits carry the binding sites for agonists and antagonists, although the precise locations within the subunit are not identified (reviewed by Heidmann and Changeux, 1978). Normal opening of the ion channel requires the binding of at least two agonists, since at low concentrations the magnitude of the transmembrane current varies with the square of the agonist concentration (Lester *et al.*, 1975; Adams, 1975; Dionne *et al.*, 1978; Neubig and Cohen, 1980; Sheridan and Lester, 1982). It has been suggested, however, that the binding of a single ligand molecule may induce brief openings of the channel (Colquhoun and Sakmann, 1981).

The ion channel of the AChR is highly asymmetric with respect to the cytoplasmic-extracellular orientation. The funnel-shaped channel has a 40Å diameter opening toward the extracellular matrix and it narrows down to about 7Å in diameter at the membrane surface level (Klymkowsky and Stroud, 1979). The transmembrane section of the channel is likely to have the same diameter of 7Å, as suggested by quantitative densitometry measurements of negatively stained electron micrographs (Kistler *et al.*, 1982) and electrophysiological determination of conductivity with variously sized organic molecules (Furukawa and Furukawa, 1959; Maeno *et al.*, 1977; Huang *et al.*, 1978; Dwyer *et al.*, 1980). The asymmetry

of the ion channel is also reflected by the asymmetry of ligand binding: While the application of agonist or antagonist from the extracellular side can activate or inactivate the AChR, the presence of intracellular agonist/antagonist does not seem to have an effect (Del Castillo and Katz, 1955; personal observation on inside-out patches).

Models for AChR topology

Several models have been proposed for the polypeptide orientation in the native plasma membrane and for the subunit involvement in the ion channel gating (Finer-Moore and Stroud, 1984; Guy, 1984; Criado *et al.*, 1985; Hucho *et al.*, 1986). These models all agree that the N-termini of the AChR subunits are located extracellularly and the C-termini intracellularly with the polypeptide chain tranversing the plasma membrane at least five times, but they differ from one another with respect to the assignments of the transmembrane segments and of the functional amino acid residues participating in the ion channel. Studies aimed at testing the validity of these models have been carried out (reviewed by Mayne, 1986), using immunochemical techniques (Lindstrom *et al.*, 1984; Young *et al.*, 1985; Ratnam *et al.*, 1986) and site-specific mutagenesis (Mishina *et al.*, 1985). The data available so far, however, are not sufficient for choosing a particular model over the others.

PHYSIOLOGICAL PROPERTIES

The physiological properties of the AChR are well documented, largely by the electrophysiological studies of the receptor in its native muscle cell membrane, in reconstituted artificial lipid bilayer membranes, and in the plasma membrane of the *Xenopus* oocytes injected with AChR mRNAs.

Early electrophysiological studies

Early studies on the endplate at the neuromuscular junction established that the effect of acetylcholine binding to its receptor is to change the electrical potential across the cell membrane by allowing certain ions to flow down their electrochemical gradients, presumably through a pore in the receptor (Fatt and Katz, 1951). The associated voltage change across the postsynaptic membrane at the neuromuscular junction serves to trigger muscle contraction. The ionic basis for the current is a conductance increase to small cations Na^+ and K^+ (Takeuchi and Takeuchi, 1960) and Ca^{++} (Jenkinson and Nicholls, 1961). When compared to nerve action potentials that also result from a conductance increase to Na^+ and K^+ (Hodgkin and Huxley, 1952), synaptic potentials show a similar relaxation time course of a few milliseconds but a very different profile for their generation and propagation: They are graded; *i. e.*, the summation is additive, rather than the all-or-none generation pattern of action potentials; and they propagate passively along the muscle fibers with a space constant of a few millimeters rather than the regenerative action potentials that can rapidly and actively propagate over long distances without attenuation (see Kuffler *et al.*, 1984; Kandel and Schwartz, 1985). These features of the ACh-induced synaptic potential render it attractive for quantitative studies.

Kinetic modeling

Based on the analysis of the voltage and temperature dependence of the ACh-induced currents at the frog neuromuscular junction by voltage-clamping the endplate, a kinetic model was proposed to account for the AChR activation (Magleby and Stevens, 1972a, b):

$$nT + R \underset{k_2}{\overset{k_1}{\rightleftharpoons}} T_n\text{-}R \underset{\alpha}{\overset{\beta}{\rightleftharpoons}} T_n\text{-}R^{*} \quad , \qquad (1)$$

where T is transmitter and R is its receptor, T_n-R is the complex with the channel closed, and T_n-R^{*} represents the channel in the open state. k_1 and k_2 are the rate constants for agonist binding and dissociation, and β and α are the rate constants for channel opening and closing. The declining phase of the observed ACh-induced currents with an exponential time course could be explained by the first-order kinetics predicted in the model, suggesting a simultaneous activation of many channels with variable duration. This view was supported by later high-resolution electrophysiological measurements (reviewed by Auerbach and Sachs, 1984a).

Because the synaptic potential is the summed effect of individual AChR channel openings, an understanding of individual channel activity was needed. The technique of noise analysis was introduced (Katz and Miledi, 1970) to distinguish the conductance of individual receptors from the mean duration of channel opening, so as to obtain a quantitative estimate of these parameters (Anderson and Stevens, 1973). The results from noise analysis indicated that the single channel conductance was relatively constant, but the mean channel duration varied with membrane potential and temperature. Because these values were inferred from macroscopic measurements and the actual shape of the single

channel response was not known, two mutually exclusive models were proposed. One envisioned an exponential time course for the single channel current similar to that of the macroscopic current (Katz and Miledi, 1972) and the other assumed a simple square pulse (Anderson and Stevens, 1973).

High resolution measurements by patch clamp recording

A breakthrough was brought about by the advent of the high- resolution patch clamp recording technique (Neher and Sakmann, 1976b; Hamill *et al.*, 1981). A great advantage of single channel recording is that the current traces of individual molecules, and thus the kinetic characteristics such as open time and conductance, can be visualized from the data rather than inferred as in noise analysis of macroscopic data.

The first single channel recordings from the AChR in denervated frog skeletal muscle (Neher and Sakmann, 1976b) immediately settled the dispute over the shape of the elementary current: It was more like a rectangular pulse, rather than the exponential decay proposed by Katz and Miledi (1972), with a fast transition from the closed to the open state and *vice versa*, and a flat plateau while open. In noise analysis of the macroscopic current, the calculated channel conductance was an averaged value. It did not tell us whether the single channel conductance was composed of a continuous spectrum of values or of discrete states. In single channel recording where the current trace can be seen, the channel conductance can be unambiguously determined by dividing the measured magnitude of the single channel currents with the corresponding membrane voltage. The analysis of the initial single channel data (Neher and Sakmann, 1976b) showed that the channel had only a single conductance value, indicating a single open conductance. Later studies revealed that there could be more than one channel conductance (Hamill and Sakmann, 1981; Trautman, 1982; Auerbach

and Sachs, 1984b; Leonard *et al.*, 1984; Leonard, 1985; Auerbach and Lingle, 1986). Because these studies were carried out with embryonic muscle cells where the existence of different types of AChR channels have been documented in later studies (Mishina *et al.*, 1986), it is not clear whether or not a single AChR channel can adopt more than one open state.

Single channel kinetics

Open time is another parameter for characterizing single channel kinetics. In the simple activation model for the AChR proposed by Magleby and Stevens (1972a, b), the open time of AChR channels is a one-step random process and follows an exponential distribution according to the mass law of chemical reaction. Then, the mean channel open duration can be defined as the average amount of time channels remain open after entering the open state and should be the reciprocal of the channel closing rate constant α (see Equation 1). Early analysis of single channel data (Neher and Sakmann, 1976b) showed that the open times of single channels did follow the expected exponential distribution and had values similar to the ones predicted from noise analysis of macroscopic data (Neher and Sakmann, 1976a). Later studies revealed that the distribution of AChR open duration times actually had two exponential components, a slow one representing the majority of events and a very brief one ten times or more shorter (Colquhoun and Sakmann, 1981). The nature of the brief component is not clear at present. The initial suggestion that it corresponds to the open channels with a single agonist bound instead of the usual two (Colquhoun and Sakmann, 1981) predicts that the short openings should become less frequent with increasing agonist concentrations. While some studies supported this hypothesis (Takeda and Trautmann, 1984; Colquhoun and Sakmann, 1985), others contradicted it (Sine and Steinbach, 1984, 1986a).

The time between successive channel openings is another parameter to be considered for the AChR channel kinetics. The closed time distribution in single channel records typically displays at least two exponential components (Horn and Lange, 1983; Sine and Steinbach, 1986a, b). The major component with the long time constant corresponds to the AChR with no agonist bound, whereas the brief component(s) seem to reflect the closed configurations of the agonist-receptor complex. Sine and Steinbach (1986b) reported the existence of two types of brief closures in addition to the long one and suggested that one type represents the AChR reopening from the closed state because its kinetic properties are agonist-dependent and that the other type of brief closure reflects an additional closed state, leading away from the pathway producing the open state because its kinetics are the same regardless of the type of agonist used.

Channel blockade

The ion channel of AChR can be blocked by its agonists as well as its antagonists, and the blockade can be viewed as another closed state. The blockers include agonists ACh, carbamylcholine (CCh), and suberyldicholine (SubCh), antagonist d-tubocurarine, and charged and uncharged local anesthetics (Sine and Steinbach, 1984; Colquhoun *et al.*, 1979; Neher and Steinbach, 1978; Ogden *et al.*, 1981). The kinetics of channel blockade vary widely. For example, the blocked time by tubocurarine is very long, while that by SubCh or QX-222 is short enough to appear as a brief interruption in the single channel current. For ACh and CCh, the blockade is too short to be resolved, resulting in a decreased amplitude and an increased open channel noise as the agonist concentration goes up. The modeling of blockade kinetics is becoming complicated. Early models for channel blockade postulate an ordered sequence with blocked state(s) leading away from the open channel state. A prediction from such a model is that the total time spent in the

open state is independent of the blocker concentration, since a blocked channel can only lose a ligand by passing through the open state. A study using QX-222 showed that at concentrations of QX-222>20μM, the total time spent in the open state went down (Neher, 1983). This implies that a channel can enter directly from the blocked state to some nonconducting, nonligand-bound state. The mechanism of blockade is also unclear. It has been suggested that the blockers exert their effects by competing for the same binding sites in the channel that ions interact with (Horn and Patlak, 1980). The channel blockers may also physically plug up the passage to the ions (Neher and Steinbach, 1978).

Desensitization

The phenomenon of desensitization (Katz and Thesleff, 1957) represents yet another closed state that the AChR can enter (Sakmann *et al.*, 1980), with the rate of desensitization dependent on the agonist concentration (Nastuk and Parsons, 1970). In fact, multiple rates of desensitization have been observed, suggesting that the phenomenon may involve more than one state (Adams, 1981). Desensitization is not caused by direct blockage of the ion channel by the agonist (Sakmann *et al.*, 1980) and may involve binding sites for agonist distinct from the ones for the channel activation by the agonist. Many compounds can enhance desensitization (Peper *et al.*, 1982) and the recovery rates seem to be compound-independent, suggesting that the AChR undergoes a slow isomerization process to the normal resting state after the dissociation of the compound (Magazanik and Vyskocil, 1973). These compounds include amine local anesthetics, nonionic detergents, aliphatic alcohols, the psychoactive tranquilizer phencyclidine, the antipsychotic chlorpromazine, and histrionicotoxin form the poison-dart frog of South America (Spivak and Albuquerque, 1982). These compounds can modulate (block) the agonist-induced AChR current but do not bind at the ACh site;

therefore, they are called noncompetitive blockers. It is unlikely that these diverse compounds all act upon the same site(s) on the AChR, but it is clear that they all enhance desensitization by stabilizing the AChR in one or more desensitized states (Heidmann and Changeux, 1979; Boyd and Cohen, 1984). Although the physiological and clinical significance is apparent, the molecular mechanism for this drug-enhanced desensitization is not known. An interesting piece of information regarding desensitization is that phosphorylation of the γ and δ subunits by a cAMP-dependent protein kinase can increase the rate of desensitization (Huganir *et al.*, 1986).

Attempts have been made to identify the local anesthetic binding sites on the AChR using photolabeling techniques (Lester *et al.*, 1980; Oswald and Changeux, 1981; Lester *et al.*, 1985; Hucho *et al.*, 1986) and alkalating derivatives (Kaldany and Karlin, 1983). These studies labeled various sites on different subunits α, β, and δ, and suggest that distinct binding sites may exist for different noncompetitive blockers.

REGULATION OF AChR BIOGENESIS

As a molecule with well-defined physiological functions, the AChR is under spatial and temporal control for its biogenesis (Fambrough, 1979; Pumplin and Fambrough, 1982; Merlie, 1984). For a complex membrane protein, the control can be exerted at any one or several of the steps leading to the ultimate appearance of functional receptor on the membrane: transcription of the AChR genes, maturation and stability of the mRNAs, translation of these mRNAs, co- and post-translational modifications of the polypeptide chains, protein insertion into the membrane, assembly of the protein complex, and maintenance/degradation of functional receptors. Although our understanding of this whole series of processes is far from complete, the available information seems to indicate that regulatory mechanisms for the AChR biogenesis do exist in most, if not all, of these processes.

Transcriptional regulation

One criterion for myogenesis at the molecular level is the appearance of muscle-specific proteins, including acetylcholine receptors (Merlie *et al.*, 1977). Early studies indicated that the large amounts of AChR molecules appearing on the muscle cell surface are synthesized *de novo* (Merlie *et al.*, 1975; Devreotes *et al.*, 1977), just like other plasma membrane proteins appearing at the onset of muscle differentiation (Prives and Patterson, 1974; Merlie and Gros, 1976). Recent studies using the cDNA clones coding for the AChR subunits have shown that the regulation of AChR gene expression plays a major role in the drastic increase of AChR synthesis during myogenesis (Yu *et al.*, 1986, and this thesis; Buonanno and Merlie, 1986). Upon induction of differentiation in cultured murine muscle cells, the mRNA levels for the α,γ, and δ subunits increased 30- to 50-

fold, accounting for 10- to 100-fold increase of the surface AChRs as measured by the α-BTX binding assay (Inestrosa *et al.*, 1983). It has also been reported that the DNA sequence 5' to the transcription initiation site of the AChR α subunit gene from chicken, when analyzed in CAT constructions (chloramphenicol acetyl transferase), provides tissue and developmental specificity of the AChR (Klarsfeld *et al.*, 1987).

The AChR subunits are synthesized and inserted into the membrane as individual polypeptide chains before the assembly of the protein complex (Anderson and Blobel, 1981). Is there a coordination for their synthesis? It seems that the mRNA level for the α subunit does not change significantly after muscle cell differentiation from a surprisingly high basal level before differentiation (Olson *et al.*, 1983). There is also a suggestion that the β subunit may have a similar pattern of overproduction to that of the α subunit (Merlie, 1984). It has been reported that the genes for the α and β subunits are located on different chromosomes in the mouse genome, while the genes for the γ and δ subunits belong to the same linkage group (Heidmann *et al.*, 1986). In fact, the γ and δ genes have been found to be in close proximity in all the species examined, including chicken (Nef *et al.*, 1984), human (Shibahara *et al.*, 1985), mouse (Crowder and Merlie, 1986), and rat (N. D. Hershey, personal communication). It has been suggested that the two genes are coregulated for their activities during development, based on the differentiation-specific pattern of DNaseI-hypersensitive sites surrounding the two genes (Crowder and Merlie, 1986). More direct and detailed studies need to be performed in order to have a better understanding of the coregulation process (or the lack of it) for the subunit genes.

Post-transcriptional modulation

Although it is known that the changes can occur in the lifetimes of the primary transcription products (nRNAs) and in the efficiency of the maturation process (defined as the nRNA/mRNA ratio of a particular gene (Davidson, 1986)), there is no direct evidence as to whether and to what extent these post-transcriptional steps are regulated for the AChR genes. It has been reported that the AChR mRNAs are more abundant in synaptic regions of differentiated skeletal muscle fibers, even when the muscle nuclei (hence the AChR genes) are quite evenly distributed along the entire length of the muscle fibers (Merlie and Sanes, 1985). An increased stability of AChR messages near synapses is one of the possible mechanisms suggested for this phenomenon.

Translational regulation and cotranslational modification

The translation of the four AChR subunits is carried out independently on membrane-bound polysomes concurrently with cotranslational insertion into the membrane (Anderson and Blobel, 1981). These polysomes loaded with AChR mRNAs are anchored on membranes of the rough endoplasmic reticulum (rough ER), and the signal recognition particle (SRP) is required for the recognition, complete translation, and membrane-insertion of the nascent polypeptide chain as well as the subsequent removal of the N-terminal signal peptide (Anderson *et al.*, 1982). Also occurring cotranslationally is the glycosylation of all four subunits (Anderson and Blobel, 1981).

Post-translational modification and receptor assembly

Another type of covalent modification is phosphorylation by protein kinases (Levitan, 1985). The nascent polypeptide chains undergo a process of conformational maturation in the first 30 min after their synthesis, acquiring the

ability to bind α-BTX and antibodies specific for the native conformations of the AChR α subunit (Merlie and Lindstrom, 1983). The β subunit is also subjected to such a conformational maturation process (Merlie, 1984).

The assembly of functional AChR is another possible step for differential regulation. While actively growing myogenic cells do not possess cell surface AChRs, growth-arrested cells undergo differentiation and exhibit a 100-fold increase of surface receptors (Olson *et al.*, 1984). This dramatic increase of surface receptors does not seem to be the result of an overall increase in AChR synthesis: Only a 4-fold increase is observed in the α subunit mRNA abundance accompanied by an even less noticeable change in the rate of α subunit synthesis. The authors suggested that the assembly rate might be regulated in this case.

Receptor localization during synapse formation

During development, the distribution of AChRs on a muscle cell surface undergoes a profound change (reviewed by Fambrough, 1979; Froehner, 1986). In uninnervated embryonic muscles, the newly synthesized and assembled AChRs are transported from the Golgi apparatus to the cell surface by a system of coated vesicles (Bursztajn and Fischbach, 1984) and inserted into the plasma membrane uniformly. But soon after a cholinergic growth cone makes contact with a muscle cell, AChRs start to accumulate at the contact site to form a synapse (Anderson *et al.*, 1977; Frank and Fischbach, 1979; Chow and Cohen, 1983).

The synapse formation has a high degree of specificity: While spinal cord motoneurons readily trigger AChR accumulation, spinal cord interneurons do not elicit the process (Role *et al.*, 1985). The AChR clustering is contributed in large part by new receptor synthesis and to a minor extent by redistribution of pre-existing receptors (Anderson and Cohen, 1977; Ziskind-Conhaim *et al.*, 1984; Role *et al.*, 1985). Since myotubes are multinucleated, the new receptors can either be

preferentially synthesized (transcription/translation) near the synapse or selectively inserted at the postsynaptic region. The recent report that the mRNAs for α and δ subunits are concentrated in the synaptic region of adult muscle fibers (Merlie and Sanes, 1985) indicates that at least the translation of receptor proteins is synapse-oriented. It is a tantalizing hypothesis that the mRNA accumulation near the synapse is the result of region-specific transcription of the AChR genes in the nuclei near the synapse. Merlie and Sanes (1985) observed that a group of nuclei, albeit a small percentage, are regularly found directly beneath the postsynaptic membrane.

There is another interesting phenomenon along this line: AChR molecules aggregate to form small patches on the membrane of cultured myotubes, and this aggregation coincides with nuclear clustering (Bruner and Bursztajn, 1986; Englander and Rubin, 1987). During rat myotube development, the change in the size and number of the nuclear clusters parallel that of the AChR aggregates, suggesting a causal relationship (Bruner and Bursztajn, 1986). Moreover, when the AChR aggregates formed on chick and rat skeletal muscle cells by the treatment of an extracellular matrix factor from *Torpedo* electric organ, the nuclei that migrated underneath these aggregates became immobilized, while the nuclei away from the AChR aggregates could translocate freely throughout the myotube (Englander and Rubin, 1987). After the AChR patches dispersed, the trapped nuclei resumed moving.

Denervation supersensitivity

The phenomenon of denervation supersensitivity (Axelsson and Thesleff, 1959; Miledi, 1960) contrasts with that of the synaptic accumulation of AChRs during normal development. In adult skeletal muscle, the majority of the AChRs is located in the neuromuscular junction area. After denervation by either

crushing the nerve tract or blocking the nerve activity with toxin, AChRs appear over the entire muscle fiber surface (reviewed by Fambrough, 1979). This renders the muscle fiber superresponsive to ACh stimulation, hence the term denervation supersensitivity.

Studies have shown that the increased AChRs are synthesized *de novo* rather than redistributed from the existing synaptic receptors (Grampp *et al.*, 1972; Brockes and Hall, 1975; Devreotes and Fambrough, 1976). The newly synthesized extrajunctional receptors are 5- to 50-fold more in number than the junctional ones, and they have a shorter half-life (24 hr compared to over a week for junctional ones).

The effect of supersensitivity to ACh can be reversed or prevented in muscle either by chronic stimulation of the remaining nerve tract beyond the site of crushing or toxin blockade, or by direct electrical stimulation of the muscle (Lomo and Rosenthal, 1972). It has been demonstrated that the effect of this electrical stimulation is to reduce the rate of receptor synthesis with continued degradation at the normal rate (Reiness and Hall, 1977; Card, 1977; Linden and Fambrough, 1979). This effect on the synthesis rate is selective: Overall protein synthesis is not suppressed by the electrical stimulation, and the proteins synthesized in stimulated and unstimulated muscles seem to exhibit identical patterns on two-dimensional gel (Reiness and Hall, 1977; Smith and Appel, 1977).

Regulation of receptor degradation

One important step in the metabolic control of AChR is degradation. While extrajunctional receptors on embryonic muscles are short-lived with a half-life of 24 hr, junctional receptors at the endplate region on adult muscles degrade at a much slower rate with a half life of 8-10 days (Salpeter and Loring, 1985). Denervation accelerates the degradation of junctional receptors (Loring and

Salpeter, 1980; Bevan and Steinbach, 1983), and this effect can be reversed by reinnervation (Salpeter *et al.*, 1986). Using a myogenic cell line, which can be manipulated to switch between differentiated and undifferentiated states, it has been shown that while differentiation induces a high level of surface AChRs, de-differentiation causes a marked shortening of the surface receptor lifespan with a half-life of 8.6 hr (Olson *et al.*, 1983). The degradation of AChR follows first-order kinetics and is carried out via proteolysis in lysosomes containing internalized receptors (Kaplan and Blau, 1986).

CONCLUDING REMARKS

The studies of AChRs have provided insightful results that are pertinent to many areas of scientific interests. Already, AChR has been a leading model in biological fields as diverse as genetic regulation in development and differentiation, molecular basis for cell-cell communication, physiological mechanism of transmembrane signaling, and relationship between protein structure and function, to list a few. Moreover, the endeavors on AChR have directly and indirectly resulted in several major advancements in research technology, including the single channel recording technique and the functional analysis of membrane ion channels using cloned cDNAs and the *in vivo* expression systems. But more importantly, the studies on AChR have forced investigators with different trainings to interact with each other and learn from each other, asking questions in the process, which often provide brand-new perspectives at the seemingly old problems. It is these kinds of new ideas that forms the foundation upon which mankind builds his pyramid of science and technology.

REFERENCES

Adams, P. R. (1981) Acetylcholine receptor kinetics. *J. Memb. Biol.* 58: 161-174.

Adams, P. R. (1975) An analysis of the dose-response curve at voltage-clamped frog endplates. *Pflugers Arch.* 360: 145-153.

Anderson, C. R., and C. F. Stevens. (1973) Voltage clamp analysis of acetylcholine-produced endplate current fluctuations at frog neuromuscular junction. *J. Physiol. (London)* 235: 655-691.

Anderson, D. J. (1983) Acetylcholine receptor biosynthesis: from kinetics to molecular mechanism. *Trends Neurosci.* 6: 169-171.

Anderson, D. J., P. Walter, and G. Blobel. (1982) Signal recognition protein is required for the integration of acetylcholine receptor δ subunit, a transmembrane glycoprotein, into the endoplasmic reticulum membrane. *J. Cell Biol.* 93: 501-506.

Anderson, D. J., and G. Blobel. (1981) *In vitro* synthesis, glycosylation, and membrane insertion of the four subunits of the *Torpedo* acetylcholine receptor. *Proc. Natl. Acad. Sci. USA* 78: 5598-5602.

Anderson, M. J., M. W. Cohen, and E. Zorychta. (1977) Effects of innervation on the distribution of acetylcholine receptors on cultured cells. *J. Physiol. (London)* 268:731-756.

Anderson, M. J., and M. W. Cohen. (1977) Nerve-induced and spontaneous redistribution of acetylcholine receptors on cultured muscle cell. *J. Physiol. (London)* 268: 757-773.

Auerbach, A., and C. J. Lingle. (1986) Heterogeneous kinetic properties of acetylcholine receptor channels in *Xenopus* myocytes. *J. Physiol. (London)* 378: 119-140.

Auerbach, A., and F. Sachs. (1984a) Patch clamp studies of single ionic channels. *Ann. Rev. Biophys. Bioeng.* 13: 269-302.

Auerbach, A., and F. Sachs. (1984b) Single channel currents from acetylcholine receptors in embryonic chick muscle: Kinetic and conductance properties of gaps within bursts. *Biophys. J.* 45: 187-198.

Axelsson, J., and S. Thesleff. (1959) A study of supersensitivity in denervated mammalian skeletal muscle. *J. Physiol. (London)* 147: 178-193.

Ballivet, M., J. Patrick, J. Lee, and S. Heinemann. (1982) Molecular cloning of cDNA coding for the γ subunit of *Torpedo* acetylcholine receptor. *Proc. Natl. Acad. Sci. USA* 79: 4466-4470.

Beeson, D. M. W., E. A. Barnard, B. M. Conti-Tronconi, S. M. J. Dunn, T. L. Anderson, A. F. Wilderspin, L. D. Bell, and J. F. Jackson. (1986) The chicken muscle acetylcholine receptor: subunit structure and α-subunit cloning. *J. Biol. Chem.* in press.

Bevan, S., and J. H. Steinbach. (1983) Denervation increases the degradation rate of acetylcholine receptors at end-plates *in vivo* and *in vitro*. *J. Physiol. (London)* 336: 159-177.

Boulter, J., K. Evans, G. Martin, P. Mason, S. Stengelin, D. Goldman, S. Heinemann, and J. Patrick. (1986) Isolation and sequence of cDNA clones coding for the precursor to the γ subunit of mouse muscle nicotinic acetylcholine receptor. *J. Neurosci. Res.* 16: 37-49.

Boulter, J., W. Luyten, K. Evans, P. Mason, M. Ballivet, D. Goldman, S. Stengelin, G. Martin, S. Heinemann, and J. Patrick. (1985) Isolation of a clone coding for the α-subunit of a mouse acetylcholine receptor. *J. Neurosci.* 5: 2545-2552.

Boyd, N. D., and J. B. Cohen. (1984) Desensitization of membrane-bound *Torpedo* acetylcholine receptor by amine noncompetitive antagonists and aliphatic

alcohols: Studies of [^{3}H] acetylcholine binding and $^{22}Na^{+}$ ion fluxes. *Biochem.* 23: 4023-4033.

Brockes, J. P., and Z. W. Hall. (1975) Synthesis of acetylcholine receptor by denervated rat diaphragm muscle. *Proc. Natl. Acad. Sci. USA* 72: 1368-1372.

Bruner, J. M., and S. Bursztajn. (1986) Acetylcholine receptor clusters are associated with nuclei in rat myotubes. *Dev. Biol.* 115: 35-43.

Buonanno, A., and J. P. Merlie. (1986) Transcriptional regulation of nicotinic acetylcholine receptor genes during muscle development. *J. Biol. Chem.* 261: 11452-11455.

Buonanno, A., J. Mudd, V. Shah, and J. P. Merlie. (1986) A universal oligonucleotide probe for acetylcholine receptor genes: Selection and sequencing of cDNA clones for the mouse muscle β subunit. *J. Biol. Chem.* 261: 16451-16458.

Bursztajn, S., and G. D. Fischbach. (1984) Evidence that coated vesicles transport acetylcholine receptors to the surface membrane of chick myotubes. *J. Cell Biol.* 98: 498-506.

Card, D. (1977) Regulation of acetylcholine receptor metabolism by electrical stimulation. *Carnegie Inst. Wash. Yearb.* 76: 17-22.

Chow, I., and M. W. Cohen. (1983) Developmental changes in the distribution of acetylcholine receptors in the myotomes of *Xenopus laevis*. *J. Physiol. (London)* 339: 553-571.

Claudio, T., M. Ballivet, J. Patrick, and S. Heinemann. (1983) Nucleic and deduced amino acid sequences of *Torpedo californica* acetylcholine receptor γ-subunit. *Proc. Natl. Acad. Sci. USA* 80: 1111-1115.

Claudio, T., and M. A. Raftery. (1977) Immunological comparison of acetylcholine receptors and their subunits from species of electric ray. *Arch. Biochem. Biophys.* 181: 484-489.

Colquhoun, D., and B. Sakmann. (1985) Fast events in single-channel currents activated by acetylcholine and its analogues at the frog muscle end-plate. *J. Physiol. (London)* 369: 501-557.

Colquhoun, D., and B. Sakmann. (1981) Fluctuation in the microsecond time range of the current through single acetylcholine receptor ion channels. *Nature* 294: 464-466.

Colquhoun, C., F. Dreyer, and R. E. Sheridan. (1979) The actions of tubocurarine at the frog neuromuscular junction. *J. Physiol. (London)* 293: 247-284.

Conti-Tronconi, B. M., M. W. Hunkapiller, J. M. Lindstrom, and M. A. Raftery. (1982) Subunit structure of the acetylcholine receptor from *Electrophorus electricus. Proc. Natl. Acad. Sci. USA* 79: 6489-6493.

Conti-Tronconi, B. M., and M. A. Raftery. (1982) The nicotinic cholinergic receptor: Correlation of molecular structure with functional properties. *Ann. Rev. Biochem.* 51: 491-530.

Criado, M., S. Hochschwender, V. Sarin, J. L. Fox, and J. Lindstrom. (1985) Evidence for unpredicted transmembrane domains in acetylcholine receptor subunits. *Proc. Natl. Acad. Sci. USA* 82: 2004-2008.

Crowder, C. M., and J. P. Merlie. (1986) DNase I-hypersensitive sites surround the mouse acetylcholine receptor δ-subunit gene. *Proc. Natl. Acad. Sci. USA* 83: 8405-8409.

Davidson, E. H. (1986) *Gene Activity in Early Development*, 3rd ed. Academic Press Inc., Orlando, Florida.

Del Castillo, J., and B. Katz. (1955) On the localization of acetylcholine receptors. *J. Physiol. (London)* 128: 157-181.

Devreotes, P. N., J. M. Gardner, and D. M. Fambrough. (1977) Kinetics of biosynthesis of acetylcholine receptor and subsequent incorporation into plasma membrane of cultured chick skeletal muscle. *Cell* 10: 365-373.

Devreotes, P. N., and D. M. Fambrough. (1976) Synthesis of the acetylcholine receptor by cultured chick myotubes and denervated mouse extensor digitorum longus muscles. *Proc. Natl. Acad. Sci. USA* 73: 161-164.

Dionne, V. E., J. H. Steinbach, and C. F. Stevens. (1978) An analysis of the dose-response relationship at voltage-clamped frog neuromuscular junctions. *J. Physiol. (London)* 281: 421-444.

Dwyer, T. M., D. J. Adams, and B. Hille. (1980) The permeability of the endplate channel to organic cations in frog muscle. *J. Gen. Physiol.* 75: 469-492.

Englander, L. L., and L. L. Rubin. (1987) Acetylcholine receptor clustering and nuclear movement in muscle fibers in culture. *J. Cell Biol.* 104: 87-95.

Fambrough, D. M. (1979) Control of acetylcholine receptors in skeletal muscle. *Physiol. Rev.* 59: 165-227.

Fatt, P., and B. Katz. (1951) An analysis of the endplate potential recorded with an intracellular electrode. *J. Physiol. (London)* 115: 320-370.

Finer-Moore, J., and R. M. Stroud. (1984) Amphipathic analysis and possible formation of the ion channel in an acetylcholine receptor. *Proc. Natl. Acad. Sci. USA* 81: 155-159.

Frank, E., and G. D. Fischbach. (1979) Early events in neuromuscular junction formation *in vitro*. *J. Cell Biol.* 83: 143-158.

Froehner, S. C. (1986) The role of the postsynaptic cytoskeleton in AChR organization. *Trends Neurosci.* 9: 37-41.

Furukawa, T., and A. Furukawa. (1959) Effects of methyl- and ethyl- derivatives of NH_4^+ on the neuromuscular junction. *Jpn. J. Physiol.* 9: 130-142.

Grampp, W., J. B. Harris, and S. Thesleff. (1972) Inhibition of denervation changes in skeletal muscle by blockers of protein synthesis. *J. Physiol. (London)* 221: 743-754.

Guy, H. R. (1984) A structural model of the acetylcholine receptor channel based on partition energy and helix packing calculations. *Biophys. J.* 45: 249-261.

Hamill, O. P., A. Marty, E. Neher, B. Sakmann, and F. J. Sigworth. (1981) Improved patch-clamp techniques for high-resolution current recording from cells and cell-free patches. *Pflugers Arch.* 391: 85-100.

Hamill, O. P., and B. Sakmann. (1981) Multiple conductance states of single acetylcholine receptor channels in embryonic muscle cells. *Nature* 294: 462-464.

Heidmann, O., Buonanno, A., B. Geoffroy, B. Robert, J. L. Guenet, J. P. Merlie, and J.-P. Changeux. (1986) Chromosomal localization of muscle nicotinic acetylcholine receptor genes in the mouse. *Science* 234: 866-868.

Heidmann, T., and J.-P. Changeux. (1979) Fast kinetic studies on the allosteric interactions between acetylcholine receptor and local anesthetic binding sites. *Eur. J. Biochem.* 94: 281-296.

Heidmann, T., and J.-P. Changeux. (1978) Structural and functional properties of the acetylcholine receptor protein in its purified and membrane-bound states. *Ann. Rev. Biochem.* 47: 317-357.

Hermans-Borgmeyer, I., D. Zopf, R.-P. Ryseck, B. Hovemann, H. Betz, and E. D. Gundelfinger. (1986) Primary structure of a developmentally regulated nicotinic acetylcholine receptor protein from *Drosophila*. *EMBO J.* 5: 1503-1508.

Hershey, N. D., D. J. Noonan, K. S. Mixter, T. Claudio, and N. Davidson. (1983) Structure and expression of genomic clones coding for the δ-subunit of the *Torpedo* acetylcholine receptor. *Cold Spring Harbor Symp. Quant. Biol.* 48: 101-108.

Hodgkin, A. L., and A. F. Huxley. (1952) A quantitative description of membrane current and its application to conduction and excitation in nerve. *J. Physiol. (London)* 117: 500-544.

Holtzman, E., D. Wise, J. Wall, and A. Karlin. (1982) Electron microscopy of complexes of isolated acetylcholine receptor, biotinyl-toxin, and avidin. *Proc. Natl. Acad. Sci. USA* 79: 310-314.

Horn, R., and K. Lange. (1983) Estimating kinetic constants from single channel data. *Biophys. J.* 43: 207-223.

Horn, R., and J. Patlak. (1980) Single channel currents from excised patches of muscle membrane. *Proc. Natl. Acad. Sci. USA* 77: 6930-6934.

Huang, L.-Y. M., W. A. Catterall, and G. Ehrenstein. (1978) Selectivity of cations and nonelectrolytes for acetylcholine-activated channels in cultured muscle cells. *J. Gen. Physiol.* 71: 397-410.

Hucho, F., W. Oberthur, and F. Lottspeich. (1986) The ion channel of the nicotinic acetylcholine receptor is formed by the homologous helices M II of the receptor subunits. *FEBS Let.* 205: 137-142.

Huganir, R. L., A. H. Delcour, P. Greengard and G. Hess. (1986) Phosphorylation of the nicotinic acetylcholine receptor regulates its rate of desensitization. *Nature* 321: 774-776.

Inestrosa, N. C., J. B. Miller, L. Silberstein, L. Ziaskind-Conhaim, and Z. W. Hall. (1983) Developmental regulation of 16S acetylcholinesterase and acetylcholine receptors in a mouse muscle cell line. *Exp. Cell Res.* 147:393-405.

Isenberg, K. E., J. Mudd, V. Shah, and J. P. Merlie. (1986) Nucleotide sequence of the mouse muscle nicotinic acetylcholine receptor α subunit. *Nucl. Acids Res.* 14: 5111.

Jenkinson, D. H., and J. G. Nicholls. (1961) Contractures and permeability changes produced by acetylcholine in depolarized denervated muscle. *J. Physiol. (London)* 159: 111-127.

Kaldany, R.-R. J., and A. Karlin. (1983) Reaction of quinacrine mustard with the acetylcholine receptor from *Torpedo californica*. *J. Biol. Chem.* 258: 6263-6242.

Kandel, E. R., and J. H. Schwartz. (1985) *Principles of Neural Science*, 2nd ed., Elsevier Sci. Publ. Co., New York, New York.

Kaplan, I. D., and H. M. Blau. (1986) Metabolic properties of human acetylcholine receptors can be characterized on cultured human muscle. *Exp. Cell Res.* 166: 379-390.

Karlin, A. (1980) Molecular properties of nicotinic acetylcholine receptors. *Cell Surf. Rev.* 6: 191-260.

Katz, B., and R. Miledi. (1972) The statistical nature of the acetylcholine potential and its molecular components. *J. Physiol. (London)* 224: 665-699.

Katz, B., and R. Miledi. (1970) Membrane noise produced by acetylcholine. *Nature* 226: 962-963.

Katz, B., and S. Thesleff. (1957) A study of desensitization produced by acetylcholine at the motor endplate. *J. Physiol. (London)* 138: 63-80.

Kistler, J., R. M. Stroud, M. W. Klymkowsky, R. A. Lalancette, and R. H. Fairclough. (1982) Structure and function of an acetylcholine receptor. *Biophys. J.* 37: 371-383.

Klarsfeld, A., P. Daubas, B. Bourachot, and J.-P. Changeux. (1987) A 5'-flanking region of the chicken acetylcholine receptor α-subunit gene confers tissue specificity and developmental control of expression in transfected cells. *Mol. Cell. Biol.* 7: 951-955.

Klymkowsky, M. W., and R. M. Stroud. (1979) Immunospecific identification and three-dimensional structure of a membrane-bound acetylcholine receptor *Torpedo californica*. *J. Mol. Biol.* 128: 319-334.

Kubo, T., M. Noda, T. Takai, T. Tanabe, T. Kayano, S. Shimizu, K. Tanaka, H. Takahashi, T. Hirose, S. Inayama, R. Kikano, T. Miyata, and S. Numa. (1985) Primary structure of δ subunit precursor of calf muscle acetylcholine receptor deduced from cDNA sequence. *Eur. J. Biochem.* 149: 5-13.

Kuffler, S. W., J. G. Nicholls, and A. R. Martin. (1984) *From Neuron to Brain*, 2nd ed., Sinauer Associates Inc. Publishers, Sunderland, Massachusetts.

Leonard, R. J. (1985) Physiological development of acetylcholine receptors in embryonic *Xenopus* muscle cells in culture. *Ph.D. thesis*, Purdue University.

Leonard, R. J., S. Nakajuma, Y. Nakajuma, and T. Takahashi. (1984) Differential development of two classes of acetylcholine receptor in *Xenopus* muscle. *Science* 226: 55-57.

Lester, H. A., L. D. Chabala, A. M. Gurney, and R. E. Sheridan. (1985) Experiments with photoisomerizable molecules at nicotinic acetylcholine receptors in cells and membrane patches from rat muscle. In *Optical Methods in Cell Physiology* Vol. 40, P. De Weer and B. Salzberg eds., John Wiley and Sons, New York, pp. 447-461.

Lester, H. A., M. M. Nass, M. E. Krouse, and J. M. Nerbonne. (1980) Electrophysiological experiments with photoisomerizable cholinergic compounds: Review and progress report. *Ann. NY Acad. Sci.* 346: 475-490.

Lester, H. A., J.-P. Changeux, and R. E. Sheridan. (1975) Conductance increases produced by bath application of cholinergic agonists to *Electrophorus* electroplaques. *J. Gen. Physiol.* 65: 797-816.

Levitan, I. B. (1985) Phosphorylation of ion channels. *J. Memb. Biol.* 87: 177-190.

Linden, D. C., and D. M. Fambrough. (1979) Biosynthesis and degradation of acetylcholine receptors in rat skeletal muscles. Effects of electrical stimulation. *Neurosci.* 4: 527-538.

Lindstrom, J., M. Criado, S. Hochschwender, J. L. Fox, and V. Sarin. (1984) Immunochemical tests of acetylcholine receptor subunit models. *Nature* 311: 573-575.

Lindstrom, J., J. Merlie, and G. Yogeeswaran. (1979) Biochemical properties of acetylcholine receptor subunits from *Torpedo californica*. *Biochem.* 18: 4465-4470.

Lomo, T., and J. Rosenthal. (1972) Control of ACh sensitivity by muscle activity in the rat. *J. Physiol. (London)* 221: 493-513.

Loring, R., and M. M. Salpeter. (1980) Denervation increases turnover rate of junctional acetylcholine receptors. *Proc. Natl. Acad. Sci. USA* 77: 2293-2298.

Maeno, T., C. Edwards, and M. Anraku. (1977) Permeability of the end-plate membrane activated by acetylcholine to some organic cations. *J. Neurobiol.* 8: 173-184.

Magazanik, L. G., and F. Vyskocil. (1973) Desensitization of the motor end plate. In *Drug Receptors*, H. P. Rang ed., Macmillan, London, pp. 105-119.

Magleby, K. L., and C. F. Stevens. (1972a) The effect of voltage on the time course of end-plate currents. *J. Physiol. (London)* 223: 151-171.

Magleby, K. L., and C. F. Stevens. (1972b) A quantitative description of endplate currents. *J. Physiol. (London)* 223: 173-197.

Mayne, K. M. (1986) Structural and functional studies on the subunits of the nicotinic acetylcholine receptor. *Ph.D. thesis.* California Institute of Technology.

Mayne, K. M., K. Yoshii, L. Yu, H. A. Lester, and N. Davidson. (1987) Expression of mouse-*Torpedo* acetylcholine receptor subunit chimeras and hybrids in *Xenopus* oocytes. *Molecular Brain Research*, in press.

McCarthy, M. P., J. P. Earnest, E. F. Young, S. Choe, and R. M. Stroud. (1986) The molecular neurobiology of the acetylcholine receptor. *Ann. Rev. Neurosci.* 9: 383-413.

Merlie, J. P. (1984) Biogenesis of the acetylcholine receptor, a multisubunit integral membrane protein. *Cell* 36: 573-575.

Merlie, J. P., and J. R. Sanes. (1985) Concentration of acetylcholine receptor mRNA in synaptic regions of adult muscle fibres. *Nature* 317: 66-68.

Merlie, J. P., K. E. Isenberg, S. D. Russell, and J. R. Sanes. (1984) Denervation supersensitivity in skeletal muscle: analysis with a cloned cDNA probe. *J. Cell Biol.* 99: 332-335.

Merlie, J. P., and J. Lindstrom. (1983) Assembly *in vivo* of mouse muscle acetylcholine receptor: Identification of an α subunit species that may be an assembly intermediate. *Cell* 34: 747-757.

Merlie, J. P., M. E. Buckingham, and F. Gros. (1977) Molecular aspects of myogenesis. *Curr. Top. Dev. Biol.* 11: 61-114.

Merlie, J. P., and F. Gros. (1976) *In vitro* myogenesis: Expression of muscle specific function in the absence of cell fusion. *Exp. Cell Res.* 97: 406-412.

Merlie, J. P., A. Sobel, J.-P. Changeaux, and F. Gros. (1975) Synthesis of acetylcholine receptor during differentiation of cultured embryonic muscle cells. *Proc. Natl. Acad. Sci. USA* 72:4028-4032.

Miledi, R. (1960) The acetylcholine sensitivity of frog muscle fibers after complete or partial denervation. *J. Physiol. (London)* 151: 1-23.

Mishina, M., T. Takai, K. Imoto, M. Noda, T. Takahashi, S. Numa, C. Methfessel, and B. Sakmann. (1986) Molecular distinction between fetal and adult forms of muscle acetylcholine receptor. *Nature* 321:406-411.

Mishina, M., T. Tobinatsu, K. Imoto, K. Tanaka, Y. Fujita, K. Fukuda, M. Kurasaki, H. Takahashi, Y. Morimoto, T. Hirose, S. Inayama, T. Takahashi, M. Kuno, and S. Numa. (1985) Location of functional regions of acetylcholine receptor α-subunit by site-directed mutagenesis. *Nature* 313: 364-369.

Mishina, M., T. Kurosaki, T. Tobimatsu, Y. Morimoto, M. Noda, T. Yamamoto, M. Terao, J. Lindstrom, T. Takahashi, M. Kuno, and S. Numa. (1984) Expression of functional acetylcholine receptor from cloned cDNAs. *Nature* 307: 604-608.

Nastuk, W. L., and R. L. Parsons. (1970) Factors in the inactivation of postjunctional membrane receptors of frog skeletal muscle. *J. Gen. Physiol.* 56: 218-249.

Nef, P., A. Mauron, R. Stalder, C. Alliod, and M. Ballivet. (1984) Structure, linkage, and sequence of the two genes encoding the δ and γ subunits of the nicotinic acetylcholine receptor. *Proc. Natl. Acad. Sci. USA* 81: 7975-7979.

Neher, E. (1983) The charge carried by single-channel currents of rat cultured muscle cells in the presence of local anaesthetics. *J. Physiol. (London)* 339: 663-678.

Neher, E., and J. H. Steinbach. (1978) Local anaesthetics transiently block currents through single acetylcholine-receptor channels. *J. Physiol. (London)* 277: 153-176.

Neher, E., and B. Sakmann. (1976a) Noise analysis of drug-induced voltage clamp currents in denervated frog muscle. *J. Physiol. (London)* 258: 705-729.

Neher, E., and B. Sakmann. (1976b) Single-channel currents recorded from membrane of denervated frog muscle fibres. *Nature* 260: 799-802.

Neubig, R. R., and J. B. Cohen. (1980) Permeability control by cholinergic receptors in *Torpedo* post-synaptic membrane: Agonist dose-response relations measured at second and millisecond times. *Biochem.* 19: 2770-2779.

Neubig, R. R., E. K. Krodel, N. D. Boyd, and J. B. Cohen. (1979) Acetylcholine and local anesthetic binding to *Torpedo* nicotinic post-synaptic membranes after removal of non-receptor peptides. *Proc. Natl. Acad. Sci. USA* 76: 690-694.

Noda, M., H. Takahashi, T. Tanabe, M. Toyosato, S. Kikyotani, T. Hirose, M. Asai, H. Takashima, S. Inayama, T. Miyata, and S. Numa. (1983a) Primary structures of β-subunit and δ-subunit precursors of *Torpedo californica* acetylcholine receptor deduced from cDNA sequences. *Nature* 301: 251-255.

Noda, M., H. Takahashi, T. Tanabe, M. Toyosato, S. Kikyotani, Y. Furutani, T. Hirose, H. Takashima, S. Inayama, T. Miyata, and S. Numa. (1983b) Structural homology of *Torpedo californica* acetylcholine receptor subunits. *Nature* 302: 528-532.

Noda, M., H. Takahashi, T. Tanabe, M. Toyosato, Y. Furatani, T. Hirose, M. Asai, H. Takashima, S. Inayama, T. Miyata, and S. Numa. (1982) Primary structure of α subunit precursor of *Torpedo californica* acetylcholine receptor deduced from cDNA sequence. *Nature* 299: 793-797.

Ogden, D. C., S. A. Siegelbaum, and D. Colquhoun. (1981) Block of acetylcholine-activated ion channels by an uncharged local anaesthetic. *Nature* 289: 596-599.

Olson, E. N., L. Glaser, J. P. Merlie, and J. Lindstrom. (1984) Expression of acetylcholine receptor α-subunit mRNA during differentiation of the BC_3H1 muscle cell line. *J. Biol. Chem.* 259: 3330-3336.

Olson, E. N., L. Glaser, J. P. Merlie, and R. Sebanne. (1983) Regulation of surface expression of acetylcholine receptors in response to serum and cell growth in the BC_3H1 muscle cell line. *J. Biol. Chem.* 258: 13946-13953.

Oswald, R. E., and J.-P. Changeux. (1981) Selective labeling of the δ-subunit of the acetylcholine receptor by a covalent local anesthetic. *Biochem.* 20: 7166-7174.

Peper, K., R. J. Bradley, and F. Dreyer. (1982) The acetylcholine receptor at the neuromuscular junction. *Physiol. Rev.* 62: 1271-1340.

Popot, J.-L., and J.-P. Changeux. (1984) Nicotinic receptor of acetylcholine: structure of an oligomeric integral membrane protein. *Physiol. Rev.* 64: 1162-1239.

Prives, J. M., and B. M. Patterson. (1974) Differentiation of cell membranes in cultures of embryonic chick breast muscle. *Proc. Natl. Acad. Sci. USA* 71: 3208-3211.

Pumplin, D. W., and D. M. Fambrough. (1982) Turnover of acetylcholine receptors in skeletal muscle. *Ann. Rev. Physiol.* 44: 319-335.

Raftery, M. A., M. W. Hunkapiller, C. D. Strader, and L. E. Hood. (1980) Acetylcholine receptor: Complex of homologous subunits. *Science* 208: 1454-1457.

Ratnam, M., D. L. Nguyen, J. Rivier, P. B. Sargent, and J. Lindstrom. (1986) Transmembrane topography of the nicotinic acetylcholine receptor: immunochemical tests contradict theoretical predictions based on hydrophobicity profiles. *Biochem.* 25: 2621-2632.

Reiness, C. G., and Z. W. Hall. (1977) Electrical stimulation of denervated muscles reduces incorporation of methionine into the ACh receptor. *Nature* 268: 655-657.

Reynolds, J., and A. Karlin. (1978) Molecular weight in detergent solution of acetylcholine receptor from *Torpedo californica*. *Biochem.* 17: 2035-2038.

Role, L. W., V. R. Matossian, R. J. O'Brien, and G. D. Fischbach. (1985) On the mechanism of acetylcholine receptor accumulation at newly formed synapses on chick myotubes. *J. Neurosci.* 5: 2197-2204.

Sakmann, B., C. Methfessel, M. Mishina, T. Takahashi, T. Takai, M. Kurasaki, K. Fukuda, and S. Numa. (1985) Role of acetylcholine receptor subunits in gating of the channel. *Nature* 318: 538-543.

Sakmann, B., J. Patlak, and E. Neher. (1980) Single acetylcholine-activated channels show burst kinetics in the presence of desensitizing concentrations of agonist. *Nature* 286: 71-73.

Salpeter, M. M., D. L. Cooper, and T. Levitt-Gilmour. (1986) Degradation rates of acetylcholine receptors can be modified in the postjunctional plasma membrane of the vertebrate neuromuscular junction. *J. Cell Biol.* 103: 1399-1403.

Salpeter, M. M., and R. H. Loring. (1985) Nicotinic acetylcholine receptors in vertebrate muscle: properties, distribution and neural control. *Prog. Neurobiol.* 25: 297-325.

Sheridan, R. E., and H. A. Lester. (1982) Functional stoichiometry at the nicotinic receptor: The photon cross section for phase 1 corresponds to two Bis-Q molecules per channel. *J. Gen. Physiol.* 80: 499-515.

Shibahara, S., T. Kubo, H. J. Perski, H. Takahashi, M. Noda, and S. Numa. (1985) Cloning and sequence analysis of human genomic DNA encoding γ subunit precursor of muscle acetylcholine receptor. *Eur. J. Biochem.* 146: 15-22.

Sine, S. M., and J. H. Steinbach. (1986a) Acetylcholine receptor activation by a site-selective ligand: Nature of brief open and closed states in BC3H-1 cells. *J. Physiol. (London)* 370: 357-379.

Sine, S. M., and J. H. Steinbach. (1986b) Activation of acetylcholine receptors on clonal mammalian BC3H-1 cells by low concentrations of agonist. *J. Physiol. (London)* 373: 129-162.

Sine, S. M., and J. H. Steinbach. (1984) Activation of a nicotinic acetylcholine receptor. *Biophys. J.* 45: 175-185.

Smith, P. B., and S. H. Appel. (1977) Development of denervation alterations in surface membranes of mammalian skeletal muscle. *Exp. Neurol.* 56: 102-114.

Sobel, A., M. Weber, and J.-P. Changeux. (1977) Large-scale purification of the acetylcholine-receptor protein in its membrane-bound and detergent-extracted forms from *Torpedo marmorata* electric organ. *Eur. J. Biochem.* 80: 215-224.

Spivak, C. E., and E. X. Albuquerque. (1982) Dynamic properties of the nicotinic acetylcholine receptor ionic channel complex: Activation and blockade. In *Progress in Cholinergic Biology*, Vol.2, I. Hanin and A. M. Goldberg eds., Raven, New York., pp. 323-357.

Stroud, R. M., and J. Finer-Moore. (1985) Acetylcholine receptor structure, function, and evolution. *Ann. Rev. Cell Biol.* 1: 317-351.

Takai, T., M. Noda, M. Mishina, S. Shimizu, Y. Furutani, T. Kayano, T. Ikeda, T. Kubo, H. Takahashi, T. Takahashi, M. Kuno, and S. Numa. (1985) Cloning, sequencing and expression of cDNA for a novel subunit of acetylcholine receptor from calf muscle. *Nature* 315: 761-764.

Takeda, K., and A. Trautmann. (1984) A patch-clamp study of the partial agonist actions of tubocurarine on rat myotubes. *J. Physiol. (London)* 349: 353-374.

Takeuchi, A., and N. Takeuchi. (1960) On the permeability of the endplate membrane during the action of transmitter. *J. Physiol. (London)* 154: 52-67.

Trautman, A. (1982) Curare can open and block ionic channels associated with cholinergic receptors. *Nature* 298: 272-275.

White, M. M., K. M. Mayne, H. A. Lester, and N. Davidson. (1985) Mouse-*Torpedo* hybrid acetylcholine receptors: Functional homology does not equal sequence homology. *Proc. Natl. Acad. Sci. USA* 82: 4852-4856.

Wise, D. S., J. Wall, and A. Karlin. (1981) Relative locations of the β and δ chains of the acetylcholine receptor determined by electron microscopy of isolated receptor trimers. *J. Biol. Chem.* 256: 12624-12627.

Yoshii, K., L. Yu, K. M. Mayne, N. Davidson, and H. A. Lester. (1987) Equilibrium properties of mouse-*Torpedo* acetylcholine receptor hybrids expressed in *Xenopus* oocytes. *J. Gen. Physiol.*, in press.

Young, E. F., E. Ralston, J. Blake, J. Ramachandran, Z. W. Hall, and R. M. Stroud. (1985) Topological mapping of acetylcholine receptor: Evidence for a model with five transmembrane segments and a cytoplasmic COOH- terminal peptide. *Proc. Natl. Acad. Sci. USA* 82: 626-630.

Yu, L., R. J. LaPolla, and N. Davidson. (1986) Mouse muscle nicotinic acetylcholine receptor γ subunit: cDNA sequence and gene expression. *Nucl. Acids Res.* 14: 3539-3555.

Zingsheim, H. P., F. J. Barrantes, J. Frank, W. Hanicke, and D. C. Neugebauer. (1982) Direct structural localization of two toxin-recognition sites on an acetylcholine receptor protein. *Nature* 299: 81-84.

Ziskind-Conhaim, L., I. Geffen, and Z. W. Hall. (1984) Redistribution of acetylcholine receptors on developing rat myotubes. *J. Neurosci.* 4: 2346-2349.

CHAPTER 2

Mouse muscle nicotinic acetylcholine receptor γ subunit: cDNA sequence and gene expression

Lei Yu, Robert J. LaPolla, and Norman Davidson

Nucleic Acids Research

14: 3539-3555 (1986)

Volume 14 Number 8 1986 Nucleic Acids Research

Mouse muscle nicotinic acetylcholine receptor γ subunit: cDNA sequence and gene expression

Lei Yu, Robert J.LaPolla[1]* and Norman Davidson[1]

Division of Biology and [1]Department of Chemistry, California Institute of Technology, Pasadena, CA 91125, USA

Received 19 December 1985; Accepted 6 February 1986

ABSTRACT

Clones coding for the mouse nicotinic acetylcholine receptor (AChR) γ subunit precursor have been selected from a cDNA library derived from a mouse myogenic cell line and sequenced. The deduced protein sequence consists of a signal peptide of 22 amino acid residues and a mature γ subunit of 497 amino acid residues. There is a high degree of sequence conservation between this mouse sequence and published human and calf AChR γ subunits and, after allowing for functional amino acid substitutions, also to the more distantly related chicken and *Torpedo* AChR γ subunits. The degree of sequence conservation is especially high in the four putative hydrophobic membrane spanning regions, supporting the assignment of these domains. RNA blot hybridization showed that the mRNA level of the γ subunit increases by 30 fold or more upon differentiation of the two mouse myogenic cell lines, BC3H-1 and C_2C_{12}, suggesting that the primary controls for changes in gene expression during differentiation are at the level of transcription. One cDNA clone was found to correspond to a partially processed nuclear transcript containing two as yet unspliced intervening sequences.

INTRODUCTION

The nicotinic acetylcholine receptor (AChR) on the postsynaptic membrane is an integral membrane protein complex composed of four subunits, α, β, γ, and δ. It functions as an agonist gated ion channel in the *Torpedo* electric organ and at the neuromuscular junction of striated muscle in other vertebrates. At present AChR is the best studied and most fully characterized ion channel. Related receptors are also present in the nervous system. The receptor is very abundant in the electric organ of the electric ray *Torpedo* and it has been extensively characterized at the biochemical, functional, and sequence levels (1-3). The amino acid sequences of the four *Torpedo* AChR subunits have been deduced from the nucleotide sequences of full-length cDNA clones (4-9). In vertebrate striated muscle and various muscle-like cell systems in culture, nicotinic AChR molecules are present in lower overall abundances. Vertebrate systems are of greater interest than *Torpedo* for most electrophysiological studies and for cell biological studies of assembly (10). The subunits of the vertebrate AChR are similar in general properties to those of *Torpedo*, but they are clearly somewhat divergent at the amino acid sequence level (11). The mouse myogenic cell line BC3H-1 (12) is one of the more abundant sources of mammalian AChRs and their mRNAs. Our

laboratory and others have described the isolation of cDNAs for several of the mouse AChR subunits from this source (13-15).

In particular, our laboratory has previously reported on the preparation of a cDNA library from membrane bound polysomal poly(A)$^+$ RNA of induced BC3H-1 cells (14). When this cDNA library was screened by low stringency hybridization with a *Torpedo* AChR γ chain probe, two groups of non-overlapping clones were isolated. A full sequence determination (14) and expression studies in *Xenopus* oocytes (16) led to the surprising conclusion that one of these groups of clones, selected by hybridization with a *Torpedo* γ probe, actually coded for a δ subunit. In the present paper, we report the sequence determination of the clones from the other group and show that this group does in fact code for the mouse AChR γ subunit. Also reported here are some features of γ subunit gene expression at the mRNA level.

MATERIALS AND METHODS

Chemicals and Reagents

Restriction endonucleases and other enzymes including T4 DNA ligase, Klenow fragment of E. coli DNA polymerase, SP6 and T7 RNA polymerases, exonuclease III and S1 nuclease were purchased from Bethesda Research Laboratories, Boehringer Mannheim Biochemicals, New England Biolabs, Promega Biotec, and Sigma.

Cloning of Mouse AChR γ cDNA and DNA Sequence Determination

A cDNA library was prepared in the vector λgt10 using membrane-associated polysomal polyadenylated RNA from differentiated BC3H-1 cells and screened with a *Torpedo* AChR γ cDNA probe as previously described (14). The screening was carried out at 42°C for 48 hours in the hybridization solution containing 33% (v/v) formamide, 0.9M NaCl, 50mM sodium phosphate, 5mM EDTA, pH 7.4, 0.1% Ficoll, 0.1% polyvinylpyrolidone, 0.1% bovine serum albumin, 0.1% sarcosine, 0.1 mg/ml denatured salmon sperm DNA, and 2μg/ml each of poly(rA), poly(rC), and poly(rG). Filters were washed in 30mM NaCl, 3mM sodium citrate, and 0.05% sarcosine at 50°C. cDNA inserts from plaques that gave positive signals were separated from the λgt10 arms by *Eco*RI restriction digestion and recloned either into the plasmid vector pUC19 (17) for restriction mapping, or into an M13 vector (18) for exonuclease III deletion (19) and subsequent sequence determination, or into the expression vector pIBI76 (International Biotechnology Inc.) for SP6 and/or T7 *in vitro* transcription.

For transformation of JM109 cells (17) with M13 RF DNA, Hanahan's protocol (20) was used with the following transformation buffer: 30mM NaAc, 30mM $CaCl_2$, 100mM KCl, 70mM $MnCl_2$, adjusted to pH5.6 with 0.1M acetic acid, and filter sterilized.

For sequence determination, full length cDNA clones or ExoIII-generated deletion clones were analyzed by the method of dideoxy nucleotide chain termination (21) with a few modifications (22).

Cell Culture

Cells were grown and fed every other day in DME (Dulbecco modified Eagle medium) supplemented with 20% fetal calf serum and Pen-Strep (100 units penicillin G/ml and 100 mcg streptomysin/ml) for BC3H-1 cells and 20% fetal calf serum and 0.5% chick embryo extract for C_2C_{12} cells. They were plated at a density of 2-2.5x10^4 cells/ml and propagated in a humidified 37°C incubator with 5% CO_2/95% air. Cells reached 40-60% confluence 2 days after plating and were harvested as undifferentiated cells. To induce differentiation, BC3H-1 cells were grown to confluence without feeding and harvested 6 days after plating. Similarly, C_2C_{12} cells were grown to confluence (4 days after plating), switched to DME medium supplemented with 2% horse serum, fed with this medium every day, and harvested 7 days after plating.

Generation of ^{32}P-labeled RNA Probes by *in vitro* Transcription

Double-stranded plasmid DNA bearing the desired insert was linearized with appropriate restriction enzymes, extracted with phenol-chloroform, precipitated with ethanol, and used as template in *in vitro* transcription. For SP6 or T7 transcription, 0.5µg of linear DNA was suspended in 20µl transcription solution (40mM Tris, pH7.9, 6mM $MgCl_2$, 2mM spermidine, 10mM DTT, 0.5mM each of ATP, GTP and UTP, 100µCi [^{32}P-α]CTP with a specific activity of 410Ci/mM, and 20 units of RNasin). 0.5µl of SP6 or T7 RNA polymerase was added, and the reaction carried out at 37°C for 60 minutes. 10µl of 1mg/ml yeast tRNA and 1µl of 1mg/ml RNase-free DNase was added, and the mixture incubated at 37°C for another 15 minutes. The mixture was then passed over a Sephadex G-50-80 column to remove the unincorporated nucleotide precursors. The radioactive RNA solution from the column was used in hybridization without further treatment.

RNA Purification, Fractionation, Blotting, and Hybridization

Cultured cells were lysed by 6M guanidine solution (6M guanidine-HCl, 0.2M NaAc, 0.1M β-mercaptoethanol, pH4.6). The lysate was homogenized manually in a glass homogenizer to reduce viscosity, and the RNA precipitated with 0.5 volumes of pure ethanol. The pellet was dissolved in 7.5M guanidine solution (7.5M guanidine-HCl, 25mM sodium citrate, 50mM β-mercaptoethanol, pH6.4), and the RNA precipitated with 0.025 volumes of 1M acetic acid and 0.5 volumes of pure ethanol. This pellet was dissolved in 0.1% SDS solution and extracted twice with equal volume of phenol-chloroform and twice with chloroform; the aqueous solution was transferred to a glass tube containing 0.1 volumes of 3M NaAc (pH4.8) and 2.5 volumes of pure ethanol; and the RNA was precipitated. The RNA pellet was dissolved in 0.05% SDS solution and precipitated again with 0.1 volumes of 3M NaAc and 2.5 volumes of pure ethanol. Finally the RNA was resuspended in 0.05% SDS solution and stored at -80°C.

For gel blots, RNA was fractionated on a glyoxal gel (23), blotted to Hybond-N

membrane (Amersham) in 20XSSC (3M NaCl, 0.3M Na-citrate) by capillary action for 18 hours, and crosslinked to the membrane by irradiation with a standard UV transilluminator for 5 minutes.

RNA blots were prehybridized for 4 hours at 60°C in hybridization solution (0.1M Na_2HPO_4/NaH_2PO_4, pH6.5, 5XSSC, 2.5X Denhardts, 50% formamide, 0.1% SDS, 1.25mM EDTA, 0.1 mg/ml denatured calf thymus DNA, 0.1 mg/ml yeast tRNA), ^{32}P-labeled RNA probe was added to 10^6cpm/ml, and the hybridization was carried out at 60°C for 16 hours. The blots were washed at 65°C three times in 2XSSC, 0.1%SDS and three times in 0.2XSSC, 0.1%SDS, wrapped in plastic sheets, and exposed to X-ray films (Kodak XAR-5).

RESULTS AND DISCUSSION

The Mouse cDNA Clones

As previously reported (14), a cDNA library was constructed in the vector λgt10 using membrane-bound polysomal polyadenylated RNA prepared from differentiated BC3H-1 cells, a relatively rich source of AChR. By screening the library at low stringency with a full length cDNA clone for the AChR γ subunit of the electric ray ***Torpedo californica***, two groups of non-overlapping clones were isolated. Surprisingly, one group of clones, selected with the *Torpedo* γ probe, turned out to code for the mouse δ subunit, even though there was no detectable hybridization in screening the library with a *Torpedo* δ probe (14). In the work reported here, we have studied the other group of clones selected by hybridization with the *Torpedo* γ probe. Restriction endonuclease mapping analysis of these inserts revealed that they formed a group of

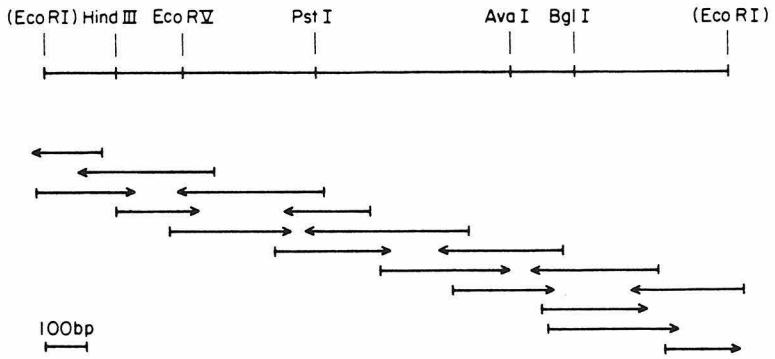

Figure 1. Restriction map of clone M169 and the exonuclease III-generated deletion clones. The restriction map of clone M169 is shown on top. The *Eco*RI sites flanking the clone were added during the cDNA library construction. The exonuclease III-generated deletion clones are aligned below and the regions sequenced are indicated by the arrowed bars.

overlapping clones (data not shown).

Nucleotide Sequence Determination and Assignment of the Protein Sequence

One of the longest cDNA clones, M169, was selected for sequence analysis. The insert was recloned into the *Eco*RI site of the M13mp18 vector and transformed into the *E. coli* host JM109. Clones containing the insert in both orientations were selected and treated with exonuclease III to generate controlled deletions (19). The restriction map of clone M169 is shown in Figure 1 and the ExoIII-generated deletion clones for sequencing are aligned below it. Sequence analysis was carried out by the dideoxy

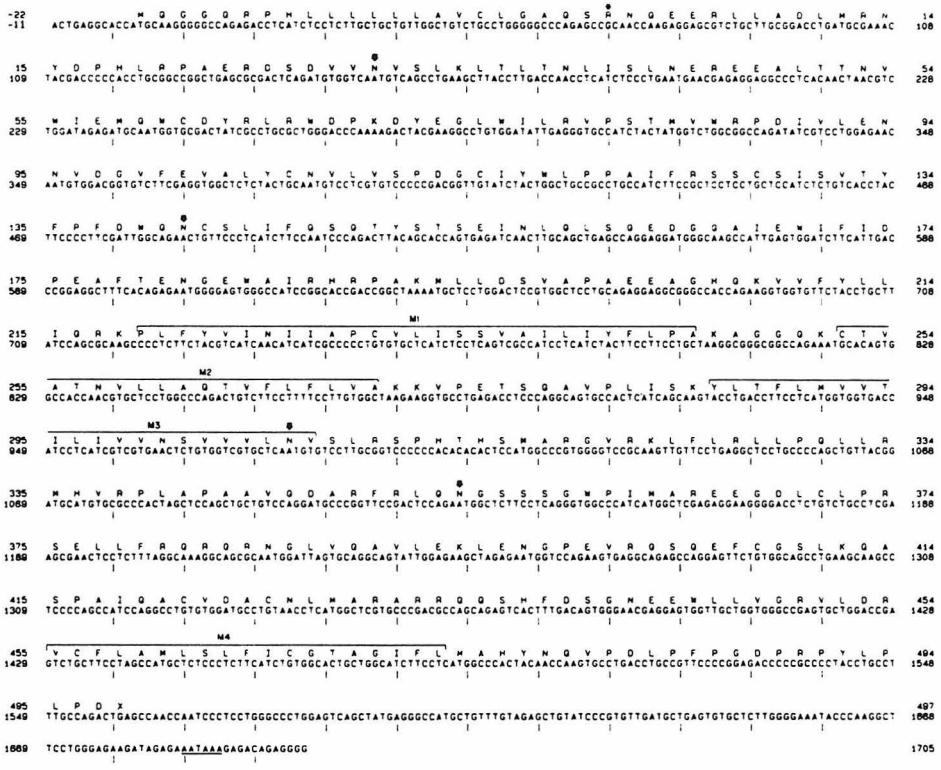

Figure 2. Nucleotide and deduced amino acid sequence of the mouse AChR γ subunit precursor. Nucleotide no. 1 indicates the first nucleotide of the initiation codon in the protein coding region, and the nucleotides 5' to the initiation codon are indicated by negative numbers. The sequence shown is followed on its 3' side by a stretch of adenosine residues (not shown). The putative polyadenylation signal sequence AATAAA is underlined. The deduced amino acid sequence is displayed above the corresponding nucleotide sequence with standard one-letter amino acid code. Amino acid no. 1 is assigned to the first amino acid residue of the mature γ subunit and marked with a *. The amino acid residues in the signal peptide are indicated by negative numbers. The four hydrophobic membrane-spanning regions are marked as M1-M4. The potential sites for asparagine N-glycosylation are indicated by vertical arrows.

nucleotide chain termination method (see Materials and Methods).

The complete nucleotide sequence of clone M169 is shown in Figure 2. It has an open reading frame of 1,557 bases flanked by 11 bases on the 5' side and 148 bases on the 3' side. The 3' untranslated region is followed by a stretch of adenosine residues (not shown in Figure 2), presumably copied from the mRNA polyadenosine tail during reverse transcription. Beginning 18 bases 5' to the polyadenosine stretch, there is a consensus polyadenylation signal AATAAA (24,25). Thus the insert appears to contain the complete 3' untranslated region of the mRNA.

The open reading frame of clone M169 has a methionine codon ATG at the third codon position following an in-frame termination codon TGA (Figure 2). If this methionine codon is used as the initiation codon, the translated polypeptide chain would consist of 519 amino acid residues. When this putative polypeptide was compared with the published AChR γ subunit sequences from other species, a high degree of homology was revealed (see below). On this basis, we assign the protein coded by clone M169 to be the mouse muscle AChR γ subunit. Using the *Xenopus* oocyte assay system (16), the RNA transcribed from clone M169 in an SP6 vector by *in vitro* transcription showed functional substitution for the *Torpedo* γ subunit, thus confirming the assignment (unpublished results, K. M. Mayne, K. Yoshii, L. Yu, and N. Davidson).

Structural Analysis of the Mouse Muscle AChR γ Subunit

The deduced amino acid sequence for the mouse muscle AChR γ subunit is displayed above the corresponding nucleotide sequence in Figure 2. The first 22 amino acid residues have the characteristic features of a signal peptide common to membrane-associated and secretory proteins (26-28). These features are a stretch of highly hydrophobic amino acid residues followed by a hydrophilic residue (glutamine), and a residue with a short side chain located at the putative cleavage site (serine). Comparison with AChR γ sequences from other species (see below) supports the interpretation that the arginine assigned as amino acid no. 1 in Figure 2 is indeed the first amino acid residue of the mature γ subunit of the mouse AChR and that the oligopeptide preceding it is the signal peptide. This signal peptide is presumably involved in the translocation of the newly synthesized protein across the rough endoplasmic reticulum membrane. Based on the above assignment, the molecular weights of the precursor and the mature γ subunit were calculated to be 58,752 and 56,493, respectively.

The mouse AChR γ subunit has structural features common to all the AChR subunits from mouse and other species (2,11,29). It has four highly hydrophobic segments characteristic of transmembrane domains. They are designated M1-M4, and their amino acid positions are M1, 219-245; M2, 252-270; M3, 286-307; and M4, 455-473 (Figure 2).

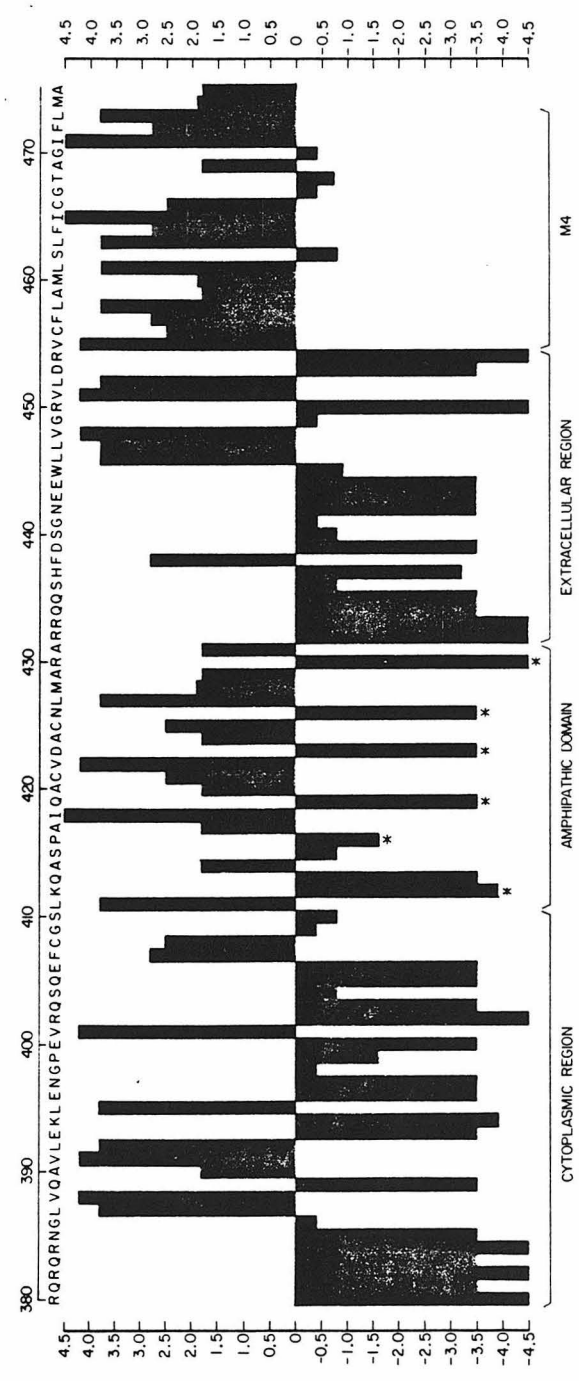

Figure 3. Analysis of the hydropathic properties of the mouse AChR γ subunit. Amino acid residues are plotted against their hydropathy index values. Positive values indicate hydrophobicity and negative values hydrophilicity. The amino acid sequence is displayed on top of the histogram and is numbered according to Figure 2. The stars mark the hydrophilic amino acid residues in the putative amphipathic membrane-spanning domain that align the inside of the ion channel.

The possible existence of a fifth membrane-spanning region, the amphipathic α-helix domain (30,31), was examined. As shown in Fig. 3, the region between amino acid residues no. 380 and no. 475 was analysed by plotting the amino acid residue numbers against their hydropathy index values (32). Positive values indicate hydrophobicity and negative ones hydrophilicity. The region between residues no. 411 and no. 431 shows a remarkable regularity of highly hydrophilic residues at the average distance of 3.5 amino acid residues while the rest of this region is largely hydrophobic, a salient feature of a membrane-spanning amphipathic α-helix. The cytoplasmic and extracellular regions on both sides of the amphipathic domain are overall hydrophilic and the membrane-spanning region M4 is highly hydrophobic (Figure 3). The hydrophilic amino acid groups in the amphipathic domain are at positions 412, 416, 419, 423, 426, and 430 with an average hydropathy index value of -3.42. The rest of this region has an average hydropathy index value of 1.81, characteristic of a hydrophobic transmembrane region. Therefore, it seems probable that this region forms an amphipathic transmembrane segment with the hydrophilic side of the α-helix contributing to the charged lining proposed for the AChR ion channel (30,31).

Many proteins, including membrane proteins, enzymes, secretory proteins without enzymatic functions, and immunoglobulins, undergo post-translational modifications to become glycoproteins by the enzymatic addition of carbohydrate chains to L-asparagine residues in the polypeptide chain (33). Analysis of many such modified proteins has revealed a consensus sequence asparagine-X-serine (threonine) where X can be any amino acid residue with the possible exception of aspartic acid (33,34). This consensus sequence is a necessary, but not a sufficient, condition for carbohydrate chain addition. There are four such potential N-glycosylation sites in the mouse AChR γ sequence (Figure 2), at positions 30, 141, 306, and 354. If the γ subunit has membrane domains as proposed, only Asn_{30} and Asn_{141} will be exposed from the membrane and thus accessible for carbohydrate attachment (35). In this interpretation, Asn_{306} is in the membrane-spanning region M3 and Asn_{354} is on the cytoplasmic side of the membrane.

Sequence Comparison of AChR γ Subunit from Different Species

cDNA and genomic clones coding for the γ subunit of the nicotinic AChR have been isolated from a number of species. To study the relatedness of the AChR γ subunit, the deduced amino acid sequence of the mouse AChR γ subunit was compared with those of human (36), calf (37), chicken (38), and *Torpedo* (4,8). As shown in Figure 4, the mouse sequence exhibits high degrees of homology with those of human and calf and somewhat lower degrees of homology with those of chicken and electric ray, indicating the close evolutionary relationship among mammals.

We have also searched for regions where, in spite of amino acid sequence

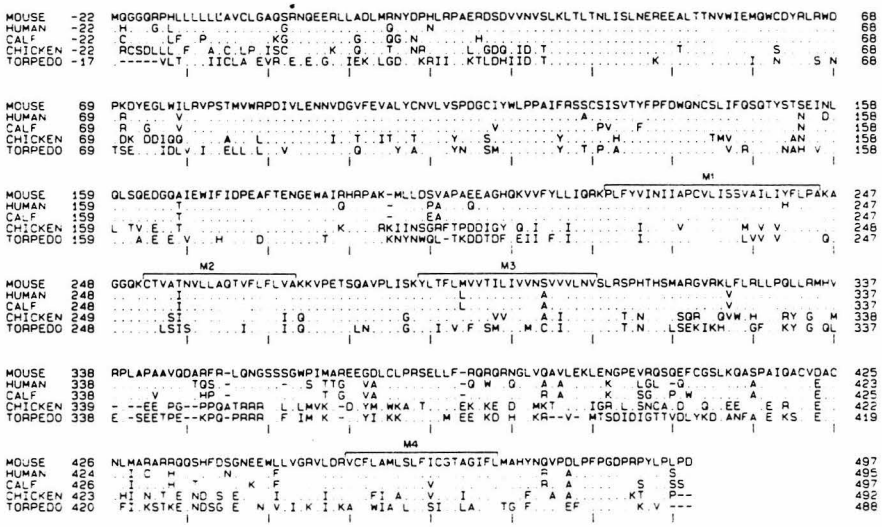

Figure 4. Comparison of the amino acid sequences for the nicotinic AChR γ subunit precursors of mouse, human, calf, chicken and electric ray *Torpedo californica*. The protein sequences are aligned with respect to the first amino acid residues in the mature proteins (marked by a *), and the amino acid residues in the signal peptides are given negative numbers. A dot indicates identity with the mouse sequence at that position. Gaps inserted to allow maximal homology are represented as dashes. The hydrophobic membrane-spanning regions are marked M1-M4.

divergence, functional features are conserved. For this purpose, amino acid substitutions by their functional equivalents were scored as homologous in the analysis. These functionally equivalent groups are: acidic, D and E; basic, H, K, and R; non-polar, A, F, I, L, M, P, Q, V, and W; and polar, C, G, N, S, T, and Y. Homology by these criteria may identify regions of conserved structure, presumably important for the assembly and function of the AChR. It is of course a mathematical necessity that the homology value between two sequences will be enhanced after the functional substitution. Nevertheless, the degree of sequence homology between the evolutionarily more distant sequences from this comparison is quite striking. As shown in Table 1, the 67% overall homology between the actual sequences of mouse and chicken AChR γ subunits is increased to 83% and the 56% between mouse and *Torpedo* to 77% after the functional group substitution. A still more striking conservation was revealed when the membrane-spanning regions were analyzed. The homology values between the actual sequences are significantly higher for the transmembrane regions than those for the entire γ subunits and, with allowance for functional substitution, these membrane segments all showed over 90% homology with each other. Both the divergence and the conservation of transmembrane regions have been reported before

TABLE 1
Amino acid sequence homology of AChR γ subunit
between mouse and human, calf, chicken, and *Torpedo*

		Human	Calf	Chicken	*Torpedo*
Homology over entire precursor	Actual sequence	90%	90%	67%	56%
	After functional substitution	93%	95%	83%	77%
Homology for M1-M4*	Actual sequence	95%	95%	80%	68%
	After functional substitution	97%	98%	97%	92%

* The sum of M1, M2, M3, and M4 as aligned in Figure 4.

(39,40). When the protein sequences were compared for class I and class II antigens of the major histocompatibility complex, it was found that the transmembrane regions are more divergent than the rest of the proteins for class I antigens (39) while they are more homologous for class II antigens (40). Since class I antigens are monomeric protein molecules and class II antigens are dimers, it may be considered that the high degree of homology for the class II antigen transmembrane domain is necessary for the interaction between the heavy and light chains to form a functional class II molecule and that there is no such evolutionary pressure for class I antigens. Our result also supprts this line of thinking and suggests that these putative membrane-spanning regions have been correctly identified and play an important role in the assembly and function of the AChR. The conservation of the membrane-spanning regions in AChR α subunits across species has been noticed before (15).

A novel γ-like subunit of AChR, the ε subunit, has been identified from a cDNA sequence from calf muscle (41). When it was compared with the mouse γ subunit, a homology of 53% was obtained. Clearly the mouse γ subunit is more homologous to the calf muscle γ subunit (90% homology).

The mouse AChR γ subunit contains two cysteine residues at positions 128 and 142 that are also conserved in the γ subunit from other species (Figure 4) as well as in all the other known subunits (11). These cysteine residues may be involved in the formation of a disulfide bridge (4).

Previously, our laboratory reported the isolation of a mouse cDNA clone by the hybridization to a *Torpedo* γ subunit cDNA probe. Sequence analysis showed that the protein coded by this clone exhibits a slightly higher degree of homology with the *Torpedo* δ subunit than with γ and thus it was tentatively assigned as a mouse AChR δ

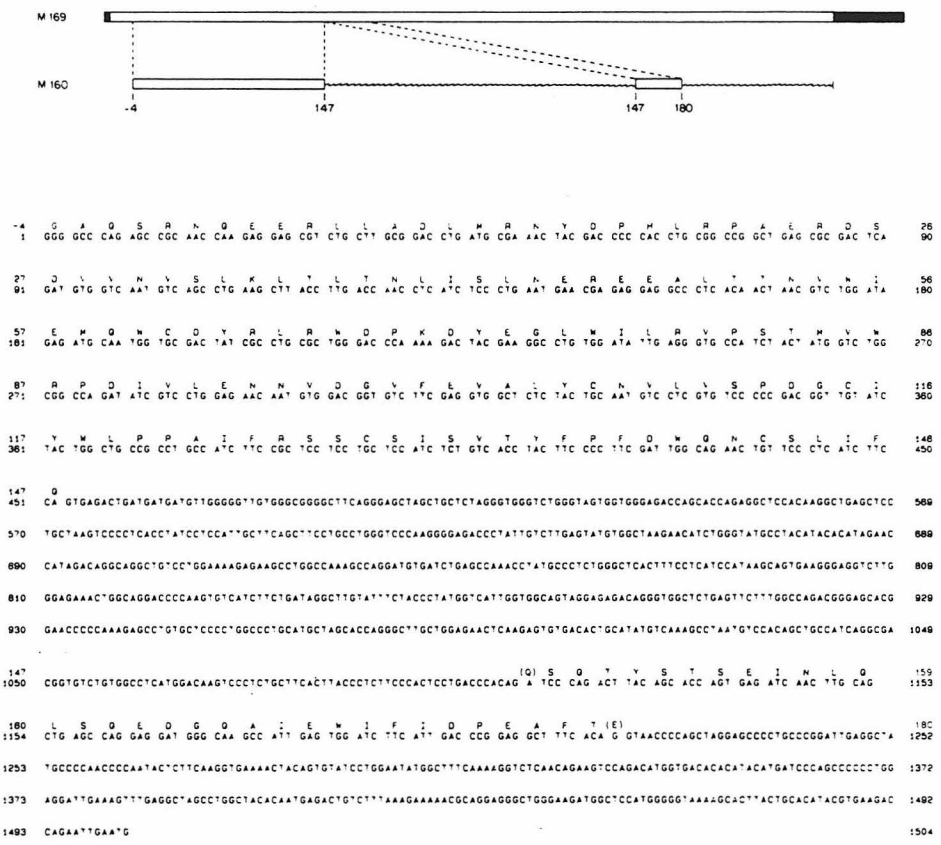

Figure 5. Mouse AChR γ subunit intervening sequences. Clone M160 is aligned with respect to the mature message clone M169 in the top panel. The open boxes represent protein coding regions, and the closed boxes in M169 indicate the 5' and 3' untranslated regions. The wavy lines in M160 represent intron sequences. The numbers at the coding region boundaries below M160 denote the amino acid positions as defined in Figure 2. DNA sequence of M160 and the translation of exons are shown in the bottom panel. Nucleotide no. 1 corresponds to nucleotide no. 55 of the M169 sequence in Figure 2. Amino acid sequences of the protein coding sections are displayed above the DNA sequence and are numbered according to Figure 2.

subunit cDNA (14). Subsequent functional analysis indicated that the RNA made from this clone could replace the RNA of the *Torpedo* δ subunit to produce a highly functional AChR hybrid protein and that it could not substitute for the *Torpedo* γ subunit RNA (16). The isolation of the mouse AChR γ subunit cDNA has further confirmed our previous identification of the mouse AChR δ subunit cDNA clone. When the mouse γ and δ subunits were compared, they showed overall homologies of 58% at the DNA sequence level and 50% at the protein sequence level (data not shown).

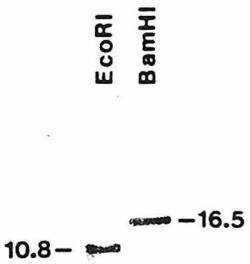

Figure 6. Genomic DNA blot analysis. 10μg of BC3H-1 DNA was digested either with *Eco*RI or *Bam*HI, size fractionated by agarose gel electrophoresis, blotted, and hybridized with nick-translated full-length M169 DNA. The sizes of the hybridizing bands are given in kilobases.

Partially Processed RNA Molecules

There are two clones that were selected from the original cDNA library by screening with the *Torpedo* γ probe that showed homology with clone M169 over some portion but not over others. One of these clones, M160, was analyzed by sequence determination. The arguments presented below lead to the conclusions that the sections in M160 nonhomologous to M169 are intron sequences and that we have isolated a clone derived from a partially processed nuclear RNA. The published genomic sequences for the AChR γ gene of human (36) and chicken (38) both have introns disrupting a codon for glutamine at position 147 and disrupting a codon for glutamic acid at position 180. When the sequences of M160 and M169 were compared, it became obvious that M160 codes for part of the AChR γ subunit with the codons for Gln_{147} and Glu_{180} interrupted by two non-coding sequences (Figure 5A). These sequences have nonsense codons in all three reading frames and are flanked by dinucleotides GT on the 5' side and AG on the 3' side (Figure 5B), the two major characteristics of intervening sequences (42,43). Therefore, we conclude that these two non-coding sequences are indeed intron sequences. The human and chicken AChR γ genes have a total of 11 introns interrupting their coding regions at identical positions. Because the two introns in M160 are present at the same positions as in the human and chicken genes, it is reasonable to believe that the same overall exon-intron structure exists for the mouse

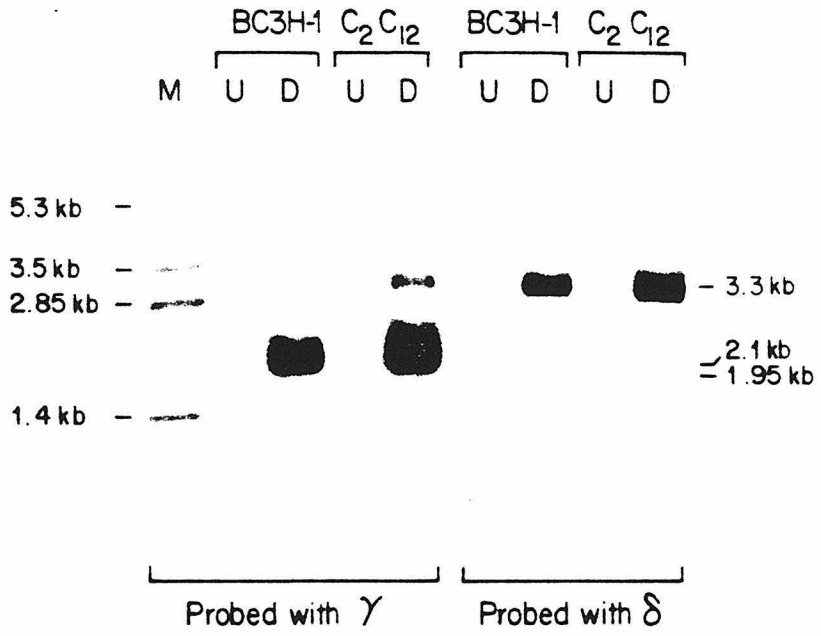

Figure 7. RNA blot hybridization. 10μg of total cellular RNA from appropriate cells were fractionated in each lane, blotted, and hybridized with ^{32}P-RNA probes. U, undifferentiated cells; D, differentiated cells. M, RNA markers made by *in vitro* SP6 transcription of mouse γ cDNA clone. Kb, kilobases.

gene. However, the protein coding region in M160 between codon -4 and codon 147 is continuous, lacking the three introns that are present in both human and chicken genes (Figure 5). Therefore, we propose that clone M160 was derived from a partially processed nuclear RNA molecule coding for the mouse AChR γ subunit. Intron-containing cDNA clones have been reported before for the calf AChR γ subunit (37).

The Gene Coding for the AChR γ Subunit

The AChR γ subunit is encoded by a unique gene in the chicken genome (38) and perhaps also a single gene in the human genome (36). For calf and *Torpedo* γ subunit, there is no available information regarding the gene number. To estimate the number of gene(s) coding for the mouse AChR γ subunit, genomic DNA blot analysis was performed using the full-length M169 DNA as the hybridization probe. As shown in Figure 6, *Eco*RI and *Bam*HI digested DNA each gives a single hybridizing fragment. This simple pattern of hybridization suggests that the mouse SChR γ subunit is probably encoded by a single gene.

γ Gene Expression in Murine Myogenic Cell Lines

The activity of the majority of eukaryotic genes is regulated both temporally and

spatially, making possible the various types of cells and tissues necessary for a multicellular organism. One of the characteristics of mammalian skeletal muscle is the high abundance of AChR molecules on the cell surface. Using the mouse γ subunit cDNA clones, we studied the γ gene expression pattern in two mouse myogenic cell lines, BC3H-1 (12) and C_2C_{12} (41). These cells grow and proliferate in rich medium under tissue culture condition. When proliferation is restricted by confluence and/or exposure to a less rich medium, the cells stop dividing and undergo differentiation, producing large amounts of muscle-specific proteins in the process (44,45). To study the AChR γ gene expression during differentiation, total cellular RNA samples were isolated from undifferentiated and differentiated cells, fractionated by gel electrophoresis, transferred to nylon membranes, and hybridized with radioactively labeled RNA probes (see Materials and Methods). As shown in Figure 7, the γ subunit probe hybridizes strongly to a 2 kb band. On a briefly exposed autoradiograph (not shown here), this band can be resolved into two RNA species with estimated molecular lengths of 1.95kb and 2.1kb, respectively. These RNA species are present at low levels in undifferentiated cells and become relatively abundant when the cells differentiate.

There is a 3.3kb RNA species that hybridizes to the γ probe (Figure 7). This appears to be due to crosshybridization between the γ probe and the message for the AChR δ subunit, as indicated by the strong hybridization at the same position to the mouse δ probe (14) in Figure 7. The δ probe also cross-hybridizes weakly with the two γ messages.

The absolute abundance of the γ messages in total cellular RNA was estimated by comparison of the signal intensity on RNA blots between the band of a 1.4kb RNA standard and the γ mRNA bands (Figure 7). The standard was generated by *BglI* restriction digestion of the γ cDNA sequence M169 subcloned into the expression vector pIBI76 and subsequent *in vitro* transcription with SP6 RNA polymerase (see Materials and Methods). The radioactive precursor [^{32}P-α]CTP was used as a tracer (1:3.5x10^4 dilution with non-radioactive CTP). The purity of the transcription product was ascertained by running an aliquot of the RNA in a gel and exposing the gel to an X-ray film. The *in vitro* transcription efficiency was calculated and the RNA concentration derived. 10pg of this *in vitro*-generated γ subunit RNA were mixed with other RNA size markers, subjected to gel electrophoresis side-by-side with 10μg of total cellular RNA samples from undifferentiated and differentiated cells, blotted to nylon membranes, and hybridized to the antisense γ probe (Figure 7). Thus, the 1.4kb RNA serves not only as an RNA size marker, but also as a mass standard for the AChR γ messages. The intensities of the RNA bands were measured by densitometry tracing, the area under each peak integrated by a graphic digitizer, and the values normalized to the standard. The results are shown in Table 2. The mRNA abundance for the AChR γ

TABLE 2
Quantitation of the mouse AChR γ mRNA

Source of RNA	SP6 RNA	BC3H-1 cells		C_2C_{12} cells	
		Undifferen-tiated	Differen-tiated	Undifferen-tiated	Differen-tiated
Quantity of RNA	10pg	10μg	10μg	10μg	10μg
Signal intensity (normalized to SP6 RNA)	100%	49%	1380%	72%	3570%
Message ratio		1 : 28		1 : 50	
Message abundance (pg/μg cellular RNA)		0.49	13.8	0.72	35.7

subunit is very low before differentiation and is dramatically increased when the cells are differentiated, reaching 13.8pg per μg total cellular RNA in BC3H-1 and 35.7pg in C_2C_{12} cells. The induction ratio is approximately 28-fold for BC3H-1 and 50-fold for C_2C_{12}. This up-regulation of AChR γ messages upon differentiation correlates well with the observation that the large amounts of AChR molecules appearing on the muscle surface during differentiation were synthesized *de novo* rather than being stored in the cytoplasm before differentiation (45-47) and suggests that the control of expression is mainly at the transcriptional level.

ACKNOWLEDGEMENTS

We are grateful to Ms. Marie Krempin for operation of the cell culture facility, to Dr. Terry Snutch for providing the RNA purification procedure, to Tim Hunkapiller for the usage of computer sequence analysis system (48), and to Dr. Jean-Paul Revel for the usage of graphic digitizer. The *Torpedo* γ probe was kindly provided by the authors of reference 8.

While this manuscript was in the final stages of preparation, we received a copy of a preprint from Dr. J. Boulter and coworkers in the laboratory of Drs. S. Heinemann and J. Patrick at the Salk Institute describing their independent isolation and sequence determination of a γ subunit cDNA clone derived from BC3H-1 cells. There are only a few minor disagreements between the two sequences. We are grateful to these authors for sharing their results prior to publication.

This work was supported by research grants to N. D. from the National Institutes of Health and the Muscular Dystrophy Association, by a California Foundation for Biochemical Research Fellowship to L. Y., and by a National Institutes of Health Fellowship to R. L. P.

*Present address: Johnson & Johnson Biotechnology Center, PO Box 8289, La Jolla, CA 92038, USA

REFERENCES

1. Karlin, A. (1980) Cell Surf. Rev. 6, 191-260.
2. Conti-Tronconi, B. M. and Raftery, M. A. (1982) Ann. Rev. Biochem. 51, 491-530.
3. Popot, J.-L. and Changeux, J.-P. (1984) Physiol. Rev. 64,1162-1239.
4. Noda, M., Takahashi, H., Tanabe, T., Toyosato, M., Furutani, Y., Hirose, T., Asai, M., Inayama, S., Miyata, T. and Numa, S. (1982) Nature 299, 793-797.
5. Sumikawa, K., Houghton, M., Smith, J. C., Bell, L., Richards, B. M. and Barnard,
6. Noda, M., Takahashi, H., Tanabe, T., Toyosato, M., Kikyotani, S., Hirose, T., Asai, M., Takashima, H., Inayama, S., Miyata, T. and Numa, S. (1983) Nature 301, 251-255.
7. Noda, M., Takahashi, H., Tanabe, T., Toyosato, M., Kikyotani, S., Furutani, Y., Hirose, T., Takashima, H., Inayama, S., Miyata, T. and Numa, S. (1983) Nature 302, 528-532.
8. Claudio, T., Ballivet, M., Patrick, J. and Heinemann, S. (1983) Proc. Natl. Acad. Sci. USA 80, 1111-1115.
9. Devillers-Thiery, A., Giraudat, J., Bentaboulet, M. and Changeux, J.-P. (1983) Proc. Natl. Acad. Sci. USA 80, 2067-2071.
10. Merlie, J. P. (1984) Cell 36, 573-575.
11. Stroud, R. M. and Finer-Moore, J. (1985) Ann. Rev. Cell Biol. 1, 369-403.
12. Schubert, D., Harris, A. J., Devine, C. E. and Heinemann, S. (1974) J. Cell Biol. 61, 398-413.
13. Merlie, J. P., Sebbane, R., Gardner, S. and Linstrom, J. (1983) Proc. Natl. Acad. Sci. USA 80, 3845-3849.
14. LaPolla, R. J., Mayne, K. M. and Davidson, N. (1984) Proc. Natl. Acad. Sci. USA 81, 7970-7974.
15. Boulter, J., Luyten, W., Evans, K., Mason, P., Ballivet, M., Goldman, D., Stengelin, S., Martin, G., Heinemann, S. and Patrick, J. (1985) J. Neurosci. 5, 2545-2552.
16. White, M. M., Mayne, K. M., Lester, H. A. and Davidson, N. (1985) Proc. Natl. Acad. Sci. USA 82, 4852-4856.
17. Yanisch-Perron, C., Vieira, J. and Messing, J. (1985) Gene 33, 103-119.
18. Messing, J. (1983) Methods in Enz. 101, 20-78.
19. Henikoff, S. (1984) Gene 28, 351-359.
20. Hanahan, D. (1983) J. Mol. Biol. 166, 557-580.
21. Sanger, F., Nicklen, S. and Coulson, A. R. (1977) Proc. Natl. Acad. Sci. USA 74, 5463-5467.
22. Hu, M. C.-T., Sharp, S. B. and Davidson, N. (1986) Mol. Cell. Biol. 6, 15-25.
23. McMaster, G. K. and Carmichael, G. C. (1977) Proc. Natl. Acad. Sci. USA 74, 4835-4838.
24. Proudfoot, N. J. and Brownlee, G. G. (1976) Nature 263, 433-438.
25. Birnstiel, M. L., Busslinger, M. and Strub, K. (1985) Cell 41, 349-359.
26. Davis, B. D. and Tai, P.-C. (1980) Nature 283, 433-438.
27. Kreil, G. (1981) Ann. Rev. Biochem. 50, 317-348.
28. Sabatini, D. D., Kreibich, G., Morimoto, T. and Adesnik, M. (1982) J. Cell Biol. 92, 1-22.
29. Stevens, C. F. (1985) Trends Neurosci. 8, 1-2.
30. Finer-Moore, J. and Stroud, R. M. (1984) Proc. Natl. Acad. Sci. USA 81, 155-159.
31. Guy, H. R. (1984) Biophys. J. 45, 249-261.
32. Kyte, J. and Doolittle, R. F. (1982) J. Mol. Biol. 157, 105-132.
33. Struck, D. K. and Lennarz, W. J. (1980) in The Biochemistry of Glycoproteins and Proteoglycans, Lennarz, W. J. Ed., pp. 35-83, Plenum, New York.
34. Marshall, R. D. (1974) Biochem. Soc. Symp. 40, 17-26.
35. Hubbard, S. C. and Ivatt, R. J. (1981) Ann. Rev. Biochem. 50, 555-583.
36. Shibahara, S., Kubo, T., Perski, H. J., Takahashi, H., Noda, M. and Numa, S. (1985)

Eur. J. Biochem. 146, 15-22.
37. Takai, T., Noda, M., Furutani, Y., Takahashi, H., Notake, M., Shimizu, S., Kayano, T., Tanabe, T., Tanaka, K., Hirose, T., Inayama, S. and Numa, S. (1984) Eur. J. Biochem. 143, 109-115.
38. Nef, P., Mauron, A., Stalder, R., Alliod, C. and Ballivet, M. (1984) Proc. Natl. Acad. Sci. USA 81, 7975-7979.
39. Fisher, D. A., Hunt, S. W. and Hood, L. (1985) J. Exp. Med. 162, 528-545.
40. Kaufman, J. F., Auffray, C., Korman, A. J., Shackelford, D. A. and Strominger, J. (1984) Cell 36, 1-13.
41. Takai, T., Noda, M. Mishina, M., Shimizu, S., Furutani, Y., Kayano, T., Ikeda, T., Kubo, T., Takahashi, H., Takahashi, T., Kuno, M. and Numa, S. (1985) Nature 315, 761-764.
42. Breathnach, R. and Chambon, P. (1981) Ann. Rev. Biochem. 50, 349-383.
43. Mount, S. M. (1982) Nucleic Acids Res. 10, 459-472.
44. Chiu, C. P. and Blau, H. M. (1984) Cell 37, 879-887.
45. Patrick, J., McMillan, J., Wolfson, H. and O'Brien, J. C. (1977) J. Biol. Chem. 252, 2143-2153.
46. Merlie, J. P., Sobel, A., Changeux, J.-P. and Gros, F. (1975) Proc. Natl. Acad. Sci. USA 72, 4028-4032.
47. Fambrough, D. M. (1979) Physiol. Rev. 59, 165-227.
48. Hunkapiller, M., Kent, S., Caruthers, M., Dreyer, W., Firca, J., Giffin, C., Horvath, S., Hunkapiller, T., Tempst, P. and Hood, L. (1984) Nature 310, 105-115.

CHAPTER 3

Expression of mouse-*Torpedo* acetylcholine receptor subunit chimeras and hybrids in *Xenopus* oocytes

Katharine Mixter Mayne, Kiyonori Yoshii, Lei Yu,
Henry A. Lester, and Norman Davidson

Molecular Brain Research

in press

SUMMARY

In this study, *in vitro* synthesized mRNA encoding mouse and *Torpedo* nicotinic acetylcholine receptor subunits was injected into *Xenopus* oocytes, followed by assays for assembly onto the oocyte surface (using α-bungarotoxin binding) and for acetylcholine-induced conductances (using voltage clamp). We constructed *hybrid* acetylcholine receptors in *Xenopus* oocytes by injecting all eight possible combinations of four subunit-specific mRNAs in which a single subunit is derived from the other species. For each hybrid combination, there are detectable assembly and conductance. We also constructed cDNA clones that encode chimeric acetylcholine receptor subunits in which part of the γ subunit from *Torpedo* was replaced by the homologous region of the δ subunit from mouse. None of the chimeric subunits was able to replace the *Torpedo* γ, mouse δ, or *Torpedo* δ subunit with regard to assembly or function. We therefore conclude that widely spaced (and unknown) parts of the protein chain are required for the intersubunit interactions that eventually lead to functional assembly of the receptor.

INTRODUCTION

The nicotinic acetylcholine receptor (AChR) is a protein complex composed of four homologous transmembrane subunits in the stoichiometry $\alpha_2\beta\gamma\delta$. AChRs are very abundant in the electric organs of *Torpedo* where they have been characterized at the structural, biochemical, and sequence levels (reviewed in 4,7,18,23). Considerable sequence homology is demonstrated by the cDNA clones for many AChR subunits isolated recently for *Torpedo*, calf, human, mouse and chick (reviewed in 23).

Xenopus oocytes are an efficient system for expressing AChRs from the *Torpedo* electric organ RNA (1,24). RNAs, transcribed *in vitro* from subunit specific cDNA clones by the phage SP6 transcription system, are mixed and injected into the oocyte cytoplasm where they are translated (13,25). The polypeptide products are processed and inserted into the oocyte membrane where they can be assayed electrophysiologically. Voltage-clamp studies show that the surface receptors resulting from injection of all four *Torpedo* mRNAs are AChRs by the criteria of ACh responsiveness with a Hill coefficient of 2.0, atropine insensitivity, and *d*-tubocurarine sensitivity (12,25).

Previous studies have shown that injection of transcripts for all four *Torpedo* subunits are needed for effective expression of functional receptors (12,13,25). For the combination $\alpha_T\beta_T\gamma_T$ without δ_T, the agonist-induced conductance is about 3% of that observed with all four; all other combinations of only three subunits gave no detectable conductance. When a mouse cDNA for one subunit was cloned and sequenced in our laboratory (8) the translated amino acid sequence was found to have *ca.* 60% amino acid homology with δ_T and 48% homology with γ_T. This result obviously suggested but did not prove the subunit identity of the mouse clone. The definitive demonstration that it was in fact a

mouse δ subunit was the observation that injection into oocytes of its RNA transcript in a mixture with α_T, β_T and γ_T gave a high yield of functional receptors whereas injection of a mixture with α_T, β_T and δ_T gave a very small signal (25).

We were thus confronted with the problem that, in spite of only 60% amino acid sequence homology, there was excellent functional homology of δ_M with δ_T; and in spite of 48% amino acid sequence homology with γ_T, there was no functional homology. In the present study, we have asked whether it is possible to identify a particular segment of the γ and δ sequences that define their functional subunit character, or whether this property is distributed over the entire chain. We have accordingly made several *chimeric* or fusion genes between the δ and γ subunits. For example, a $\delta_M\gamma_T$ construct contains an amino terminal segment of the δ_M chain attached, at a homologous point, to the carboxy terminal fragment of the γ_T chain. The reciprocal chimera $\gamma_T\delta_M$ would have the amino terminus of the γ chain fused to the carboxy terminal segment of the δ chain with the same crossover point. By varying the position of the crossover point, chimeric chains were prepared with more or less of the amino terminal segment of one subunit and less or more, respectively, of carboxy terminal segment of the other subunit.

In the course of this work, we have also studied the rules for the formation of functional *hybrid* receptor complexes, that is, complexes containing three subunits from one species (*Torpedo* or mouse) with the other from another species (mouse, *Torpedo*, or chicken).

MATERIALS AND METHODS

Plasmids

The mouse cell line BC3H-1 γ subunit was isolated in this laboratory (27) and transferred into pSP65 (11). The chick muscle α cDNA clone (2) was provided by Drs. J. Jackson and E. Barnard of Imperial College and MRC Molecular Neurobiology Unit and was subcloned into pSP64 (11). The mouse α and β subunits from BC3H-1 cells were provided by J. P. Merlie of Washington University, St. Louis and recloned into pGEM1 and pGEM2, respectively (Promega Biotec).

Construction of cDNA chimera plasmids

The chimeras that have been made are shown in Fig. 1. The general principles of the construction procedures are explained in the first section of Results. In each case, two or more partially complementary synthetic oligonucleotides with appropriate protruding ends were used to ligate the 5' segment of one cDNA that had been cut at a suitable restriction site to the 3' segment of the other cDNA, also cut at a suitable enzyme site.

The phosphorylated oligonucleotide pairs were heated to 50°C in 100 mM NaCl and allowed to cool to 40°C over 1 h. Other components and the two restricted cDNAs were added to give a final reaction containing 50 mM Tris (pH 7.6), 50 mM NaCl, 10 mM $MgCl_2$, 10 mM dithiothreitol, 1 mM spermidine, and 1 mM ATP in a total of 20 μl. The mixture was held at 40°C for 5 min before chilling to 15°C. 400 units of T4 DNA ligase (Boehringer Mannheim) were added and the reaction was incubated at 15°C overnight. Each ligation contained approximately 1 μg of vector DNA, 0.5-0.2 μg of each cDNA fragment, and 10 ng of each oligonucleotide, each of which was previously gel-isolated. The ligations were extracted with phenol and passed through a 1 ml spun column of Sephadex G-

50 (9,17). An aliquot was used to transform HB101 competent cells (Bethesda Research Laboratories). Ampicillin-resistant transformants were replica-plated and screened with three ^{32}P-labeled probes: each nick-translated cDNA fragment and one of the oligonucleotides. The structure of the selected clones was confirmed by DNA sequencing (10).

The oligonucleotides (5' to 3') and restriction sites they spanned for each ligation are given below. In the ligation leading to chimera δ_M-γ_T-1 (see Fig. 1), oligonucleotides KM3, 5'gatcAACCTAGTCTTCTACCTGCCAGGCGACTGTGGG3', and its partial complement KM4, 3'TTGGATCAGAAGATGGACGGTCCGCTGACACCCccg5' (lower-case letters indicate protruding single strand ends, upper-case letters indicate complementary parts of the oligonucleotides) span the gap between the BclI site in δ_M and the Sau96I site in δ_T. In γ_T-δ_M-2 the space between the Sau96I site in γ_T and the NaeI site in δ_M is spanned by four oligonucleotides: KM5, 5'ggcGAGAAGACCTCCGTGGCCATCTCAGTGCTCCTGGCCC3'; KM6 5'AATCTGTCTTCCTGCTGCTTATCTCCAAGAGGCTGCC3'; KM7 3'CTCTTCTGGAGGCACCGGTAGAGTCACGAG5' and KM8, 3'GACCGGGTTAGACAGAAGGACGACGAATAGAGGTTCTCCGACGG5'. Oligonucleotides KM9, 5'cgCCTCACCACAGCCCGCAGGCCTCCAGCAAGCG3', and KM10, 3'GGAGTGGTGTCGGGCGTCCGGAGGTCGTTCGCagct5', span the gap between the Nar I site of δ_M and the SalI site of γ_T in chimera δ_M-γ_T3. The α_T-δ_T chimera was formed by a direct ligation event fusing the α_T Bst NI site to the δ_T cutting site for FokI. This results in a net six amino acid deletion in the subunit encoded by this clone. The oligonucleotides intended to span this gap were not correctly ligated in any transformants from multiple attempts.

In vitro transcription

Plasmid DNAs were linearized by restriction endonuclease digestion at sites within the plasmid vectors. In order to prevent artifactual transcripts arising from initiation at the 3' protruding ends produced by AatII and PvuI, the protruding ends of the template DNA were removed by treatment with the Klenow fragment of DNA polymerase I (22). Templates were purified and transcribed essentially as described in White *et al.* (25), except that the SP6 polymerase was present at a concentration of 300 units/ml. These transcripts were capped at the 5' end by including diguanosine triphosphate, a cap analogue, in the transcription reaction, as described by White *et al.* (25). The reaction was incubated at 37°C for 2 h, followed by a 10 min incubation with 2 units/ml RNase-free DNase. Unincorporated nucleotides were then removed by spun column (17).

Preparation of oocytes, RNA injection, and electrophysiology

To obtain oocytes free from adhering cell layers, excised ovarian tissue was incubated in ND-96 solution containing collagenase (type 1A, Sigma) at 2 mg/ml for 3 h at room temperature.

RNA was dissolved in distilled water at 1 mg/ml, and 50 nl was injected into the cytoplasm. The oocytes were incubated in ND-96 solution (96 mM NaCl, 2 mM KCl, 1.8 mM $CaCl_2$, 1 mM $MgCl_2$, 5 mM HEPES/NaOH, pH 7.6) supplemented with 100 units of penicillin and 100 µg of streptomycin per ml, 0.5 mM theophylline, 2.5 mM pyruvic acid, and incubated at room temperature for 48-72 h. Surface binding of α-bungarotoxin (α-BTX) was measured in 5 nM [^{125}I]-α-BTX in ND-96 solution with 1 mg/ml bovine serum albumin and 0.1 mg/ml cytochrome C for 1 h at room temperature.

Voltage-clamp experiments were performed as described by White *et al.* (1985). Agonist-induced currents were measured at a membrane potential of -60 mV. Agonist-induced conductances were calculated from these currents and from the reversal potentials, which ranged from 0 to -10 mV.

RESULTS

Construction of chimeras

In the ligation reactions used to generate each of the chimeras, a double-stranded oligonucleotide "adaptor" was used to ligate the 5' end of one cDNA restriction fragment onto the 3' end of another restriction fragmentation from a different subunit. The oligonucleotide portions were each designed to bring the two halves of the protein sequence together in-frame, as well as to encode 6-25 amino acids. The specific overhanging ends of the oligonucleotides were complementary to the protruding ends left by the restriction enzymes used to generate the cDNA fragments. The protruding ends of the vector, cDNA, and oligonucleotide components specify one theoretically possible ligation event in each ligation reaction, as discussed in Methods. This recombinant cDNA was then ligated into the vector in proper orientation with respect to the SP6 promotor.

The alignment and numbering of the amino acid sequences of the AChR subunits follow that of Stroud and Finer-Moore (23). Chimeric cDNAs were constructed that encode intersubunit fusion proteins as shown schematically in Fig. 1. In Fig. 1 the membrane spanning helices (M1, M2, M3, MA, and M4) as proposed by Guy (6) and Finer-Moore and Stroud (5) are included as landmarks for the locations of the breakpoints (transition points in the amino acid sequence) in the amino acid sequence. The alignment of the whole subunits is retained across these transitions so that no putative functional regions are deleted.

Fig. 1. Schematic representation of chimeric subunit constructions. The amino acid sequences extend from the amino terminus on the left to the carboxy terminus on the right. The breakpoint for each chimera is indicated by the slanted vertical pair of lines. – – – – , δ_M sequences;···—···— , γ_T sequences; —·—·—·, α_T; ·····, δ_T.

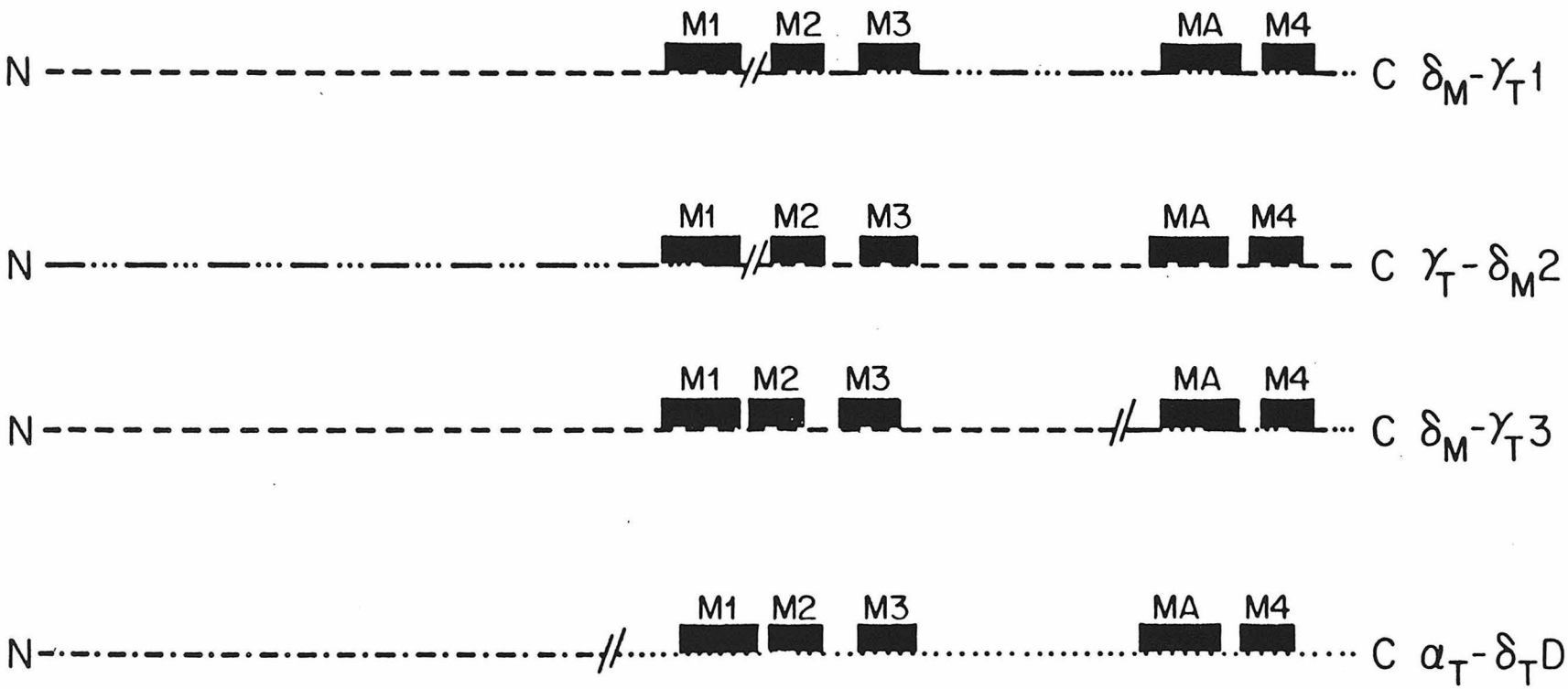
M1
M2
M3
MA
M4
N
C
δ_M-γ_T1
γ_T-δ_M2
δ_M-γ_T3
α_T-δ_TD

We created three chimeras between the δ_M and γ_T subunits, as well as one chimera between the α_T and δ_T subunits. δ_M-γ_T1 was constructed as the exact reciprocal of γ_T-δ_M2; each has gly-258 from γ_T as the first residue from the γ_T half of the chimera. As indicated by the name, δ_M-γ_T1 derives its N-terminal portions from δ_M and its C-terminal residues from γ_T, and γ_T-δ_M2 has the reciprocal arrangement. The breakpoints for this pair of chimeras lie between M1 and M2, which is roughly in the middle of the protein sequences. The chimera δ_M-γ_T3 consists of the N-terminal 412 amino acids from δ_M and the remaining 100 amino acids from the C-terminus of γ_T. This breakpoint falls just before the suggested MA helix (5). The breakpoint in the α_T-δ_T chimera lies on the N-terminal side of M1; in the model of Finer-Moore and Stroud (5), all the membrane spanning helices of this chimera are derived from δ_T. That is, in this construction , leucine 216 of α is joined to isoleucine 222 of δ_T. As stated in Methods, for reasons unknown, the oligonucleotide adaptors were not incorporated into α_T-δ_T, resulting in a deletion of six amino acids in the chimeric subunit encoded by this clone.

In vitro transcription and expression in Xenopus oocytes

Linearized plasmid DNAs were used as templates for *in vitro* transcription of RNA by phage SP6 polymerase. Equal amounts of the *in vitro* synthesized mRNAs were mixed together in several combinations and injected into *Xenopus* oocytes. The ACh-induced conductance displayed a sigmoidal dependence on the amount of RNA injected. The minimum readily detectable ACh response for the all *Torpedo* AChR was measured in oocytes injected with 1.5 ng of RNA, and the response approached saturation for 100 ng of injected RNA (data not shown). For the results reported here, oocytes were injected with 50 or 75 ng of RNA.

For any one mixture of RNAs, the agonist-induced conductance of an oocyte is proportional to: a) the number of complexes that are produced by translation and assembled on the surface of the oocyte, and b) the average conductance per AChR on the surface. For each mixture, we measured the number of complexes on the surface by measuring the binding of ^{125}I-α-bungarotoxin (α-BTX). From the measured agonist-induced conductance, we then calculated the conductance per unit-amount of α-BTX binding.

Chimeras

In one set of experiments, we tested the ability of the several chimeras to replace δ_T or δ_M by coinjecting the chimera RNA with RNAs for α_T, β_T and γ_T. These data (Table 1) show that the $\delta_M\gamma_T1$ construct and its reciprocal $\gamma_T\delta_M2$, as well as $\delta_M\gamma_T3$, all give a moderate level of increase of ^{125}I-α-BTX binding per oocyte compared to $\alpha_T\beta_T\delta_T$, alone (76%, 57%, and 109%, respectively, as compared to 476% for $\alpha_T\beta_T\gamma_T\delta_T$ and 338% for $\alpha_T\beta_T\gamma_T\delta_M$). However, the agonist-induced ion conductance per mole of surface binding is not significantly increased over $\alpha_T\beta_T\gamma_T$ alone. That is, the chimeric units can promote assembly of complexes on the surface to a modest extent, but these complexes function about as well as the receptors without chimeric subunits.

When the same chimeric RNAs were tested for their ability to function as γ subunits, both binding and conductance were so small that they were near the lower limit of our resolution (Table 2). In only one case, when chimera δ_M-γ_T (#1) was included in place of γ, α-BTX binding was significantly increased, but the ACh response was still low (~6 μs/fmole at 20 μM). The other δ_M-γ_T or γ_T-δ_M chimeras (2 and 3) do not substitute effectively for γ. Their presence has no effect on the α-BTX binding detected with α, β, δ_M alone, and ACh-induced conductance is actually reduced. The α_T-δ_T D chimera also has no effect on ACh-induced conductance or α-BTX binding when compared to controls.

TABLE I

Tests of chimeric subunits as replacements for δ

δ-RNA	α-BTX bound, fmol	Response at [ACh] = 1 μM μS	Response at [ACh] = 1 μM μS/fmol
T	8.29 ± 0.8 (9)	10.2 ± 0.9 (3)	1.23
M	4.86 ± 1.2 (7)	61.8 ± 17.6 (3)	12.70
none	1.44 ± 0.1 (9)	0.29 ± 0.14 (9)	0.20
1	2.53 ± 0.2 (13)	0.65 ± 0.31 (5)	0.26
2	2.25 ± 0.2 (16)	0.48 ± 0.20 (3)	0.21
3	3.01 ± 0.5 (7)	0.68 ± 0.09 (3)	0.23
D	1.29 ± 0.2 (9)	0.22 ± 0.07 (3)	0.17

In each case, the *Torpedo* α, β, and γ subunit RNAs were injected along with the indicated candidate for δ.

T = *Torpedo* δ; M = mouse δ.

Binding and conductance data are given as mean ± S. E. M. (number of oocytes).

TABLE II

Tests of chimeric subunits as replacements for γ

γ-RNA	α-BTX bound, fmol	Response at 20 μM ACh μS
none	0.07 ± 0.02 (7)	4.25, 2.38
1	0.52 ± 0.08 (9)	1.7 ± 0.7 (3)
2	0.05 ± 0.01 (8)	0.7 ± 0.3 (3)
3	0.05 ± 0.01 (9)	0.03 ± 0.03 (3)

In each case, the *Torpedo* α and β and the mouse δ subunit of RNAs were injected along with indicated candidate for γ. Binding and conductance data are given as the mean ± S. E. M. (number of oocytes). Oocytes were injected and assayed during the same experiment as for Table 1.

We tested the $\alpha_T\delta_T$ chimeras for α subunit character by coinjection with $\beta_T\gamma_T$ and δ_M. The results (data not shown) were negative.

Hybrids

The experiments reported in Table 3 address the ability of the *Torpedo* subunits to form functional AChRs in combination with mouse and chick subunits. All mouse subunits and the α_C subunit were each tested individually as replacements of the analogous *Torpedo* subunit. The simple replacement of δ_M for δ_T has been discussed previously (25). We find that each substitution gives detectable α-BTX binding and detectable ACh-induced conductance, although the level of binding varies by more than 10-fold and the response per receptor varies by nearly 1000 fold. In particular, β_M with $\alpha_T\gamma_T\delta_T$ gives very low levels of assembly and of ACh-induced conductance. The combination $\alpha_T\beta_T\gamma_M\delta_T$ gives a detectable, albeit low, level of toxin binding, but very low ACh-induced conductance.

DISCUSSION

There is a considerable degree of amino acid homology among all of the subunits of the AChR from all of the vertebrate studies (23). Generally speaking, there is a greater degree of homology among the same subunits from different species, than among subunits of any one species. For example, there is *ca.* 60% homology between δ_M and δ_T. Each of these subunits functions very well in conjunction with $\alpha_T\beta_T\gamma_T$ (25 and Table 3a,b). The same is true for the δ subunit of calf with $\alpha_T\beta_T\gamma_T$ (21).

The γ and δ subunits are more closely related to each other than either is to α and β. For example, there is *ca.* 45% homology between γ_T and δ_M, and 57% homology between γ_T and δ_T (15,16). Yet, δ_M and δ_T can substitute for each

TABLE III

Properties of mouse-chick-Torpedo *receptor hybrids*

RNAs α β γ δ	α-BTX bound, fmol	Response at [ACh] = 1 μM μS	Response at [ACh] = 1 μM μS/fmol
T T T T	3.48 ± 0.3 (11)	3.8 ± 0.1 (11)	1.09
T T T M	5.45 ± 0.64 (5)	55 ± 7 (5)	10.09
T T M T	1.36 ± 0.39 (5)	0.35 ± .6 (5)	0.26
T M T T	0.65 ± 0.33 (5)	0.03 ± 0.15 (3)	0.05
M T T T	2.53 ± 0.38 (5)	110 ± 7 (5)	43.48
M M M M	6.49 ± 0.68 (5)	95 ± 11 (5)	14.64
M M M T	0.49 ± 0.24 (5)	1.1 ± 0.2 (5)	2.24
M M T M	8.06 ± 0.15 (5)	265 ± 77 (5)	32.88
M T M M	1.01 ± 0.30 (5)	39 ± 3.8 (5)	38.61
T M M M	0.91 ± 0.33	0.62 ± .04 (5)	0.68
C T T T	n.m.	2.16 ± 0.44 (3)	
C T T M	n.m.	2.52 ± 0.20 (3)	

n.m. = not measured. Binding and conductance data are given as mean ± S.E.M. (number of oocytes)

other, but neither can substitute for a γ subunit or *vice versa*. In our initial studies with the γδ and αδ chimeras, we have attempted to determine whether the "δ" character of the subunit can be localized to any major segment of the polypeptide chain. We find that a reciprocal exchange between γ_T and δ_M more or less in the middle of each chain ($\delta_M\gamma_T1$ and $\gamma_T\delta_M2$, Fig. 2) gives polypeptides that can function neither as γ or δ. A long amino terminal segment of δ_M fused to a short carboxy terminal of γ_T in the region around amino acid 412 of δ_M ($\delta_M\gamma_T3$) is also nonfunctional. This exchange takes place just upstream of the putative MA helix of the models of Finer-Moore and Stroud (5) and of Guy (6). In the model of Ratnam *et al.* (19,20), the exchange is entirely within the final cytoplasmic region of the peptides. The final chimera we have tested, $\alpha_T\delta_T$ (Fig. 1), contains only extracellular regions of the α chain and all of the membrane spanning regions of δ in the models of Finer-Moore and Stroud (5) and of Guy (6), but does not include the upstream M_6 and M_7 membrane-spanning regions of δ proposed by the Ratnam *et al.* (19,20) models. This chimera is nonfunctional as either δ or α.

Further studies with more chimeras would probably identify some short regions of the δ chain that are not essential for its "δ" identity. Nevertheless, the straightforward interpretation of the present results is that the sequences necessary for a δ subunit to interact with the α, β, and γ subunits are distributed over most of the chain for efficient assembly into a receptor complex in the plasma membrane and to respond to agonists by gating an ion channel.

Our subunit substitution experiments (Table 3) demonstrate that many combinations of mouse and *Torpedo* subunits can form functional acetylcholine receptors in the oocyte expression assay, as long as each of the α, β, γ and δ subunits is represented. (The same is true for the chick α subunit; other chick subunits have not been tested.) The quantitative variability between the various

combinations in both the assembly and the response per assembled complex emphasizes that while there are essential common features in the conformation and packing of the same subunit from different species, there are also important differences.

Detailed dose-response studies are under way for the hybrid receptors described here (26). At low agonist concentrations, the agonist-induced conductance increases more than linearly with the ACh concentration. On double-logarithmic coordinates, the slope of the dose-response relation approaches two for all of the hybrids. This finding suggests that the hybrid receptors have been assembled so that they function normally: The open state of the receptor channel is more likely to be associated with the presence of two bound agonist molecules than with a single such molecule. These results thus generalize the findings of White *et al.* (25), who showed that the mouse δ subunit could substitute for the *Torpedo* δ; and of Sakmann *et al.* (21), who showed that the calf α and δ, and perhaps the β and γ subunits, could substitute for the analogous *Torpedo* subunit. Another subunit analogous to γ, termed ε, can also substitute for γ (14).

Most available studies also demonstrate that omission of the δ subunit gives a small fraction (<10%) of the response of the all-*Torpedo* receptor; Hill coefficients have not been reported. The results in Table 1 confirm this finding but show that, when normalized to conductance per receptor so that the probability of opening can be assessed, the receptors without a δ subunit suffer only a modest decrement: they function roughly one-fifth as well as the complete *Torpedo* receptor.

ACKNOWLEDGEMENTS

We thank Drs. T. Claudio, S. Heinemann, and D. Noonan for kindly providing *Torpedo* AChR cDNA clones; Drs. D. Mead and D. Melton for providing SP6 expression plasmids and information concerning the SP6 transcription system; Drs. J. Jackson and E. Barnard for the chick α cDNA clone; Dr. J. P. Merlie for the mouse α cDNA clone; and Drs. R. Stroud and J. Finer-Moore for helpful discussions. This work has been supported in part by research grants GM-10991 and NS-11756 from the National Institutes of Health, a research grant for the Muscular Dystrophy Association, support from the government of Japan for K.Y., Predoctoral Training Grant GM-07616 from the National Institutes of Health to K.M.M., and a California Foundation for Biochemical Research Fellowship to L.Y.

REFERENCES

1. Barnard, E. A., Miledi, R. and Sumikawa, K., Translation of exogenous messenger RNA coding for nicotinic acetylcholine receptors produces functional receptors in *Xenopus* oocytes. *Proc. R. Soc. Lond. Ser. B.* 215 (1982) 241-246.
2. Beeson, D. M. W., Barnard, E. A., Conti-Tronconi, B. M., Dunn, S. M. J., Anderton, T. L., Wilderspin, A. F., Bell, L. D. and Jackson, J. F., The chicken muscle acetylcholine receptor: subunit structure and α-subunit cloning. *J. Biol. Chem.*, in press.
3. Boulter, J., Evans, K., Goldman, D., Martin, G., Treco, D., Heinemann, S. and Patrick, J., Isolation of a cDNA clone coding for a possible neural nicotinic acetylcholine receptor α-subunit. *Nature*, 319 (1986) 368-374.
4. Conti-Tronconi, B. M. and Raftery, M. A., The nicotinic cholinergic receptor: Correlation of molecular structure with functional properties. *Ann. Rev. Biochem.* 51 (1982) 491-530.
5. Finer-Moore, J. and Stroud, R. M., Amphipathic analysis and possible formation of the ion channel in an acetylcholine receptor. *Proc. Natl. Acad. Sci. USA* 81 (1984) 155-159.
6. Guy, H. R., A structural model of the acetylcholine receptor channel based on partition energy and helix packing calculations. *Biophys. J.* 45 (1984) 249-261.
7. Karlin, A., Kao, P. N. and DiPaola, M., Molecular pharmacology of the nicotinic acetylcholine receptor. *Trends in Pharm. Sci.* 7 (1986) 304-308.
8. LaPolla, R. J., Mayne, K. M. and Davidson, N., Isolation and characterization of cDNA clone for the complete protein coding region of the δ-subunit of the mouse acetylcholine receptor. *Proc. Natl. Acad. Sci. USA* 81 (1984) 7970-7984.

9. Maniatis, T., Fritsch, E. F., and Sambrook, J., *Molecular cloning.* Cold Spring Harbor Lab., NY (1982).

10. Maxam, A. M., and Gilbert, W. Sequencing end-labeled DNA with base specific chemical cleavages. *Meth. Enzymol.* 65 (1980) 499-560.

11. Melton, D. A., Krieg, P. A., Rebagliati, M. R., Maniatis, R., Zinn, K. and Green, M. R., Efficient *in vitro* synthesis of biologically active RNA and RNA hybridization probes from plasmids containing a bacteriophage SP6 promoter. *Nucl. Acids Res.* 12 (1984) 7035-7056.

12. Mishina, M., Kurosaki, T., Tobimatsu, T., Morimoto, Y., Noda, M., Yamamoto, T., Terao, M., Lindstrom, J. Takahashi, T., Kuno, M. and Numa, S., Expression of functional acetylcholine receptor from cloned cDNAs. *Nature* 307 (1984) 604-608.

13. Mishina, M., Tobimatsu, T., Imoto, K., Tanaka, K.-I., Fujita, Y., Fukuda, K., Kurasaki, M., Takahashi, H., Morimoto, Y., Hirose, T. Inayama, S., Takahashi, T., Kuno, M. and Numa, S., Location of functional regions of acetylcholine receptor α subunit by site-directed mutagenesis. *Nature* 313 (1985) 364-369.

14. Mishina, M., Takai, T., Imoto, K., Noda, M., Takahashi, T., Numa, S., Methfessel, C., Sakmann, B., Molecular distinction between fetal and adult forms of muscle acetylcholine receptor. *Nature (England)* 321 (1986) 406-411.

15. Noda, M., Takahashi, H., Tanabe, T., Toyosato, M., Kikyotani, S., Furutani, Y., Hirose, T., Takashima, H., Inayama, S., Miyata, T. and Numa, S., Structural homology of *Torpedo californica* acetylcholine receptor subunits. *Nature* 302 (1983a) 528-532.

16. Noda, M., Takahashi, H., Tanabe, T., Toyosato, M., Kikyotani, S., Hirose, T., Asai, M., Takashima, H., Inayama, S., Miyata, T. and Numa, S., Primary structures of β- and δ-subunit precursors of *Torpedo californica* acetylcholine receptor deduced from cDNA sequences. *Nature* 301 (1983b) 251-255.

17. Penefsky, H. S., Reversible binding of P_i by beef heart mitochondrial adenosine triphosphate. *J. Biol. Chem.* 252 (1977) 2891-2899.

18. Popot, J.-L. and Changeux, J.-P., Nicotinic receptor of acetylcholine: Structure of an oligomeric integral membrane protein. *Physiol. Rev.* 64 (1984) 1162-1239.

19. Ratnam, M., Nguyen, D. L., Rivier, J., Sargent, P. B. and Lindstrom, J., Transmembrane topography of the nicotinic acetylcholine receptor: immunochemical tests contradict theoretical predictions based on hydrophobicity profiles. *Biochemistry*, 25 (1986a) 2621-2632.

20. Ratnam, M., Sargent, P. B., Sarin, V., Fox, J. L., Nguyen, D. L., Rivier, J., Criado, M. and Lindstrom, J., Location of antigenic determinants on primary sequences of the subunits of the nicotinic acetylcholine receptor by peptide mapping. *Biochemistry*, 25 (1986b) 2633-2644.

21. Sakmann, B., Methfessel, C., Mishina, M., Takahashi, T., Takai, T., Kurasaki, M., Fukuda, K. and Numa, S., Role of acetylcholine receptor subunits in gating of the channel. *Nature* 318 538-543.

22. Schenborn, E. T., and Mierendorf, R. C., A novel transcription property of SP6 and T7 polymerases: dependence on template structure. *Nucl. Acids Res.* 13 (1985) 6223-6236.

23. Stroud, R. M. and Finer-Moore, J., Acetylcholine receptor structure, function, and evolution. *Ann. Rev. Cell. Biol.* 1 (1985) 317-351.

24. Sumikawa, K., Houghton, M., Emtage, J. S., Richards, B. M. and Barnard, E. A., Active multi-subunit ACh receptor assembled by translation of heterologous mRNA in *Xenopus* oocytes. *Nature* 292 (1981) 862-864.

25. White, M. M., Mayne, K. M., Lester, H. A. and Davidson, N., Mouse-*Torpedo* hybrid acetylcholine receptors: Functional homology does not equal sequence homology. *Proc. Natl. Acad. Sci. USA* 82 (1985) 4852-4856.

26. Yoshii, K., Yu, L., Mayne, K. M., Davidson, N., and Lester, H. A., Mouse-torpedo acetylcholine receptor subunit hybrids expressed in *Xenopus* oocytes: equilibrium properties. *Biophys. J.* 51 (1987) 60a.

27. Yu, L., LaPolla, R. J. and Davidson, N., Mouse muscle nicotinic acetylcholine receptor γ subunit: cDNA sequence and gene expression. *Nucl. Acids Res.* 14 (1986) 3539-3555.

CHAPTER 4

Equilibrium properties of mouse-*Torpedo* acetylcholine receptor hybrids expressed in *Xenopus* oocytes

Kiyonori Yoshii, Lei Yu, Katharine Mixter Mayne,
Norman Davidson, and Henry A. Lester

Journal of General Physiology
in press

ABSTRACT

This study utilized messenger RNA encoding each subunit (α, β, γ, and δ) of the nicotinic acetylcholine (ACh) receptor from mouse BC3H-1 cells and from *Torpedo* electric organ. The mRNA was synthesized *in vitro* by transcription with SP6 polymerase from cDNA clones. All 16 possible combinations that include one mRNA species for each of α, β, γ, and δ were injected into oocytes. After allowing 2-3 d for translation and assembly, we assayed each oocyte for (1) receptor assembly, measured by the binding of [^{125}I]α-bungarotoxin (α-BTX) to the oocyte surface, and (2) ACh-induced conductance, measured under voltage clamp at various membrane potentials. All combinations yielded detectable assembly (30-fold range among different combinations) and ACh-induced conductances (> 1000-fold range at 1 μM). On double-logarithmic coordinates, the dose-response relations all had a slope near two for low [ACh]. Data were corrected for variations in efficiency of translation among identically injected oocytes by expressing ACh-induced conductance per fmol of α-bungarotoxin binding sites. Five combinations were tested for d-tubocurarine inhibition by the dose-ratio method; the apparent dissociation constant ranged from 0.08 to 0.27 μM. Matched responses and geometric means are used for describing the effects of changing a particular subunit (mouse vs *Torpedo*) while maintaining the identity of the other subunits. The most dramatic subunit-specific effect is that of the β subunit on voltage sensitivity of the response: $g_{ACh}(-90\ mV)/g_{ACh}(+30\ mV)$ is always at least 1, but this ratio increases by an average of 3.5-fold if β_M replaces β_T. Also, combinations including γ_T or δ_M usually produce greater receptor assembly than combinations including the homologous subunit from the other species. Finally, E_{ACh} is defined as the ACh concentration inducing 1 μS/fmol at -60 mV; E_{ACh} is lowest for α_M and for β_T. We conclude that receptor assembly, voltage sensitivity, and E_{ACh} are governed by different properties.

INTRODUCTION

All four subunits of the nicotinic acetylcholine receptor have been isolated and sequenced as cDNA clones from muscle and electric organ for several species. This accomplishment has encouraged several theoretical and experimental studies dealing with the relationship between structure and function of this membrane protein (Stroud & Finer-Moore, 1985). Important unanswered questions concern the nature of the coupling between agonist binding and channel activation, structure and selectivity properties of the channel itself, and details of open-channel and closed-channel blockade.

One way to test such theories exploits the fact that the cDNA clones themselves can be combined and mutated in various ways to encode novel receptors. At present, it appears that the most appropriate functional assay for such manipulations consists of *in vitro* RNA synthesis, using a viral RNA polymerase system (Melton *et al.*, 1984; Krieg & Melton, 1984; Mishina *et al.*, 1985; White *et al.*, 1985), followed by injection into *Xenopus* oocytes and by electrophysiological measurements on the newly expressed receptors (Gurdon *et al.*, 1971; Sumikawa *et al.*, 1981; Barnard *et al.*, 1982a; Mishina *et al.*, 1984, 1985; White *et al.*, 1985; Sakmann *et al.*, 1985; Methfessel *et al.*, 1986). The more recent work shows an excellent quantitative correspondence between the characteristics of the receptors expressed in oocytes and those in the native tissue; this correspondence extends to functional stoichiometry, desensitization, single-channel conductance and lifetime, and voltage sensitivity (White *et al.*, 1985; Sakmann *et al.*, 1985; Methfessel *et al.*, 1986). The faithful translation and assembly suggest that useful insights will indeed be obtained from the study of modified receptors expressed in *Xenopus* oocytes. Our study therefore extends that of White *et al.* (1985) and of Sakmann *et al.* (1985) on interspecies hybrid receptors. We have studied all 16 possible combinations of mouse and *Torpedo* α, β, γ, and δ subunits.

This report concerns the equilibrium properties of these hybrid receptors--Hill coefficient, steady-state activation, voltage sensitivity, and blockade by d-tubocurarine. Because we wanted to concentrate on the details of receptor function rather than on the biosynthesis, assembly, and membrane insertion, α-bungarotoxin (α-BTX) binding has been measured on the same oocytes, and most of results are expressed on a "per receptor" basis. A preliminary analysis of some of the data has been submitted for publication (Mayne *et al.*, 1987) and also published in abstract form (Yoshii *et al.*, 1987).

METHODS

Plasmids

A cDNA clone for the mouse AChR α subunit precursor was generously provided by Dr. J. P. Merlie (Isenberg *et al.*, 1986) and was transferred to the vector pGEM1 (Promega Biotec) containing the SP6 promoter. Two sequenced cDNA clones covering the 5' and 3' portions of the mouse AChR β subunit were also provided by Dr. Merlie in the vector M13mp18. A composite cDNA sequence coding for the entire β subunit precursor was constructed from restriction fragments. Both plasmids were digested with SacII, which has a unique recognition site in the β sequence, as well as with PvuI, which cuts once in the vector but not in the β sequence. The desired DNA fragments were isolated by agarose gel electrophoresis and treated with T4 DNA ligase. The sequence was confirmed by the dideoxy nucleotide technique (Sanger *et al.*, 1977). The complete protein-coding cDNA sequence was then recloned into the vector pGEM2 (Promega Biotec) containing the SP6 promoter.

The cDNA clones for the mouse AChR γ and δ subunits were isolated at Caltech (Yu *et al.*, 1986; LaPolla *et al.*, 1985) and recloned into the vectors pSP65 (Melton *et al.*, 1984) and pSP64T (Krieg & Melton, 1984) respectively. The clones for the *Torpedo* AChR subunits were as described by White *et al.* (1985).

In vitro transcription

The protocol of White *et al.* (1985) was used for *in vitro* transcription of AChR mRNAs with the following modifications. The linearized DNA templates were present at a concentration of 30 μg/ml and the SP6 RNA polymerase at 300 units/ml. The reaction was carried out for 2 h at 37°C, followed by 10 min incubation with 2 units/ml ribonuclease-free DNAase. Unincorporated nucleotide precursors were removed by spun column (Penefsky, 1977). The RNA was

extracted once with phenol-chloroform and twice with chloroform, precipitated twice with ethanol, and redissolved in distilled water (1 mg/ml) for microinjection into oocytes.

Preparation of oocytes and RNA injection

Mature *Xenopus* females were obtained from commercial sources. They were anesthetized by immersion in water containing 0.17% tricaine (3-aminobenzoic acid ethyl ester). An incision was made in the abdomen and a portion of the ovary was removed and placed in 82.5 mM NaCl/2 mM KCl/1 mM $MgCl_2$ /5 mM HEPES-NaOH, pH 7.5. Follicle cells were removed by incubating the tissue in this solution containing collagenase (Type IA, Sigma), 2 mg/ml for 2-3 h at room temperature.

50 nl of the mRNA solution was injected into the ooplasm of stage V and VI oocytes (Dumont, 1972) with a microdispenser (Drummond Scientific Co., Broomall, PA) through a needle with the tip diameter of ~20 μm. The oocytes were then transferred to Barth's medium supplemented with penicillin (100 unit/ml) and streptomycin (100 μg/ml). Oocytes were incubated at room temperature for 48-72 h.

Electrophysiology

Individual oocytes were transferred to a recording chamber (volume, 0.3 ml) continually perfused, by a system of valves and stopcocks, at a rate of 3.5 ml/min. The Ringer solution contained 96 mM NaCl/2 mM KCl/1 mM $MgCl_2$/0.3 μM atropine sulfate/5 mM HEPES-NaOH, pH 7.5, plus ACh as indicated.

We employed a two-microelectrode voltage-clamp circuit (Axoclamp-2A, Axon Instruments, Burlingame CA 94010). Electrodes were filled with 3 M KCl and had tip resistances of 0.5-1 MΩ. Oocytes were continually clamped to a

membrane potential of -60 mV and 100-ms steps were generated to various test potentials using standard instrumentation (Sheridan & Lester, 1977; Kegel *et al.*, 1985). Oocytes were typically exposed to each test solution for ~30 s. For the conditions of these experiments, holding currents reached a plateau in ~10 s and showed little or no desensitization. Marked desensitization occurs in the presence of higher ACh concentrations or with ACh receptors containing chick α subunits (K. Yoshii, K. M. Mayne, unpublished data). ACh-induced currents were measured by subtracting voltage-clamp currents in the absence and presence of ACh. All experiments were conducted at room temperature.

Toxin-binding assay

Oocytes were prewashed for 5 min in 96 mM NaCl/ 2 mM KCl/ 1 mM $MgCl_2$/ 5 mM HEPES, pH 7.6/ 1 mg/ml BSA. They were then transferred to the same solution containing ^{125}I-α-bungarotoxin (New England Nuclear) and incubated for 1 h. Oocytes were then washed 4 times and counted individually in a γ counter. All incubations were at room temperature.

RESULTS

All Combinations Produce Detectable Assembly and Function

Conductance per α-bungarotoxin binding site: a measure that minimizes variations

Among oocytes from the same ovary receiving identical injections, there was a > 10-fold range in the conductance generated from a given concentration of ACh. This variation among oocytes is a general phenomenon in our laboratory and in many others that study channels and receptors generated from foreign RNA; it is seen, for instance, with Ca and Na channels from rat RNA (Dascal *et al.*, 1986a; Goldin *et al.*, 1986; Leonard *et al.*, 1987). In the present study, we attempted to draw functional conclusions despite the presence of these large variations. For this purpose, we subjected individual oocytes to two experimental manipulations: we measured both ACh-induced conductance and surface α-bungarotoxin binding. The large variations in ACh-induced conductance were indeed accompanied by large variations in the α-bungarotoxin binding; and there was a good correlation between the two parameters with each of the combinations studied. An example is given in Fig. 1 for the case of all-*Torpedo* receptors. We therefore express most of the conductance data with a normalization to the number of α-bungarotoxin binding sites. This ratio, μS/fmol, has a coefficient of variation of roughly 30% for all cells injected with a given combination of subunits.

We also found that the average μS/fmol values varied little when among oocytes from different frogs, typically by only 30%. Nonetheless, the data presented in this paper were all gathered from a single frog's oocytes, tested over a period of one week.

Range of the data

Assembly. Table 1 summarizes several aspects of the measurements on each combination. The *assembly* of receptors is simply expressed as the number

Fig. 1. Binding and conductance compared for 11 individual oocytes from the same ovary that received identical injections with $(\alpha\beta\gamma\delta)_T$ RNA. ACh-induced conductance was measured at -60 mV. The line is a least-squares fit to the data, constrained to pass through the origin, and has a slope of 1.07 μS/fmol.

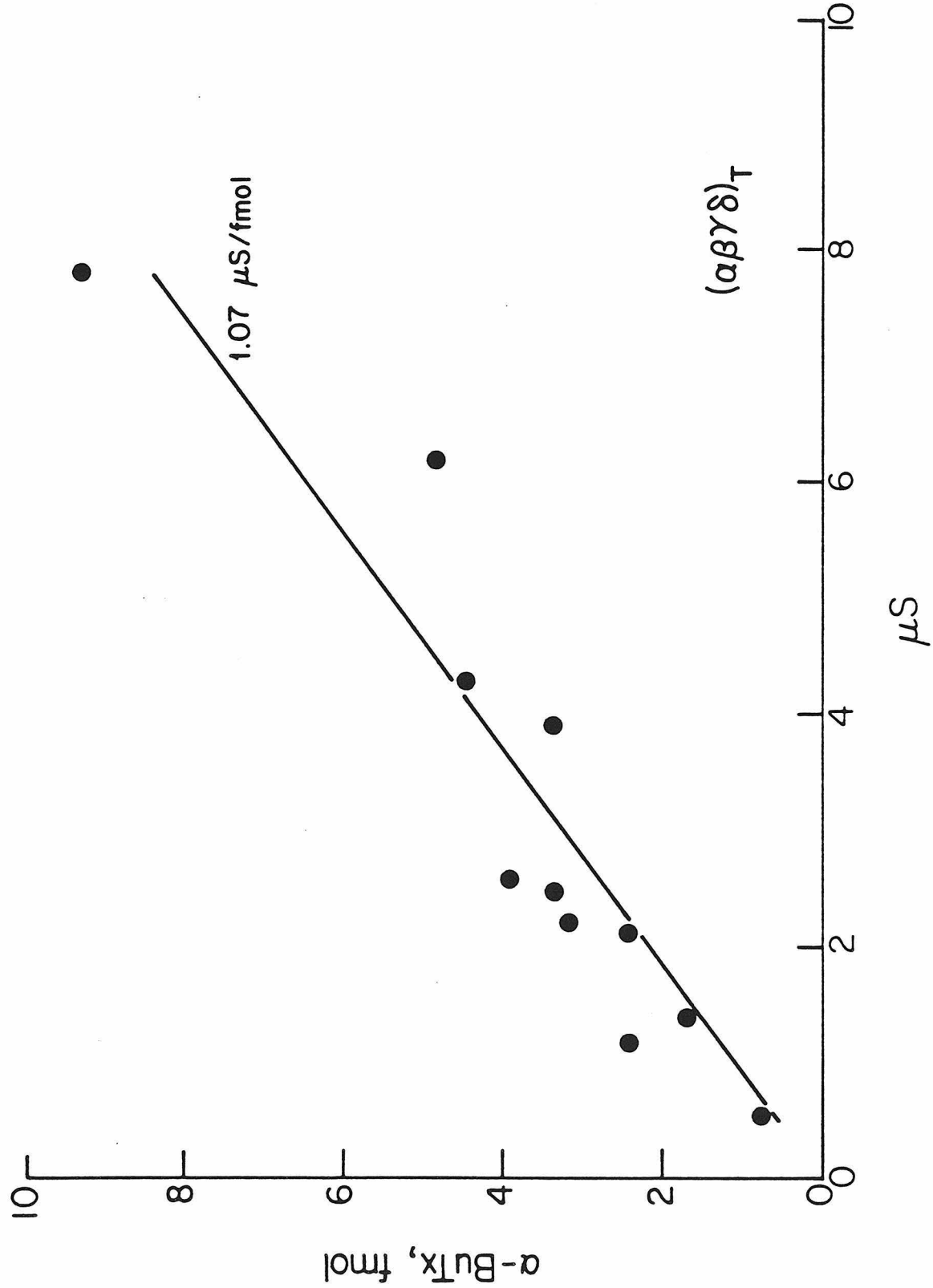
α-BuTx, fmol
0
2
4
6
8
10
μS
1.07 μS/fmol
$(\alpha\beta\gamma\delta)_T$

Table 1. Summary of Some Parameters for Each of the 16 Combinations.

RNAs	α-bungarotoxin per oocyte	EACh at -60 mV	g[-90] / g[+30]	Hill coefficient	KdTC
αβγδ	fmol	μM			μM
MMMM	6.49 ± 0.67 (n = 5)	0.20 ± 0.006 (n = 5)	4.3 ± 0.2 (n =4)	2 ± 0.1 (n =4)	0.27
MMMT	0.49 ± 0.04 (n = 5)	0.61 ± 0.018 (n = 5)	16. ± 2.2 (n =4)	1.8 ± 0.1 (n =4)	
MMTM	8.06 ± 0.05 (n = 5)	0.16 ± 0.002 (n = 8)	6.6 ± 1.1 (n =4)	1.9 ± 0.1 (n =4)	
MTMM	1.01 ± 0.08 (n = 5)	0.09 ± 0.004 (n = 8)	2.8 ± 0.2 (n =4)	2 ± 0.2 (n =4)	
TMMM	0.91 ± 0.14 (n = 5)	1.67 ± 0.089 (n = 8)	6.1 ± 0.6 (n =4)	1.5 ± 0.1 (n =4)	
MMTT	0.76 ± 0.12 (n = 5)	0.45 ± 0.075 (n = 8)	11. ± 0.9 (n =4)	1.5 ± 0.3 (n =4)	
MTTM	2.02 ± 0.17 (n = 5)	0.16 ± 0.009 (n = 8)	3.7 ± 0.3 (n =4)	1.9 ± 0.1 (n =4)	
MTMT	0.67 ± 0.05 (n = 5)	0.29 ± 0.023 (n = 8)	1.3 ± 0.1 (n =4)	1.6 ± 0.1 (n =4)	
TMMT	0.39 ± 0.04 (n = 5)	2.75 ± 0.14 (n = 4)	7.1 ± 1.1 (n =4)	1.8 ± 0.2 (n =4)	
TMTM	11.4 ± 1.48 (n = 5)	0.76 ± 0.066 (n = 8)	4.1 ± 0.3 (n =4)	2.1 ± 0.1 (n =4)	
TTMM	0.53 ± 0.08 (n = 5)	2.20 ± 0.13 (n = 8)	2.8 ± 0.3 (n =4)	1.8 ± 0.1 (n =4)	
MTTT	2.53 ± 0.37 (n = 5)	0.20 ± 0.016 (n = 4)	1.7 ± 0.1 (n =4)	2.3 ± 0.3 (n =4)	0.08
TMTT	0.65 ± 0.18 (n = 5)	13.5 ± 0.71 (n = 8)	8.9 ± 2.5 (n =4)	1.5 ± (n =1)	
TTMT	1.36 ± 0.21 (n = 5)	1.33 ± 0.099 (n = 8)	1 ± 0.1 (n =4)	1.5 ± 0.1 (n =4)	0.19
TTTM	5.45 ± 0.64 (n = 5)	0.29 ± 0.02 (n = 8)	3 ± 0.1 (n =4)	1.9 ± 0.1 (n =4)	0.19
TTTT	3.48 ± 0.27 (n = 11)	0.96 ± 0.044 (n = 11)	1.6 ± 0.2 (n =4)	1.8 ± 0.2 (n =4)	0.16

of binding sites for α-bungarotoxin per oocyte. There is a > 30-fold variation in the average number of α-bungarotoxin binding sites/oocyte for the various combinations, ranging from 0.39 fmol for the $\alpha_T\beta_M\gamma_M\delta_T$ hybrid to 11.5 fmol for the $\alpha_T\beta_M\gamma_T\delta_M$ hybrid.

Functional efficiency. There was an even larger range in the average ACh-induced conductance. At 1 μM ACh and -60 mV, some combinations--for instance, $(\alpha\beta\gamma\delta)_M$--yielded signals too large for reliable clamping (> 5-10 μA); others, such as $\alpha_T\beta_M\gamma_T\delta_T$, yielded signals too small for accurate measurement (< 5 nA). This range of $>10^3$ is due to three factors. (1) There are real differences in the fractional receptor activation produced by a given [ACh]. (2) If these differences arise primarily from the agonist-receptor interaction, they are amplified by the necessity for activation by two bound agonist molecules and the resultant parabolic dose-response relation. (3) Finally, there are differences in the assembly for each combination. As explained above, we account for factor (3) by referring to response per fmol of bound α-bungarotoxin (Fig. 2). We propose to account for point (2) by using a form of "response matching" similar to the principle of the dose-ratio method for studying antagonist dissociation constants. We therefore define E_{ACh} as the *equipotent* concentration of ACh that induces the response of 1 μS/fmol. Differences in E_{ACh} can eventually be compared with differences in the binding of competitive antagonists and open-channel blockers. E_{ACh} ranged over 100-fold among the combinations tested.

Voltage sensitivity is always in the same direction. Many combinations showed nonlinear current-voltage relations for the ACh-induced conductance (Fig. 3). Voltage sensitivity is expressed as the ratio of two slope conductances: g(-90 mV)/g(+30 mV). This parameter ranged from unity to about 16. The voltage sensitivity does not vary detectably with [ACh] in the concentration range tested; the constancy shown in Fig. 4 is typical of all the combinations.

Fig. 2. Dose-response relations for representative oocytes injected with each of the 16 combinations. In this and subsequent Figures, the source of each subunit RNA is represented by the pattern of the symbol. Each quadrant is either empty (mouse) or filled (*Torpedo*). Clockwise from upper right, the quadrants denote α, β, γ, and δ. The form of the symbols bears no intended relation to the molecular structure of the receptor. A, combinations containing mostly or all mouse subunits. B, combinations containing 2 mouse and 2 *Torpedo* subunits. C, combinations containing mostly or all *Torpedo* subunits.

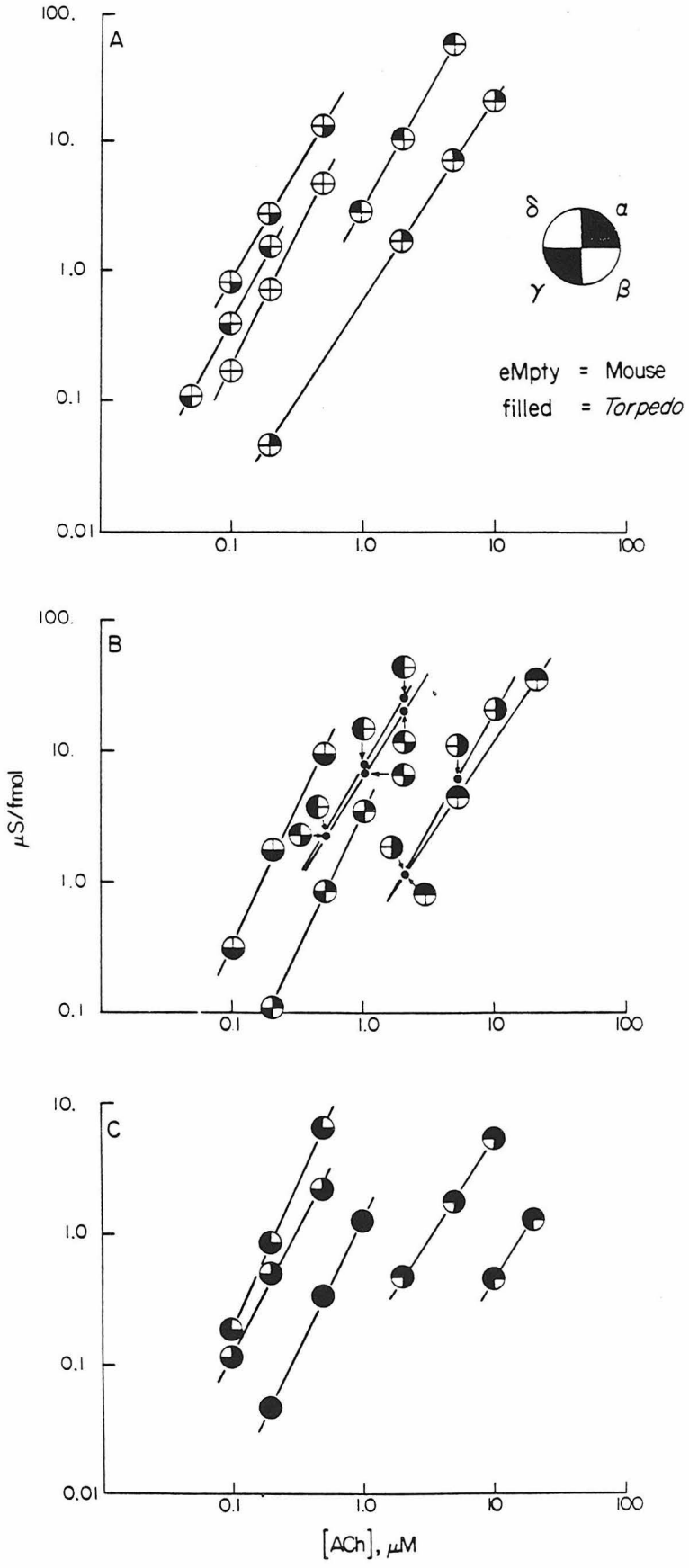
A
B
C
100.
10.
1.0
0.1
0.01
0.1
1.0
10
100
δ
α
γ
β
eMpty = Mouse
filled = Torpedo
μS/fmol
[ACh], μM

Fig. 3. Current-voltage relation for representative responses from all 16 combinations. For clarity, each combination is identified only at the extrema of the plot; for key to the combinations, see Fig. 2. A, combinations containing mostly or all mouse subunits. B and C, combinations containing 2 mouse and 2 *Torpedo* subunits. D, combinations containing mostly or all *Torpedo* subunits.

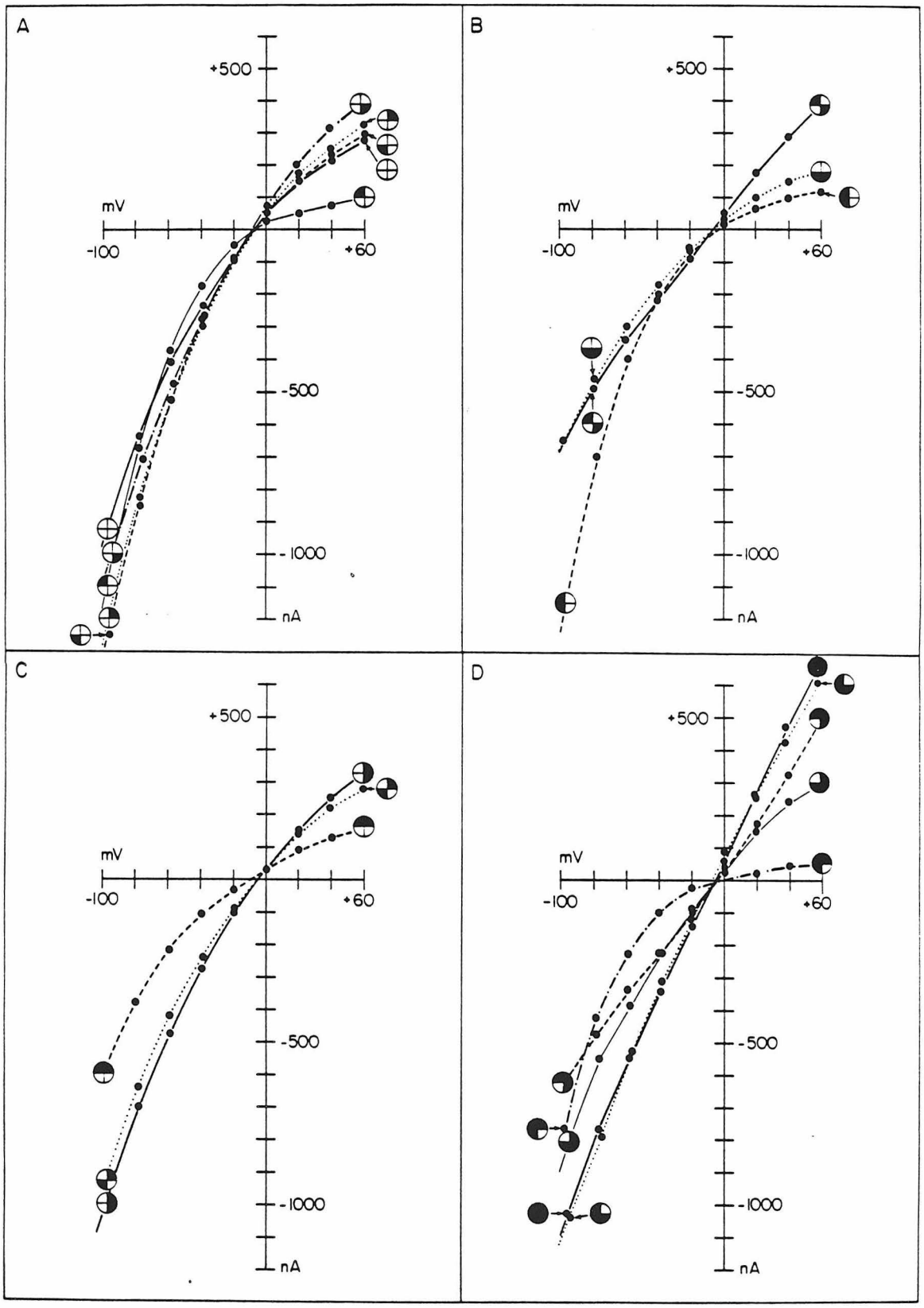
A
+500
mV
-100
+60
-500
-1000
nA
B
+500
mV
-100
+60
-500
-1000
nA
C
+500
mV
-100
+60
-500
-1000
nA
D
+500
mV
-100
+60
-500
-1000
nA

Fig. 4. Voltage sensitivity vs [ACh] for 5 oocytes injected with the $\alpha_T\beta_T\gamma_M\delta_M$ combination. Each oocyte was tested at several ACh concentrations.

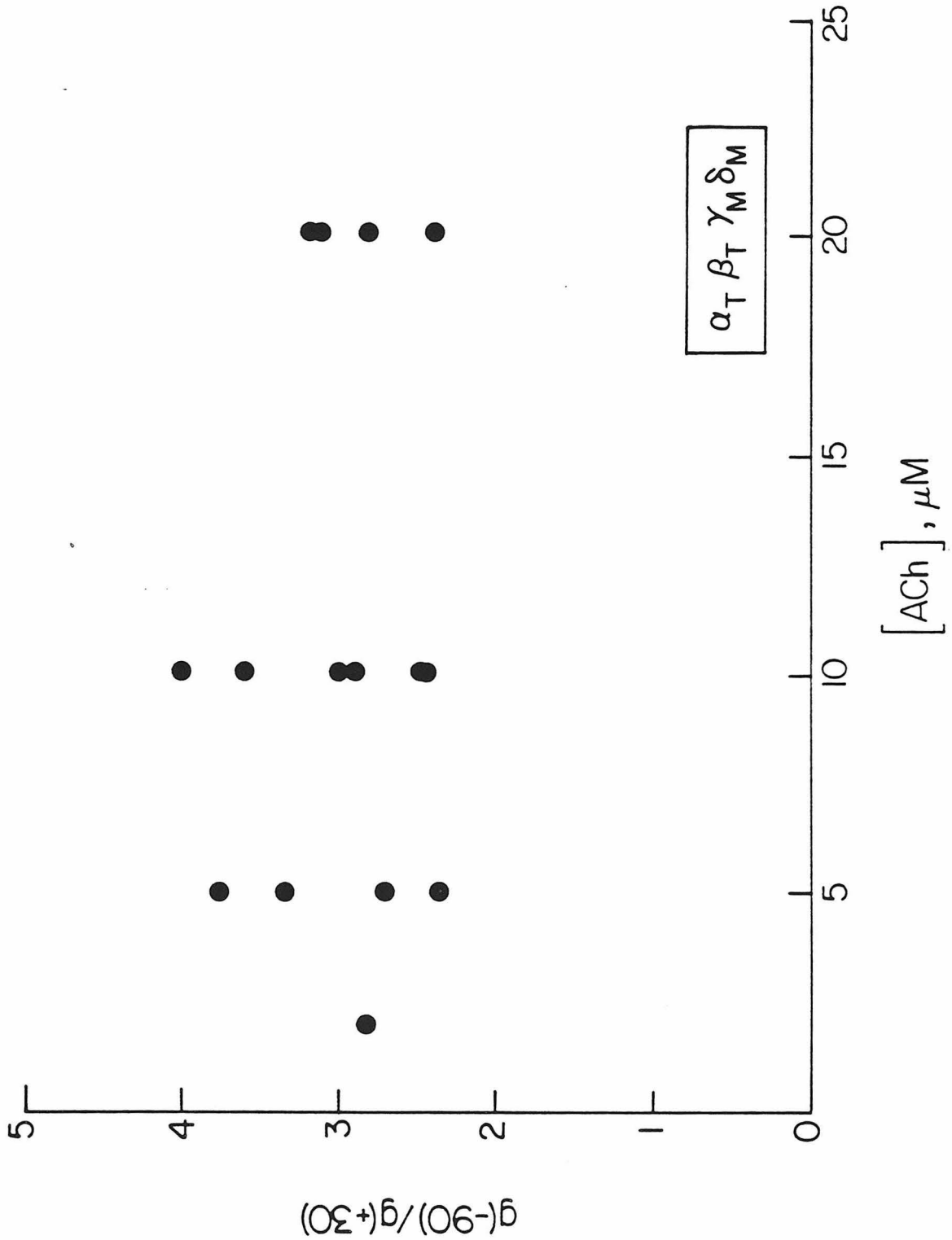
$\alpha_T \beta_T \gamma_M \delta_M$
g(-90)/g(+30)
0
1
2
3
4
5
5
10
15
20
25
[ACh], μM

There is little correlation among function, assembly, and voltage sensitivity

Figs. 5, 6, and 7 present scatter plots comparing these parameters for the sixteen combinations. It is evident that these three parameters have little or no correlation with each other.

Features Common to All Combinations

Functional stoichiometry of the response to ACh is near two

We have abstracted the functional stoichiometry as the slope of the dose-response relation at low [ACh] on double-logarithmic coordinates. This slope is near two for all of the hybrids (Table 1), suggesting that, as usually found for ACh receptors, the open state of the receptor channel is more likely to be associated with the presence of two bound agonist molecules than with a single one. The slope decreased slightly for those combinations yielding the smallest conductance per oocyte (Fig. 8). The least-squares linear fit to the data in Fig. 8 has a correlation coefficient of only 0.37; if one omits the combination $\alpha_T\beta_M\gamma_M\delta_T$ (which gave the lowest conductances), the correlation coefficient is 0.54. We doubt that this trend represents a real change in functional stoichiometry; it seems more likely that at the higher ACh concentrations necessary to test these combinations, the dose-response relation was distorted by desensitization, open-channel blockade, or partial saturation.

Reversal Potential

The reversal potential for the agonist-induced currents ranged between -2 mV and -9 mV for all the combinations tested. There was little or no significant difference among the combinations.

Fig. 5. Scatter plot, assembly vs E_{ACh} for all 16 combinations. For meaning of symbols, see Fig. 2. In this and subsequent figures, S. E. M. is shown where it exceeds the size of the symbol.

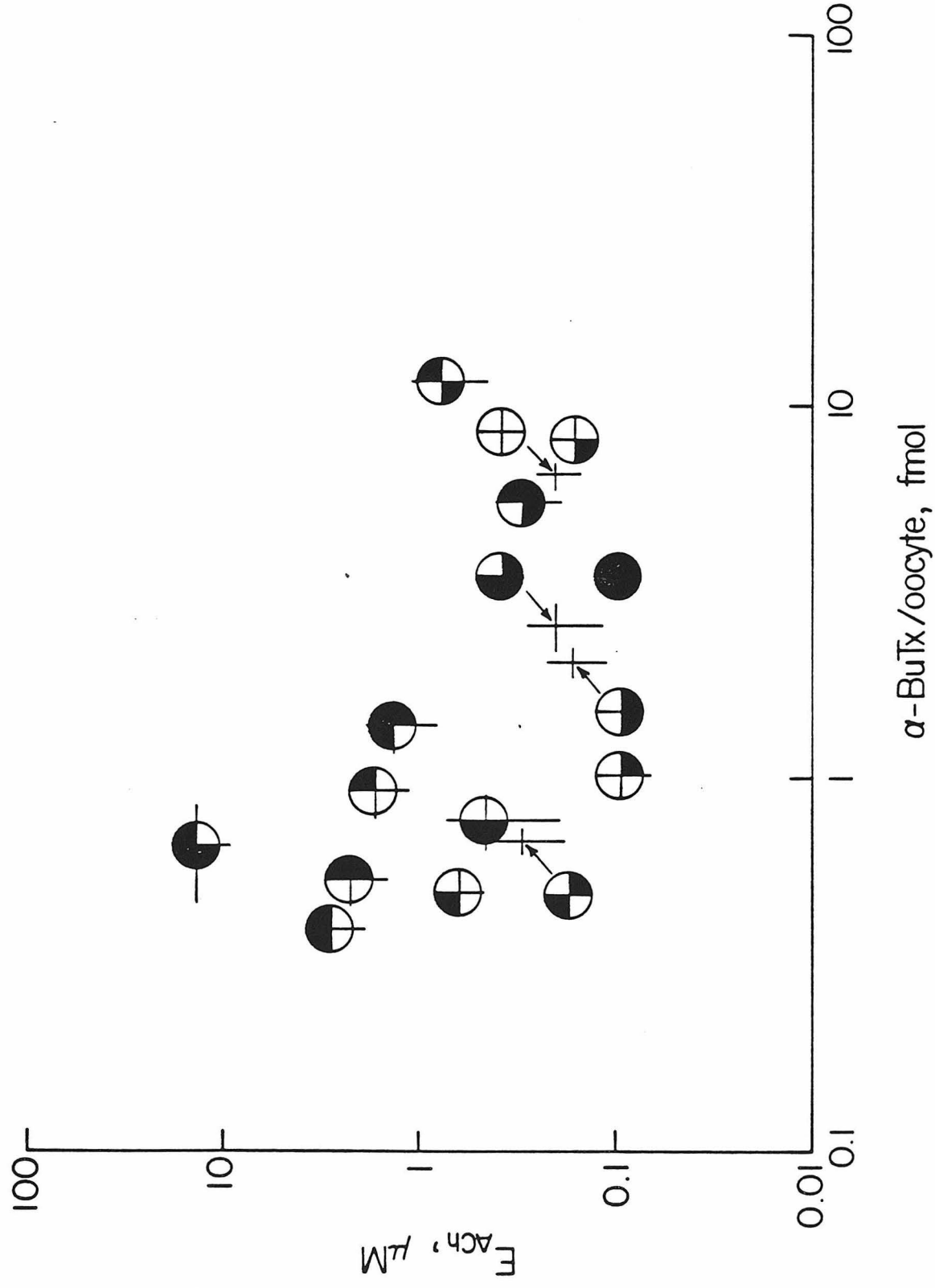
100
10
1
0.1
0.01
E_{ACh}, μM
0.1
1
10
100
α-BuTx/oocyte, fmol

Fig. 6. Scatter plot, voltage sensitivity vs. assembly. For the meaning of symbols, see Fig. 2.

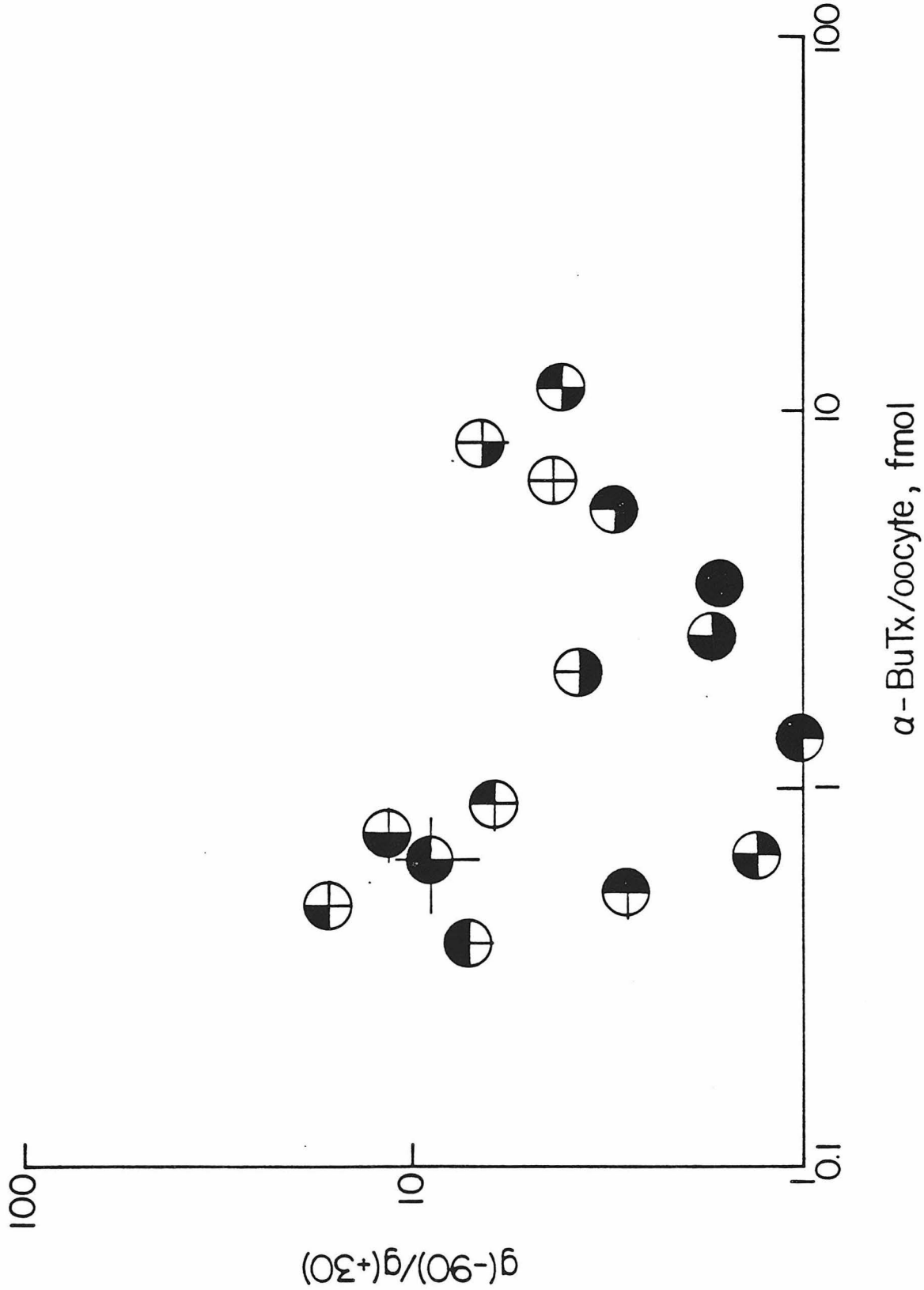
g(-90)/g(+30)
100
10
0.1
1
10
100
α-BuTx/oocyte, fmol

Fig. 7. Scatter plot, voltage sensitivity vs. E_{ACh}. For the meaning of symbols, see Fig. 2.

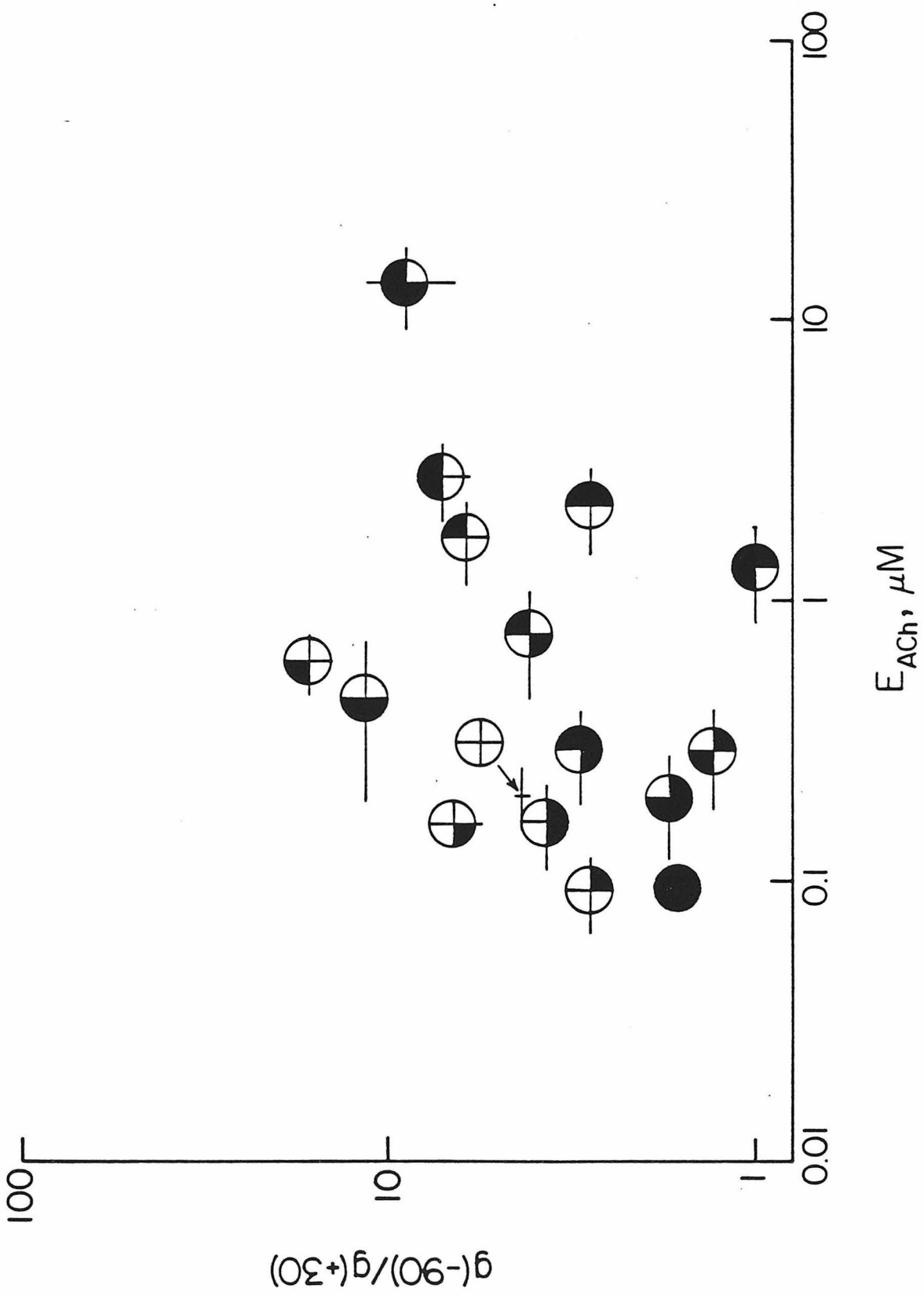
100
10
1
g(-90)/g(+30)
0.01
0.1
1
10
100
E_{ACh}, μM

Fig. 8. Scatter plot of Hill coefficient vs Ach concentration inducing 1 μS. Note that the abscissa refers to the conductance per oocyte, rather than per fmol as in previous figures. For meaning of the symbols, see Fig. 2.

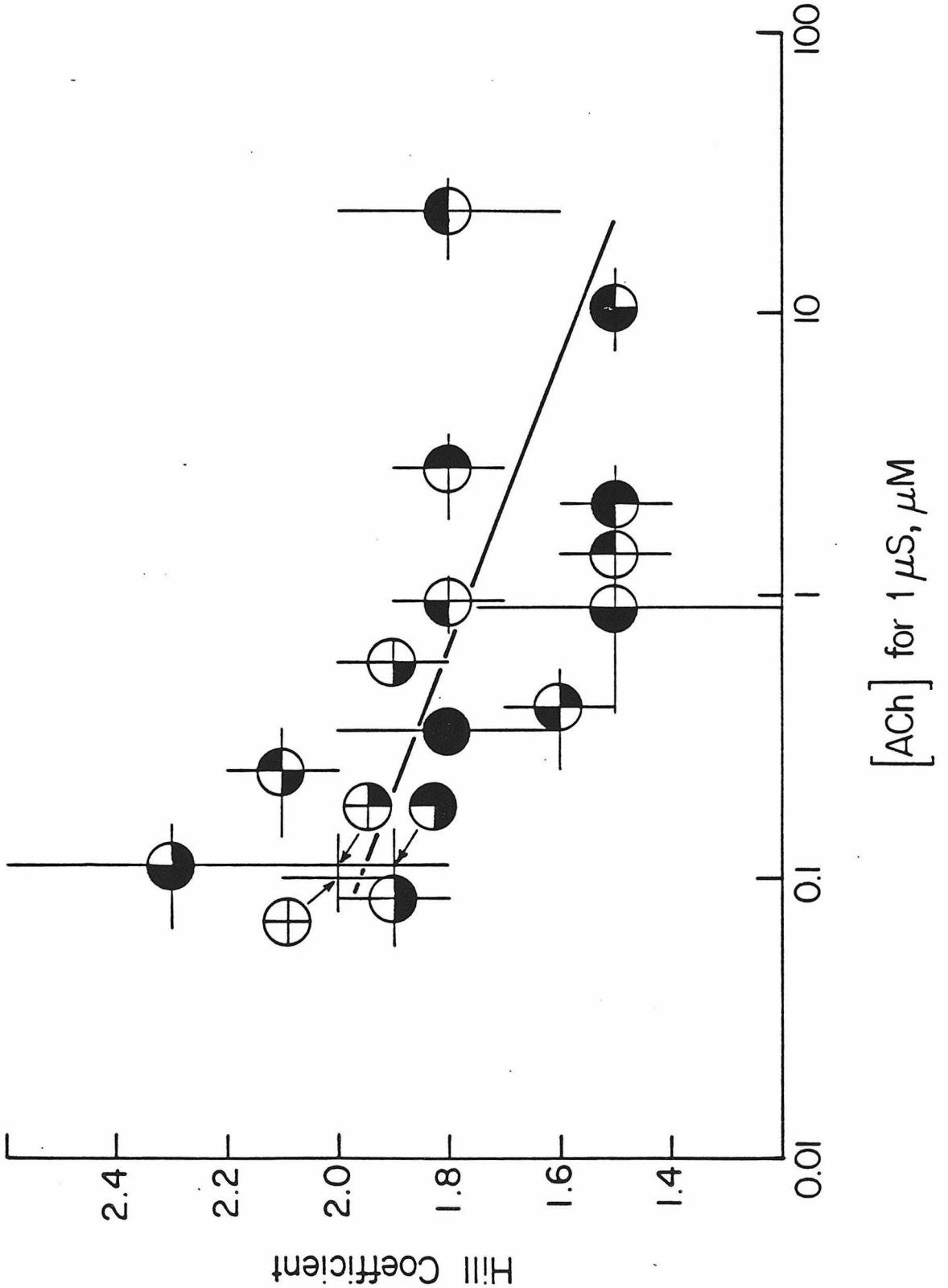
Hill Coefficient
2.4
2.2
2.0
1.8
1.6
1.4
0.01
0.1
1
10
100
[ACh] for 1 μS, μM

Effects of Individual Subunits: Quantitative Measures

A major purpose of this study is to decide whether the identity of any particular subunit (*Torpedo* vs. mouse) determines a property of the AChR complex. To address this question in a quantifiable way, we introduce several simple measures. The first, the ***subunit specific T/M ratio***, compares two hybrids that differ by only one subunit. This quantity is simply the ratio between the values for *Torpedo* and mouse. To provide an unbiased measure over the entire dynamic range, we will actually be dealing with logarithms of this ratio and abbreviate it qS.

Assembly efficiency

From the data in Table 1, qS values can be readily calculated. For example, qS for ***assembly*** associated with the $\alpha_T\beta_T\gamma_T\delta_{T/M}$ pair is -.195. The qS values for assembly in this study range from -1.25, for the $a_T\beta_M\gamma_T\delta_{T/M}$ pair, to 1.1, for the $\alpha_T\beta_M\gamma_{T/M}\delta_M$ pair, and include several values close to 0, e.g. the $\alpha_{T/M}\ \beta_M\gamma_T\delta_T$ pair which differ by less than 20%. We generalize this measure by averaging over the 8 qS values for each subunit; the resulting parameter is the ***subunit average*** qS(subunit). This measure (Table 2) shows that the identity of the α subunit had no consistent effect upon assembly: $qS(\alpha) = -.03$. The same lack of effect was noted for β, because $qS(\beta) = -.005$. In both cases, there were equal numbers of positive and negative values. The *Torpedo* γ subunit appeared to give better assembly, however; $qS(\gamma) = 0.45$ and all 8 values were greater than zero. Finally, the mouse δ subunit seems to produce better assembly ($qS(\delta) = -0.45$, with 6 of 8 values negative). The final measure, the ***global average*** $qS(\alpha\beta\gamma\delta)$, includes all 32 pairs. For the α-bungarotoxin binding measurements, $qS(\alpha\beta\gamma\delta)$ is very close to 0, showing no preferential incorporation of *Torpedo* or mouse proteins.

α_M consistently gives higher responses

Fig. 2 presents dose-response relations for some of the combinations. Clearly, α_M produces receptors that function with a higher degree of response than α_T. It also appears that $\delta_M > \delta_T$ and $\beta_T > \beta_M$ (Table 3).

β_M consistently gives the highest voltage sensitivity

As noted above, most of the combinations display a voltage-sensitive response (Fig. 3): for only one case, $\alpha_T\beta_T\gamma_M\delta_T$, the ratio g(-90 mV)/g(+30 mV) does not differ significantly from unity. Table 4 presents the qS ratios for voltage sensitivity and also arranges the various combinations in order of decreasing voltage sensitivity. Clearly, the most consistent correlation is with the β subunit: the 8 highest voltage sensitivities are all associated with β_M. Also, for a given β subunit, combinations with a heterogenous δ subunit were more voltage-sensitive than those with a homogeneous δ subunit.

All Four Subunit RNAs are Required for Substantial Responses

In actuality, there are not just 16 possible combinations, but 80, because each subunit could be selected from mouse (M) or *Torpedo* (T), or omitted entirely (0). We have not tested all 64 additional combinations involving 1, 2 or 3 omitted subunits, or even all 32 combinations involving only 1 omitted subunit. The available data suggest, however, that omission of even a single subunit RNA leads to rather inefficient assembly, so that the data reported with a complete set of subunits in this paper would not be distorted by such incomplete complexes.

***Omission of* δ.** White *et al.* (1985) found that the combination $\alpha_T\beta_T\gamma_T\delta_0$ produced roughly 3% the agonist-induced conductance of $\alpha_T\beta_T\gamma_T\delta_T$ and an even smaller percentage of $\alpha_T\beta_T\gamma_T\delta_M$. Therefore, any δ_0 complexes would have

Table 2. Subunit effects on assembly.

Measure: surface [^{125}I]α-bungarotoxin binding, T/M

Subunit	average qS (of 8)	qS number > 0
α	-0.03	4
β	-0.005	4
γ	0.49	8
δ	-0.45	2

Global	average qS(αβγδ)	qS number > 0
	-0.001	18

See text for definition of qS.

Table 3. Subunit effects on E_{ACh}.

Measure : E_{ACh}, T/M

Subunit	average qS (of 8)	qS number > 0
α	0.84	8
β	-0.35	1
γ	-0.11	2
δ	0.41	7

Global	average qS(αβγδ)	qS number > 0
	0.020	17

Table 4. Subunit effects on voltage sensitivity

Measure: g[-90]/g[+30], T/M

A. *Subunit average qS*

Subunit	average qS (of 8)	qS number > 0
α	-0.10	1
β	-0.55	0
γ	0.05	6
δ	-0.02	4

Global average qS(αβγδ)

-0.15 12 of 32

B. *Rank order*

DECREASING SENSITIVITY --->

α	M	M	T	T	M	T	M	T	M	T	M	T	M	T	M	T
β	M	M	M	M	M	M	M	M	T	T	T	T	T	T	T	T
γ	M	T	T	M	T	M	M	T	T	T	M	M	T	T	M	M
δ	T	T	T	T	M	M	M	M	M	M	M	M	T	T	T	T

contributed an insignificant amount of conductance to the macroscopic measurements reported here. However, Mayne *et al.* (1987) reported that $\alpha_T\beta_T\gamma_T\delta_0$ assembles much less efficiently than combinations including a δ subunit, so that the ACh-induced conductance per α-bungarotoxin site is roughly 20% that of $\alpha_T\beta_T\gamma_T\delta_T$.

Omission of β *or* γ. In the present study, the rather low agonist-induced conductances for some combinations (such as $\alpha_T\beta_M\gamma_T\delta_T$) and the rather low assembly for some combinations (such as $\alpha_T\beta_M\gamma_M\delta_T$) lead to the question, can function or assembly be detected in the absence of β or γ subunits? In one experiment, we tested the combinations $\alpha_T\beta_T\gamma_M\delta_M$, $\alpha_T\beta_M\gamma_M\delta_M$, and $\alpha_T\beta_0\gamma_M\delta_M$. For the former two combinations, ACh (10 μM) induced conductances of 3 to 4 μS/fmol; however, the latter combination yielded no detectable assembly (< 0.05 fmol) and no detectable ACh-induced conductances (< 0.1 μS).

We also compared the combinations $\alpha_T\beta_M\gamma_T\delta_T$ and $\alpha_T\beta_M\gamma_0\delta_T$. The α-bungarotoxin binding was 1.80 $\mp$ 1.1 and 0.15 $\mp$ 0.06 fmol respectively (mean $\mp$ S. E. M., 5 oocytes). Conductances induced by ACh (20 μM) were 25.8 and 1.5 pS, respectively. Furthermore, the voltage-dependence values were 10.2 and 1.3, respectively. Thus, there seems to be little contribution by γ_0 combinations to the macroscopic conductances. Nonetheless, it must be pointed out that the functional efficiency, μS/fmol, seems to be little decreased for those few receptors that are correctly assembled in the absence of the γ subunit.

Omission of α. Mayne *et al.* (1987) reported no detectable binding or function when the α subunit was omitted.

α *alone*. We tested oocytes injected with α_T, α_M, or α_{Chick} RNA without other subunit RNAs. In some cases, ACh concentrations of ~500 μM induced detectable conductances (L. Yu, unpublished data). However, no responses were detected at [ACh] < 50 μM as employed in the present study.

Dissociation Constant for d-Tubocurarine

For five of the combinations, we used the dose-ratio method to measure the apparent dissociation constant for the competitive inhibition by d-tubocurarine (Fig. 9). This method involves assessing the parallel shift in dose-response relations at various inhibitor concentrations; its use for the nicotinic acetylcholine receptor has been frequently discussed (Jenkinson, 1960; Armstrong & Lester, 1979; Krouse *et al.*, 1985). Combinations including δ_M showed a small (30%) decrease in the dose-ratio slope at -100 mV, probably because of open-channel block by d-tubocurarine; therefore, Table 1 presents the values for potentials between -60 mV and +40 mV. The differences in K_i cover a fold of 3.5-fold; this is substantially less than the differences in criterion concentration for the same combinations. The dissociation constant for agonists often depends on voltage, but at +40 mV the criterion concentrations still cover a range of 9.5 fold.

Fig. 9. Dose-ratio analysis of inhibition by d-tubocurarine. A, parallel shift of dose-response curves. B, dose-ratio plots at several voltages.

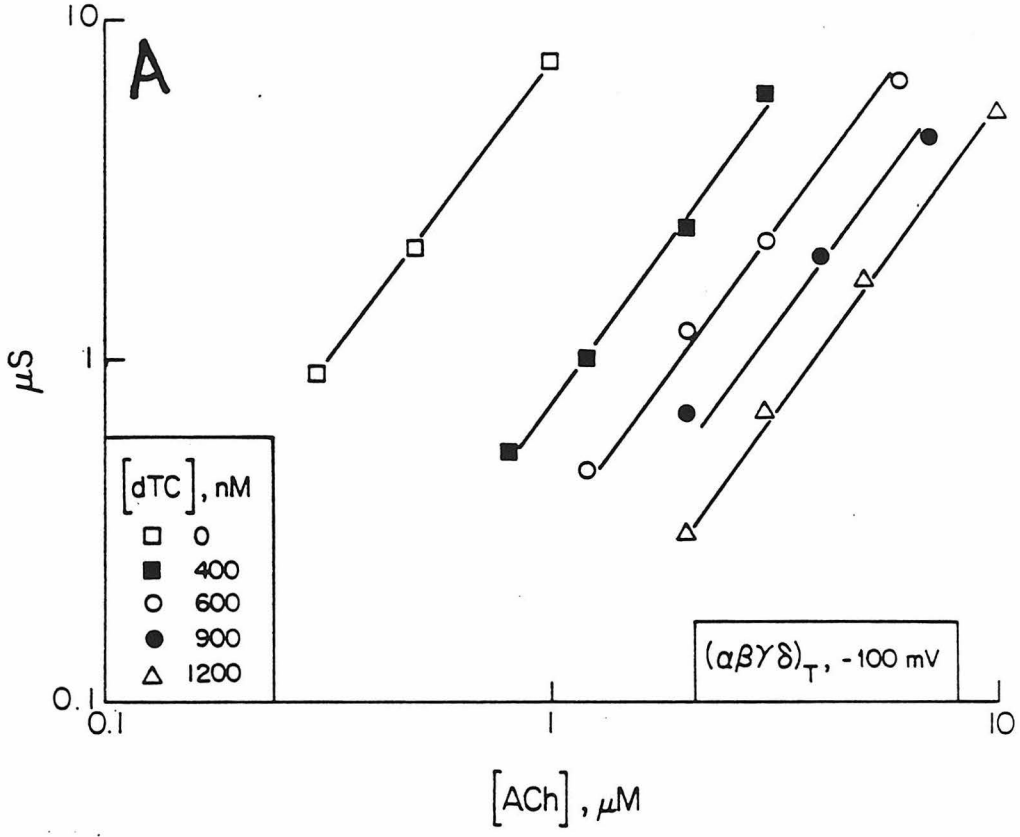
A
10
1
0.1
μS
[dTC], nM
0
400
600
900
1200
(αβγδ)T, -100 mV
0.1
1
10
[ACh], μM

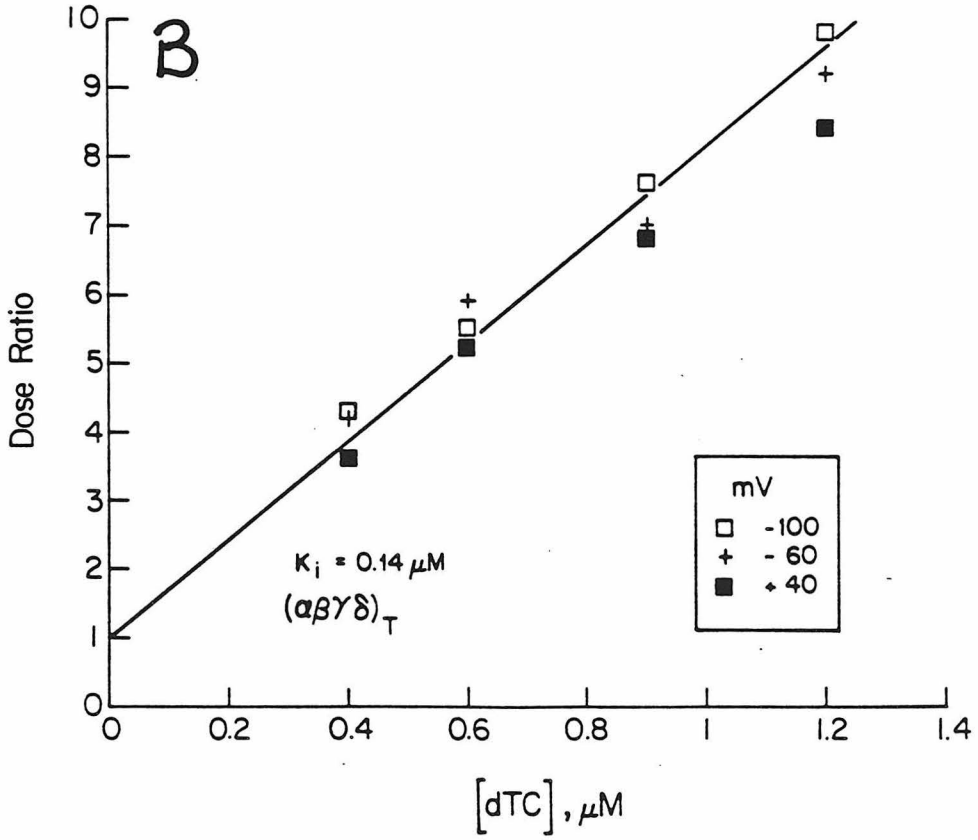
B
Dose Ratio
0
1
2
3
4
5
6
7
8
9
10
0
0.2
0.4
0.6
0.8
1
1.2
1.4
[dTC], μM
mV
-100
- 60
+ 40
Ki = 0.14 μM
(αβγδ)T

DISCUSSION

In this study, we surveyed the properties of all 16 possible hybrid acetylcholine receptors involving a complete set of α, β, γ, and δ subunits from two species. A major conclusion is that the identities of particular subunits determine different receptor properties. Thus, γ_T always gives better receptor assembly, α_M always gives higher receptor function, and β_M always gives higher voltage sensitivity. It must therefore be concluded that receptor assembly, function, and voltage sensitivity are governed by different subunits.

Receptor Function Appears Normal

E_{ACh} is roughly as expected

We adapted the somewhat arbitrary response of 1 μS/fmol for comparing equipotent ACh concentrations among the hybrid combinations. Because the dose-response relations are nearly parallel in the range studied here, this choice for E_{ACh} does not strongly influence the conclusions concerning relative functional efficiencies. It should be pointed out that 1 μS/fmol equals 8.3×10^{-4} pS per ACh receptor (assuming 2 α-bungarotoxin binding sites per receptor). Assuming an open-channel conductance of 40 pS, this in turn corresponds to an average activation of 2×10^{-5}. We note that this value is roughly in agreement with expectations from physiological measurements of dose-response relations for mouse and *Torpedo* receptors. For a Hill coefficient of 2, a fractional activation of 2.1×10^{-5} corresponds to an agonist concentration of 4.6×10^{-3} times the half-maximal concentration. The lowest concentrations giving this value are in the range 0.1 to 1 μM (see Table 1). Taking the value of 0.5 μM as an average, this would suggest that half-maximal activation would occur at roughly 100 μM ACh.

This value is in good agreement with actual measurements on BC3H-1 cells (Brett *et al.*, 1986; Sine & Taylor, 1980) and on *Torpedo* membrane fragments (Neubig & Cohen, 1980; Heidmann *et al.*, 1983), although it should be pointed out that the half-maximal concentration is liable to be voltage-sensitive in the case where the response is voltage-sensitive (as observed here for nearly all combinations).

Blockade by tubocurarine is roughly as expected

There have been no previous quantitative electrophysiological studies of d-tubocurarine blockade at *Torpedo* acetylcholine receptors. The values we found (0.08 to 0.27 μM for all five mouse-*Torpedo* combinations tested) are close to the ranges usually found for mouse muscle (0.04-0.15 μM, Pennefather & Quastel, 1981), frog muscle (0.39-0.43 μM, Jenkinson, 1960; Adams, 1975), and *Electrophorus* electroplaques (0.2 μM, Lester *et al.*, 1975). It is unclear how the present values should be interpreted in terms of the existing binding studies on *Torpedo* electric organ (Neubig & Cohen, 1979) and BC3H-1 cells, the source of the mouse clones used here (Sine & Taylor, 1981), both suggesting that the receptor has two distinguishable sites for competitive antagonist binding (see discussions by Pennefather & Quastel, 1981; Krouse *et al.*, 1985).

Regardless of the detailed binding mechanism, however, we find only a modest range in the apparent dissociation constant for dTC, whereas the criterion concentration for agonists varies by more than 100 fold. If the range of inhibitory constants remains small for the other 11 combinations to be tested, this would presumably agree with present concepts of receptor function: antagonists interact in a relatively simple and constant fashion with the receptor binding site; the subsequent conformational steps that open the channel are more complex and more greatly affected by subunit substitutions.

Voltage Sensitivity

The β subunit and voltage sensitivity

Another clear result of this study is that the voltage sensitivity ratio is at least unity; where present, voltage sensitivity is always in the same direction. Furthermore, the voltage sensitivity depends on the identity of the β subunit. The subunit qS was greater than zero for all $\alpha\beta_{T/M}\gamma\delta$ pairs, yielding a subunit average qS of 0.55. Furthermore, all 8 combinations containing β_M are more voltage-sensitive than all 8 combinations involving β_T. On the average, the mouse β subunit renders a combination 3.55 times more voltage-sensitive than does the *Torpedo* β subunit.

According to present concepts, a voltage-sensitive ACh-induced conductance could arise from voltage sensitivity in at least one of three separate parameters: (1) the single-channel conductance, (2) the rate constant for channel closing, or (3) the rate constant for opening. The first two of these parameters, and probably the third as well, can be assessed with single-channel recordings; and these are now under way in our laboratory. One hopes for a decisive assignment of the voltage sensitivity to one of the three parameters.

In a study of some calf-*Torpedo* ACh receptor hybrids, Sakmann *et al.* (1985) found no evidence that the single-channel conductance is voltage-sensitive. The combination $(\alpha\beta\gamma)_T\delta_{calf}$, but not $\alpha_{calf}(\beta\gamma\delta)_T$ combination, showed the same channel duration (including voltage sensitivity) as the $(\alpha\beta\gamma\delta)_{calf}$ combination. Quantitative data were not reported for other combinations. On the basis of these data, it was suggested that the δ subunit governs the voltage sensitivity of the closing rate constant. Our data are not strictly comparable to the study cited, because (a) we studied *Torpedo*-mouse rather than *Torpedo*-calf hybrids; and (b) as noted above, our data do not address the channel duration alone. We do find a more subtle effect of the δ subunit on the equilibrium voltage

sensitivity of the ACh-induced conductance. The subunit average qS (δ) for g(-90)/g(+30) is nearly zero, with 4 positive and 4 negative values; but the 4 most voltage-sensitive combinations involving δ_M also involve β_M, and the 4 least voltage-sensitive combinations involving δ_M also involve β_T.

A final difference between the two studies is that we used roughly 10-fold more RNA per oocyte. We have found (unpublished results) that the combinations differ widely with respect to the amount of RNA injected that yields half-maximal assembly and response. Thus, we may have been able to detect responses from some combinations that might give undetectable responses with the smaller injections used by Sakmann *et al.* (1985). Yet, we have presented evidence that even the "worst" combinations were not substantially aided by endogenous subunits or by incomplete complexes: all four subunit RNAs were required for substantial responses.

Origin of voltage sensitivity

Voltage-sensitive responses presumably have their origin in Coulombic interactions. Several specific types of interaction can be envisioned. Among these are interactions between the dipole moment of the channel and the membrane field, between permeant ions and a barrier or binding site in the channel, or between ions bathing the membrane and the binding sites on the receptor. At present there is no strong basis for choosing among these possibilities. However, because the voltage sensitivity is also in the same direction, one might tentatively conclude that the Coulombic interaction energy has the same sign for all of the 16 combinations (except for the single combination $\alpha_T\beta_T\gamma_M\delta_T$, for which the energy is presumably zero). A dipole moment (Magleby & Stevens, 1972a,b) could presumably have either sign, in disagreement with this idea. However, if the Coulombic interaction involves an ion in the solution and a

binding site on the receptor (Armstrong & Matteson, 1986), the energy would always have the same sign.

The most voltage-sensitive combination showed a ratio of 16 over a voltage range of 120 mV. This would correspond to an e-fold change per 43 mV. Such a variation could be caused by the motion of a single charge halfway through the membrane. The binding site might be either weaker or nearer the membrane surface for the more weakly voltage-dependent combinations.

Regardless of the detailed mechanism, it seems difficult to escape the conclusion that the difference of the voltage sensitivity between the mouse and *Torpedo* β subunits arises because of a difference in the charges on their amino-acid residues. One possibility is that the mouse and *Torpedo* subunits fold in exactly the same way, so that there are one or two regions with charge differences. Fig. 10 presents a simple superposition of the charge distributions. There are several regions of substantial difference; the range of residues 210 to 220 is especially interesting because it lies between the region homologous to the binding site on the α subunit and the highly conserved M2-M3 region thought to be involved in permeation (Hucho *et al.*, 1986; Giraudat *et al.*, 1986; Imoto *et al.*, 1986).

A more subtle possibility is that the mouse and *Torpedo* β subunits fold differently because of differences in nonpolar interactions, again resulting in three-dimensional structures with different charge distributions. This possibility would be more difficult to analyze from primary sequence data alone. The problem calls for further analysis using chimeric and mutant subunits (Imoto *et al.*, 1986).

Fig. 10. Charge distributions on mature mouse and Torpedo β subunits. The plot was generated by assigning a value of +1 to lys and arg, -1 to glu and asp, and 0 to other residues. The data were then subjected to a running average of 10 residues; gaps were then introduced to provide a good homology. The bars give positions of the disulfide bond in the putative extracellular region (S-S), putative α-helices M1-M4, and the putative amphipathic helix MA (Stroud & Finer-Moore, 1985).

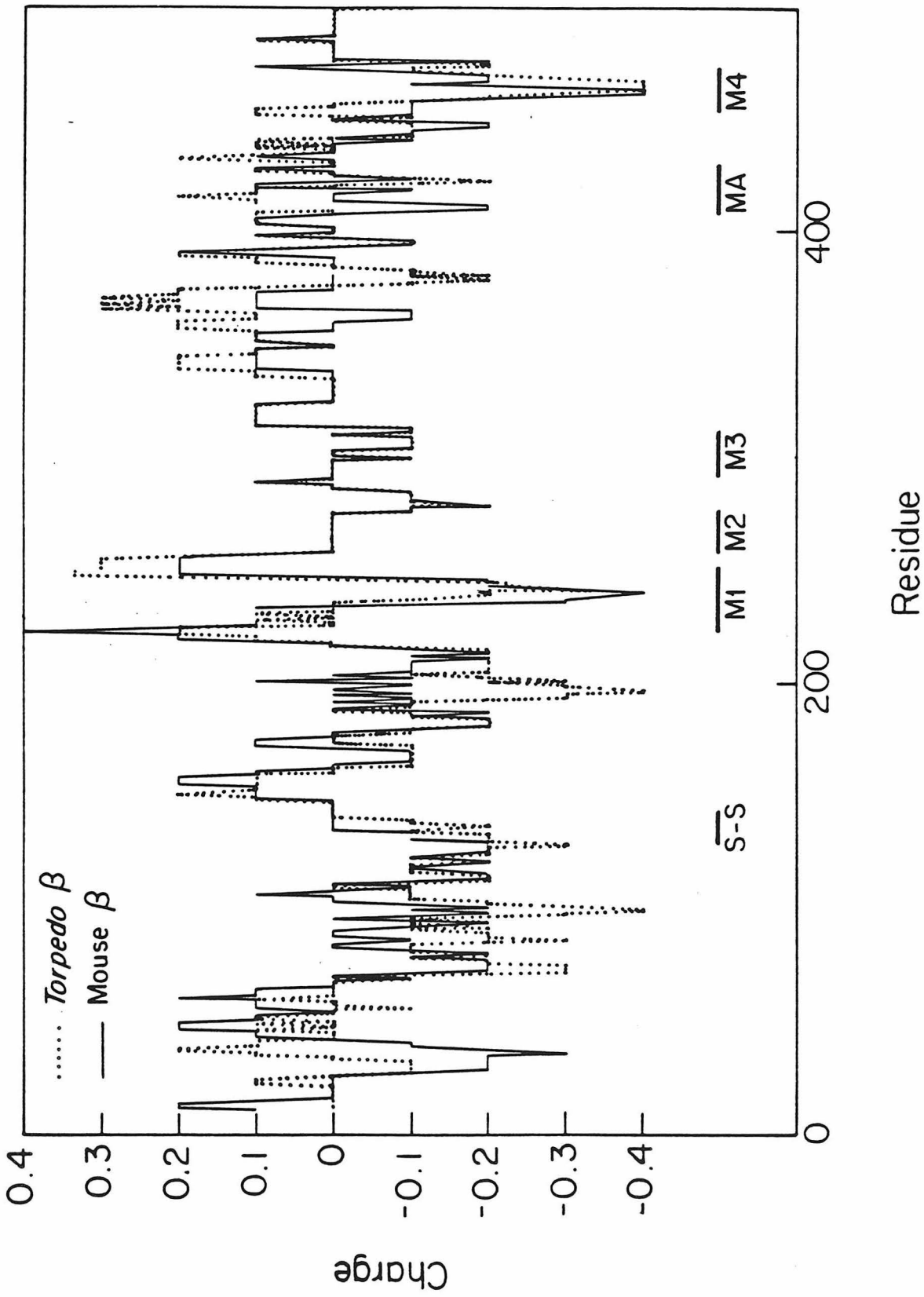
Torpedo β
Mouse β
S-S
M1
M2
M3
MA
M4
0.4
0.3
0.2
0.1
0
-0.1
-0.2
-0.3
-0.4
Charge
0
200
400
Residue

ACKNOWLEDGMENTS

We thank Dr. J. P. Merlie for providing clones and Dr. Reid Leonard for discussion.

This research was supported by grants from the Muscular Dystrophy Association and from the National Institutes of Health (NS-11752).

REFERENCES

Adams, P. R. 1975. Drug Interactions at the Motor Endplate. *Pflugers Arch.* **360:**155-164.

Armstrong, D., and H. A. Lester. 1979. The kinetics of curare action and restricted of diffusion within the synaptic cleft. *J. Physiol.* **294:**365-386.

Armstrong C. M., and D. R. Matteson. 1986. The role of calcium ions in the closing of K channels. *J. Gen. Physiol.* **87:**817-832.

Barnard, E.A., R. Miledi, and K. Sumikawa. 1982a. Translation of exogenous messenger RNA coding for nicotinic acetylcholine receptors produces functional receptors in *Xenopus* oocytes. *Proc. R. Soc. Lond. B.* **215:**241.

Brett, R. S., J. P. Dilger, P. R. Adams, and B. Lancaster. 1986. A method for the rapid exchange of solutions bathing excised membrane patches. *Biophys. J.* **50:**987-992.

Dascal, N., T. P. Snutch, H. Lubbert, N. Davidson, and H. A. Lester, 1986. Expression and modulation of voltage gated-calcium channels after RNA injection in *Xenopus* oocytes. *Science* **231:**1147-1150.

Dumont, J. N. 1972. Oogenesis in *Xenopus laevis* (Daudin). I. Stages of oocyte development in laboratory maintained animals. *J. Morphol.* **136:**153-180.

Giraudat, J., M. Dennis, T. Heidmann, J.Y. Chang, and J. P. Changeux. 1986. Structure of the high-affinity binding site for noncompetitive blockers of the acetylcholine receptor: serine-262 of the delta subunit is labeled by [^{3}H]chlorpromazine. *Proc. Natl. Acad. Sci. USA* **83:**2719-2723.

Goldin, A. L., A. Dowsett, H. Lubbert, T. Snutch, R. Dunn, H. A. Lester, W. Catterall, and N. Davidson. 1986. Messenger RNA conding for only the α subunit of the rat brain Na channel is sufficient for expression of functional

channels in *Xenopus* oocytes. *Proc. Natl. Acad. Sci. USA* **83:**7503-7507.

Gurdon, J. B., C. D. Lane, H. R. Woodland, and C. Marbaix. 1971. Use of frog eggs and oocytes for the study of messenger RNA and its translation in living cells. *Nature* **233:**177-182.

Heidmann, T., J. Bernhardt, E. Neumann and J.-P. Changeux. 1983. Rapid kinetics of agonist binding and permeability response analyzed in parallel on acetylcholine receptor rich membranes from *Torpedo marmorata*. *Biochemistry* **22:**5452.

Hucho, F., W. Oberthur, and F. Lottspeich. 1986. The ion channel of the nicotinic acetylcholine receptor is formed by the homologous helices M II of the receptor subunits. *FEBS Lett.* **205:**137-142.

Imoto, K., C. Methfessel, B. Sakmann, M. Mishina, Y. Mori, T. Konno, K. Fukuda, M. Kurasaki, H. Buho, Y. Fujita, and S. Numa. 1986. Location of a delta-subunit region determining ion-transport through the acetylcholine-receptor channel. *Nature* **324:**670-674.

Isenberg, K. E., J. Mudd, V. Shah, and J. P. Merlie. 1986. Nucleotide sequence of the mouse muscle nicotinic acetylcholine receptor alpha subunit. *Nucleic Acids Res.* **14:**5111.

Jenkinson, D. H. 1960. The antagonism between tubocurarine and substances which depolarize the motor endplate. *J. Physiol.* **152:**309-324.

Kegel, D. R., B. D. Wolf, R. E. Sheridan, and H. A. Lester. 1985 Software for electrophysiological experiments with a personal computer. *J. Neurosci. Meth.* **12:**317-330.

Krieg, P. A. and D. A. Melton. 1984. Functional messenger RNAs are produced by SP6 *in vitro* transcription of cloned cDNAs. *Nucleic Acids Res.* **12:**7057-7070.

Krouse, M. E., H. A. Lester, N. H. Wasserman and B. F. Erlanger. 1985. Rates and equilibria for a photoisomerizable antagonist at the acetylcholine receptor of *Electrophorus* electroplaques. *J. Gen. Physiol.* **85:**235-256.

LaPolla, R. J., K. M. Mayne, and N. Davidson. 1985. Isolation and characterization of cDNA clone for the complete coding region of the δ subunit of the mouse acetylcholine receptor. *Proc. Natl. Acad. Sci. USA* **81:**7970-7984.

Leonard, J. P., J. Nargeot, T. P. Snutch, N. Davidson, and H. A. Lester. 1987. Ca channels induced in *Xenopus* oocytes by rat brain mRNA. *J. Neurosci.*, **7:**875-881.

Lester, H. A., J.- P. Changeux, and R. E. Sheridan. 1975. Conductance increases produced by bath application of cholinergic agonists to *Electrophorus* electroplaques. *J. Gen. Physiol.* **65:**797-816.

Magleby, K. L., and C. F. Stevens. 1972a. The effect of voltage on the time course of end-plate currents. *J. Physiol.* **223:**151-171.

Magleby, K. L., and C. F. Stevens. 1972b. A quantitative description of endplate currents. *J. Physiol.* **223:**173-197.

Mayne, K. M., K. Yoshii, L. Yu, H. A. Lester, and N. Davidson. 1987. Expression of mouse-*Torpedo* acetylcholine receptor subunit chimeras and hybrids in *Xenopus* oocytes. *Mol. Brain Res.*, in press.

Melton, D. A., P. A. Krieg, M. R. Rebagliati, T. Maniatis, K. Zinn, and M. R. Green. 1984. Efficient *in vitro* synthesis of biologically active RNA and RNA hybridization probes from plasmids containing a bacteriophage SP6 promoter. *Nucleic Acids Res.* **12:**7035-7056.

Methfessel, C., V. Witzeman, B. Sakmann, T. Takahashi, M. Mishina, and S. Numa. 1986. Patch clamp measurements on *Xenopus laevis* oocytes: currents through endogenous channels and implanted acetylcholine receptor and Na^+ channels. *Pflugers Arch.* **407:**577-588.

Mishina, M., T. Kurosaki, T. Tobimatsu, Y. Morimoto, M. Noda, T. Yamamoto, M. Terao, J. Lindstrom, T. Takahashi, M. Kuno, and S. Numa. 1984. Expression of functional acetylcholine receptor from cloned cDNAs. *Nature* **307:**604-608.

Mishina, M., T. Tobimatsu, K. Imoto, K.-I. Tanaka, Y. Fujita, K. Fukuda, M. Kurasaki, H. Takahashi, Y. Morimoto, T. Hirose, S. Inayama, T. Takahashi, M. Kuno, and S. Numa. 1985. Localization of functional regions of acetycholine receptor α-subunit by site- directed mutagenesis. *Nature* **313:**364-369.

Neubig, R. R., and J. B. Cohen. 1979. Equilibrium binding of [^{3}H]tubocurarine and [^{3}H]acetylcholine by *Torpedo* postsynaptic membranes: stoichiometry and ligand interactions. *Biochemistry* **18:**5464-5475.

Neubig, R. R., and J. B. Cohen. 1980. Permeability control by cholinergic receptors in *Torpedo* postsynaptic membranes: agonist dose-response relations measured at second and millisecond times. *Biochemistry* **19:**2770-2779.

Penefsky, H. S. 1977. Reversible binding of P_1 by beef heart mitochondrial adenosine triphosphate. *J. Biol. Chem.* **252:**2891-2899.

Pennefather, P. and D. M. J. Quastel. 1981. Relationship between subsynaptic receptor blockade and response to quantal transmitter at the mouse neuromuscular junction. *J. Gen. Physiol.* **78:**313-344.

Sakmann, B., C. Methfessel, M. Mishina, T. Takahashi, T. Takai, M. Kurasaki, K. Fukuda, and S. Numa. 1985 Role of acetylcholine receptor subunits in gating of the channel. *Nature* **318:**538-543.

Sanger, F., S. Nicklen, and A. R. Coulson. 1977. DNA sequencing with chain-terminating inhibitors. *Proc. Natl. Acad. Sci. USA* **74:**5463-5467.

Sheridan, R. E., and H. A. Lester. 1977. Rates and equilibria at the acetylcholine receptor of *Electrophorus* electroplaques. A study of neurally evoked

postsynaptic currents and of voltage-jump relaxations. *J. Gen. Physiol.* **70:**187-219.

Sine, S. M. and P. Taylor. 1980. The relationship between agonist occupation and the permeability response of the cholinergic receptor revealed by bound cobra α-toxin. *J. Biol. Chem.* **255:**10144-10156.

Sine, S. M. and P. Taylor. 1981. Relationship between antagonist occupancy and the functional capacity of the acetylcholine receptor. *J. Biol. Chem.* **256:**6692-6699.

Stroud, R. M. and J. Finer-Moore. 1985., Acetylcholine receptor structure, function, and evolution. *Ann. Rev. Cell. Biol.* **1:**317-351.

Sumikawa, K., M. Houghton, J. S. Emtage, B. M. Richards, and E.A. Barnard. 1981. Active multi-subunit ACh receptor assembled by translation of heterologous mRNA in *Xenopus* oocytes. *Nature* **292:**862.

White, M. M., K. M. Mayne, H. A. Lester, and N. Davidson. 1985. Mouse-*Torpedo* hybrid acetylcholine receptors: functional homology does not equal sequence homology. *Proc. Natl. Acad. Sci. USA* **82:**4852-4856.

Yoshii, K., L. Yu, K. M. Mayne, N. Davidson, and H. A. Lester. 1987. Mouse-*Torpedo* acetylcholine receptor subunit hybrids expressed in *Xenopus* oocytes: equilibrium properties. *Biophys. J.* **51:**60a.

Yu, L., R. J. LaPolla, and N. Davidson. 1986. Mouse muscle nicotinic acetylcholine receptor γ subunit: cDNA sequence and gene expression. *Nucleic Acids Res.* **14:**3539-3555.

CHAPTER 5

Acetylcholine receptor ion channel properties:

A study of elementary currents

Lei Yu, Reid J. Leonard, Norman Davidson, and Henry A. Lester

SUMMARY

The single channel properties of nicotinic acetylcholine receptors (AChRs) have been studied by patch clamp recording. We have examined homogeneous and hybrid receptors expressed on the membrane of *Xenopus* oocytes microinjected with the desired combinations of *in vitro* transcribed mRNAs coding for the mouse and *Torpedo* AChRs.

In order to understand the mechanism underlying the phenomenon of voltage sensitivity previously observed at the level of whole cell electrophysiological recording, three parameters of the mouse AChR ion channel were examined for their relationship with the membrane electrical potential: a conductive parameter, the single-channel conductance, and two kinetic parameters, the channel-opening rate and the channel-closing rate. It was found that the single-channel conductance is independent of the membrane potential and that both the opening rate and the closing rate of the ion channel are influenced by the voltage. The relative extent of the voltage dependence for both rates was evaluated. It appears that while both the opening and closing rates form the basis for the voltage sensitivity of the whole-cell response to the agonist, the channel-closing rate makes the major contribution.

The subunit involvement in the determination of the gating properties between *Torpedo* and mouse AChRs was also studied. It was found that the δ subunit dictates the species specificity of mean open duration time, in agreement with an independent study using AChRs from calf and *Torpedo* (Sakmann *et al.*, 1985). Our results also demonstrated the roles of the β and the δ subunits in determining voltage sensitivity, supporting the findings of our previous work by whole-cell recording and thus extending its conclusions to the level of single ion channels.

INTRODUCTION

Ion channels in cell membranes are generally classified into two groups according to their stimuli. Voltage-gated channels are activated by changes in membrane potential, are selective in their permeability to ions, and are named for their ion selectivity, such as sodium channel, potassium channel, and chloride channel. Ligand-gated channels, on the other hand, are activated by the binding of certain organic molecules, are often not selective in their permeability to ions beyond cation/anion specific, and are called receptors for their chemical "activators," such as acetylcholine receptor (AChR), serotonin receptor, and GABA receptor. These receptors are often referred to as "electrically inexcitable channels" (Hille, 1984), meaning the onset of their activity is not responsive to changes in membrane potential. In studies of the AChR, however, it became clear that once the channel is activated by ligand binding, its behavior *is* influenced by the membrane potential (Takeuchi and Takeuchi, 1959; Kordas, 1969; Magleby and Stevens, 1972a,b). This effect, known as the voltage sensitivity of AChR, has been studied extensively with the use of whole cell voltage clamp technique.

The advent of the patch-clamp technique (Neher and Sakmann, 1976) provided the high resolution in electrophysiological recording necessary to detect currents through single ion channels. The methodology has been improved significantly since its inception and is described in great detail in a book edited by Sakmann and Neher (1983). The principle of the technique is illustrated schematically in Figure 1. A glass microelectrode is moved toward the cell till its fine tip touches the cell membrane. Under favorable conditions, the heat-polished rim of the electrode tip and the membrane forms a tight seal with an electrical resistance of the order of giga-ohms. The high resistance isolates the membrane patch electrically and ensures that all the currents flowing through this membrane

Fig. 1. Patch-clamp technique.

The schematic representation shows the various ways to obtain a membrane patch for single channel recording. A by-product enroute to obtain an excised "outside-out" patch is a "tight-seal" for whole-cell recording.

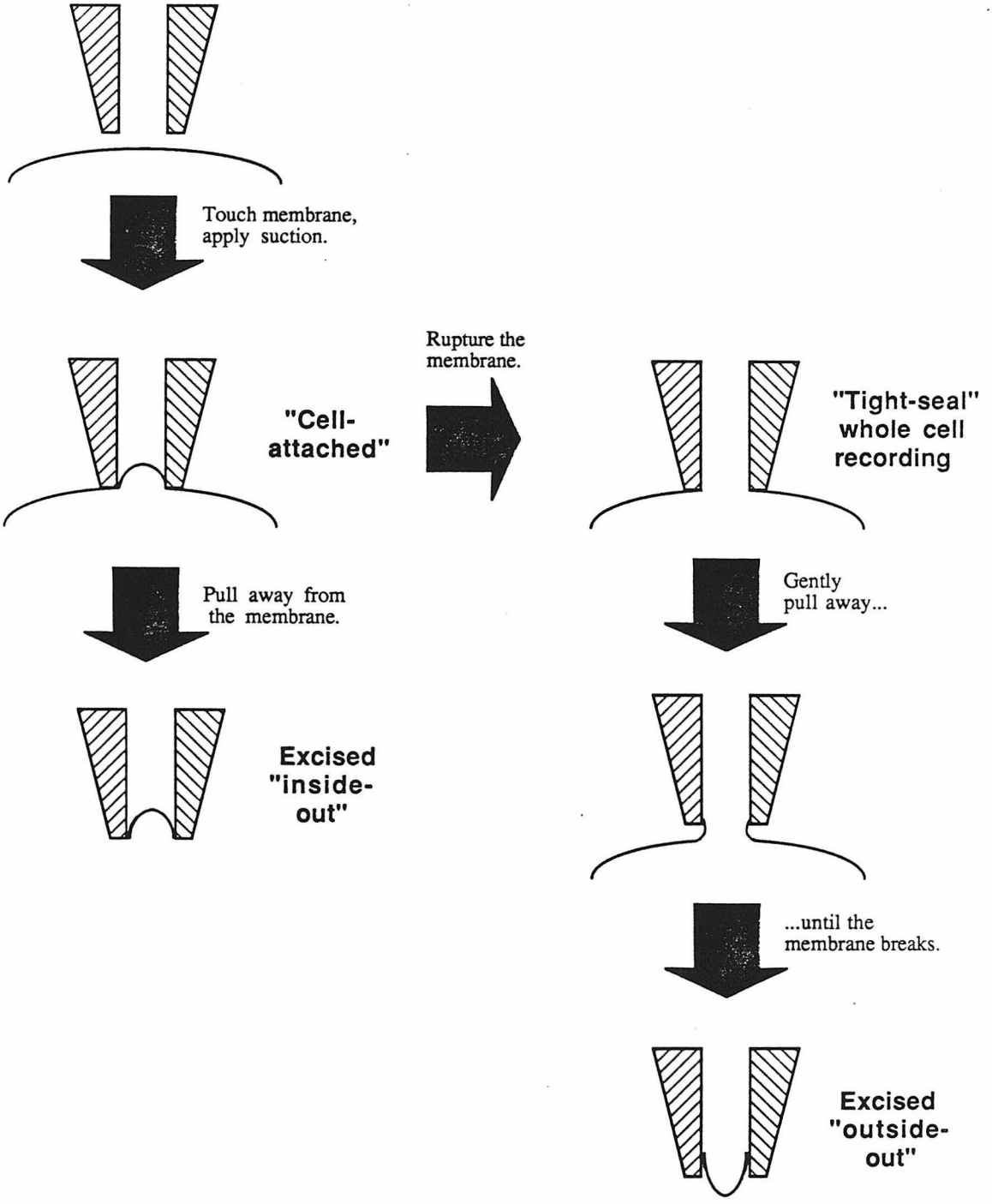
Touch membrane,
apply suction.
"Cell-
attached"
Rupture the
membrane.
"Tight-seal"
whole cell
recording
Pull away from
the membrane.
Gently
pull away...
Excised
"inside-
out"
...until the
membrane breaks.
Excised
"outside-
out"

area also flow through the recording circuit. Since the microelectrode has a very small opening (a few square microns), the recording is restricted to only a few channels at a time. This technique thus enables one to resolve elementary currents as small as 1 pA, *i. e.*, the flow of ~6000 monovalent ions per millisecond. There are several variations for the membrane patch configuration. After a giga-ohm seal is formed, the membrane patch underneath the electrode can be voltage-clamped for membrane current recording while the cell is still attached to the electrode ("cell-attached" mode). Alternatively, the membrane patch can be ripped off from the cell by pulling away the microelectrode to form an "excised" patch, leaving the cytoplasmic side of the membrane facing the bath solution and the extracellular side in contact with the electrolyte inside of the electrode ("inside-out" mode). If, on the other hand, the membrane underneath the microelectrode is ruptured before excision by a negative pressure (the traditional method) or a positive pressure (our recent variation), a conductive pathway is established between the electrode lumen and the cell interior. The entire cell can be voltage-clamped at this point ("tight-seal" whole cell recording, appropriate for small cells). If the electrode is gently pulled away from the cell, the membrane will be stretched until it breaks. With a certain percentage (inversely proportional to the operator's blood pressure), the membrane snaps back to seal the electrode tip. The patch formed this way has the exterior side facing the bath solution ("outside-out" mode) and can be voltage-clamped. Using the patch-clamp technique, the properties of AChRs have been studied extensively in cultured cells and animal tissues (Auerbach and Sachs, 1984). One drawback of these studies is the uncertainty of the homogeneity of the AChR channels under investigation, since it is known that vertebrate muscles express different types of AChRs with different kinetic and conductive properties (Katz and Miledi, 1972; Neher and Sakmann, 1976; Auerbach and Lingle, 1986). One way to overcome this

uncertainty is to generate a homogeneous population of AChRs. The molecular cloning of the cDNA sequences coding for all four AChR subunits from several species (see Chapter 1 for references) has provided such an opportunity. Using the AChR cDNA clones to produce *in vitro* transcribed mRNAs, Mishina *et al.* (1986) studied the fetal and adult forms of bovine AChR and confirmed that the heterogeneity of the AChR channel properties in animal tissue is indeed due to differences in AChR amino acid sequences.

Oocytes from the African frog *Xenopus* have provided an adequate system for the expression of foreign mRNAs and subsequent electrophysiological analysis of membrane ion channels (Miledi and Sumikawa, 1982; Miledi *et al.*, 1982; Barnard *et al.*, 1982; White *et al.*, 1985; Mishina *et al.*, 1986; Dascal *et al.*, 1986). Using the oocyte expression system and the cDNA clones from mouse and *Torpedo*, we have investigated the AChR ion channel properties at the level of whole-cell recording (Mayne *et al.*, 1987, and this thesis; Yoshii *et al.*, 1987, and this thesis). In the present study, we used the patch-clamp technique to study the single-channel properties of AChRs expressed in oocytes following injection of RNAs encoding the AChR subunits from mouse and *Torpedo*. We also studied hybrid AChRs constructed by mixing subunit RNAs from both mouse and *Torpedo* AChR. Our results confirm the conclusions from the whole-cell voltage clamp study reported earlier (Yoshii *et al.*, 1987, and this thesis). Our results further indicate that the influence of membrane potential on the channel opening rate is small and that the voltage dependence of the channel closing rate is the main source of the voltage sensitivity in the whole-cell response to stimulation by agonist.

MATERIALS AND METHODS

AChR cDNAs and mRNAs

The source of cDNA clones for the AChR subunits was as described by Yoshii *et al.* (1987, and this thesis) for the mouse receptor and by White *et al.* (1985) for the *Torpedo* receptor.

The synthesis of AChR mRNAs by *in vitro* transcription followed the protocol of White *et al.* (1985) with some modifications (Mayne *et al.*, 1987, and this thesis).

Preparation and maintenance of oocytes and RNA injection

The procedures were as described (Yoshii *et al.*, 1987, and this thesis) with the following modifications. The concentration of mRNA for microinjection varied from 0.1 to 1mg/ml, in order to obtain a receptor density on the oocyte surface which was optimal for patch-clamp recording. A new injection needle was used every time the RNA solution was changed in order to prevent cross-contamination between different combinations of AChR mRNAs. Oocytes were incubated at 20^{o}C in a humidified incubator and the bath solution was changed every day. After 48-60 h incubation, oocytes were transferred to 4^{o}C for storage for up to 10 days.

Electrophysiology

The whole-cell response to ACh was recorded with the technique of the two intracellular microelectrode voltage clamp as described (Yoshii *et al.*, 1987, and this thesis) with the following modifications. The temperature of the oocyte was lowered during recording to improve the resolution of kinetic measurements. A Plexiglas recording chamber with a volume of 170µl was attached to a metal

thermotransfer platform. A layer of heat-transferring silicone compound (Type Z9, GC Electronics, Rockford, Illinois) was sandwiched between the chamber and the platform to ensure efficient heat transfer. The chamber was continuously perfused during voltage-clamp experiments at a rate of 5ml/min. The superfusion solution was temperature-controlled via a Gizmo (Model A, Lester Instruments Inc., Pasadena, California), using the double-circulation cooling method (Lester, 1970). The temperature in all the experiments was held at 12+0.5^{o}C using a Lauda/Brinkmann circulator (Model K-2/R, Brinkmann Instruments Inc., Westbury, New York) connected to the chamber-cooling and superfusion-cooling devices. The superfusion solution contained 100mM KCl, 1mM $MgCl_2$, 10mM EGTA, 0.3μM atropine sulfate, and 10mM HEPES, pH7.2, 240mOsm. ACh was added to the solution when desired. Generation of command voltages, recording of response currents, and data analysis were aided with the computer programs CLAMPEX/CLAMPAN (Kegel *et al.*, 1985, commercially available with pCLAMP, Axon Instruments, Burlingame, California).

For single-channel recording, individual oocytes were transferred to hypertonic Barth's medium containing 100mM NaCl for 2-5min, washed in Barth's medium, and then transferred to the recording chamber for the removal of vitelline membrane. The removal was performed manually with forceps. The oocyte was transferred back to Barth's medium after an excised patch was obtained and before the superfusion of ACh-containing solution to prevent desensitization of the oocyte. This procedure allowed us to obtain multiple patches from the same oocyte.

Patch pipettes were fabricated from hard glass capillaries (KG-33, Garner Glass Company, Claremont, California) by a two-step pulling procedure (Hamill *et al.*, 1981) with a vertical pipette puller (Newport Research Corp., Fountain Valley, California), heat-polished on a microforge (Sensaur, France), and filled with

superfusion solution before use. Pipettes typically had a resistance of 10-40MΩ. A Dagan 8900 patch clamp amplifier (Dagan Corp., Minneapolis, Minnesota) was used with a 10GΩ feedback resistor. The patch-clamp probe was controlled mechanically with an oil drive (Narishige Scientific Instrument Lab., Tokyo, Japan). Command voltages were generated by a voltage calibrator (Model 2001, World Precision Instrument Inc., New Haven, Connecticut).

The single-channel currents were monitored simultaneously on an oscilloscope and a chart recorder. During the experiments, the single-channel currents and holding potential were filtered to 5kHz with an 8-pole low-pass Bessel filter (Model 902LPF, Frequency Devices Inc., Haverhill, Massachusetts), digitized with a modified Nakamichi digital mastering processor (Model DMP-100 with a PS-10 power supply, Nakamichi Corp., Japan), and recorded with a Betamax stereo videocassette recorder (Model SL-2700, Sony Corp., Japan) on magnetic videotapes.

Single channel data acquisition and analysis

Data acquisition and subsequent analysis were aided with a set of computer programs FETCHEX/FETCHAN/PSTAT (Kegel *et al.*, 1985). New features were added to these programs as the need developed (Floyd Shon, personal communication).

The digitized single channel currents stored on videotape were converted back to analog signals via the Nakamichi processor, filtered at 2kHz with the 8-pole Bessel filter (except 3kHz for *Torpedo* AChR), and fed into a window discriminator. Current signals triggered by AChR channel openings were led to an analog-to-digital convertor (Labmaster, Scientific Solutions, Ohio) and stored by a microcomputer (IBM PC-AT, IBM Corp., Armonk, New York). The signals were sampled with FETCHEX at 10kHz and the digitized data were written to a "data

file" on a 30 megabyte hard disk. Each data file contained openings from a single patch at a particular holding potential.

The data analysis of single channel currents consisted of two discrete steps: construction of idealized records and statistical analysis of the idealized records (see Results and Discussion). The construction of idealized records was performed either in manual or in automatic mode with FETCHAN. The program compiled channel openings as a list of "events." For each event, the following information was recorded, the time since the end of the last opening, the duration of the present opening, the amplitude and its standard deviation, and the cumulative time since the beginning of the data file. The event file, which amounted to an idealized record of the original data, constituted the permanent record of the experiment and was saved on diskette. Statistical analyses of the idealized records were performed with PSTAT, which employs a BASIC program (Schreiner *et al.*, 1985) for curve fitting using the Marquardt algorithm for least-squares estimation (Marquardt, 1963).

RESULTS AND DISCUSSION

Voltage Sensitivity of the Acetylcholine Receptor

A description of the phenomenon

When a cell with AChR molecules on its surface is stimulated by agonist, a transmembrane current flow can be recorded with voltage clamp techniques. It has been found that the amount of current is not linearly related to the electric driving force across the membrane: it becomes less as the membrane potential becomes more positive, thus the term "voltage sensitivity" (Kordas, 1969; Magleby and Stevens, 1972a,b). This effect is illustrated by the experiment shown in Figure 2. *Xenopus* oocytes injected with mouse AChR mRNAs (see Materials and Methods) were held in the voltage-clamp mode with two intracellular microelectrodes. A series of voltage steps (Figure 2A) was applied to the cell with a 20-mV increment. The response of the cell was measured as the amount of the current, supplied by the feedback circuit of the electronic instruments, necessary to hold the cell at the desired membrane potential. When the cell was not perturbed by the ligand, its response was linearly related to the voltage command, as reflected by the equal space between current traces in Figure 2B. After acetylcholine was applied to the bath solution to activate the receptors, the response of the cell to command voltage was increased (Figure 2C). However, this increase was not linear over the voltage range: As the potential became more positive, the increase in the response became less. This nonlinearity was more evident when the net ACh-induced current obtained by subtraction of the control current trace from the ACh-induced current trace was plotted, as shown in Figure 2D. This phenomenon is referred to as the voltage sensitivity of the AChR (Magleby and Stevens, 1972a,b).

Fig. 2. AChR voltage sensitivity.

The effect of membrane potential on the whole cell response to the agonist ACh is illustrated. The data shown are from an oocyte with the mouse AChR.

A. Command voltages. The holding potential for the whole-cell voltage clamp is -60mV. A set of 10 command voltages is applied to the cell, starting at -100mV and increasing with a 20mV step.

B. Response of the cell in the absence of ACh. The transmembrane currents of the cell in response to the command voltages are shown. The initial peak is due to the transient capacitative current.

C. Response in the presence of ACh.

D. Net current induced by ACh. The currents shown in **B** are subtracted from those in **C** to give the net ACh-induced currents.

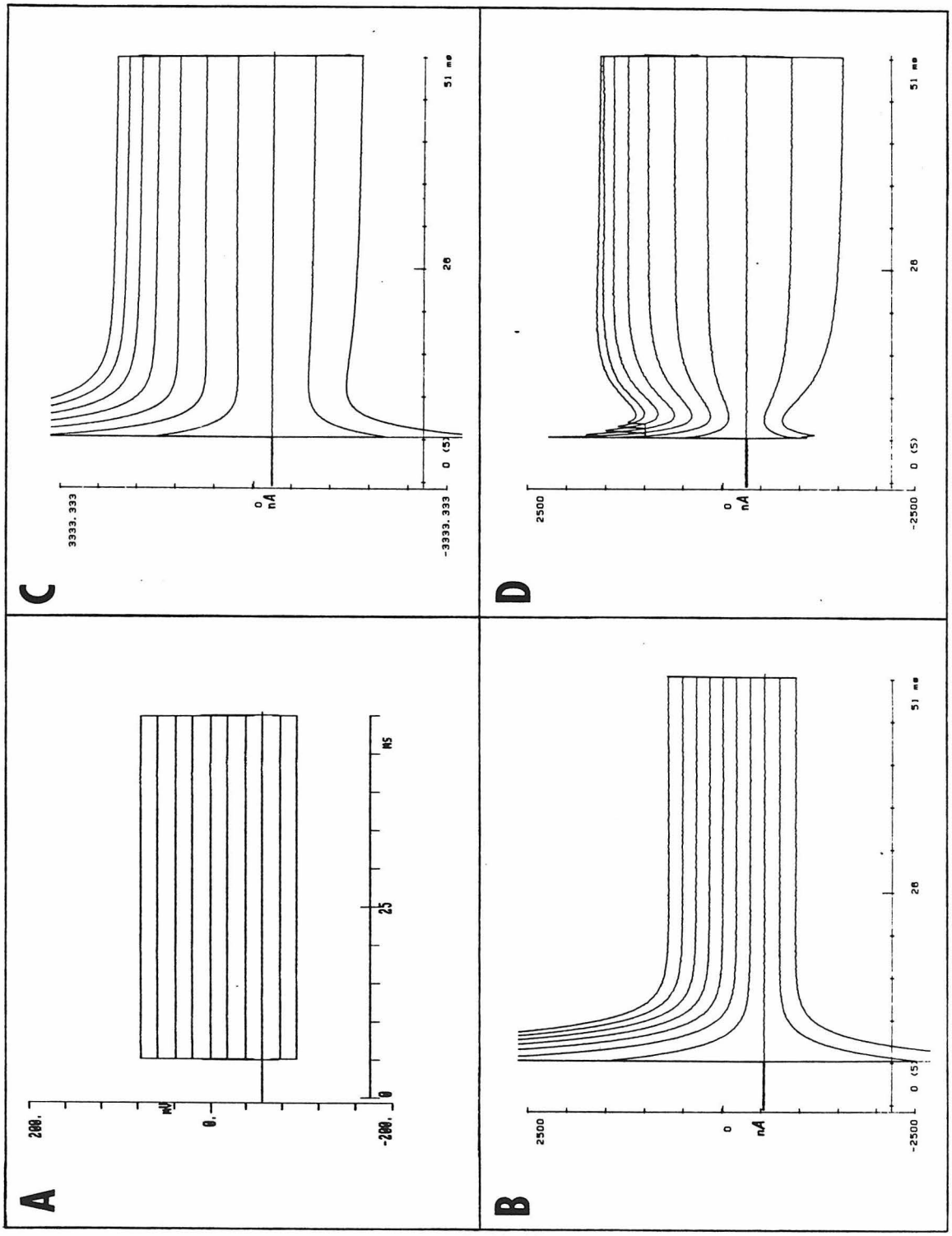
A
200.
mV
0.
-200.
25
MS
0
B
2500
0
nA
-2500
20
51 ms
0 (S)
C
3333.333
0
nA
-3333.333
20
51 ms
0 (S)
D
2500
0
nA
-2500
20
51 ms
0 (S)

Not all the AChRs from different species are influenced by voltage to the same extent. Figure 3 shows the current-voltage plots of the AChRs from *Torpedo* (Figure 3A) and from mouse (Figure 3B). It is apparent that while the I-V curves for both receptors are nonlinear, the voltage influence is stronger for the mouse AChR than for the *Torpedo* AChR. The slope between any two points in the I-V plots, *i. e.*, the difference in net current between these two points divided by the difference in corresponding potentials, gives the whole-cell slope conductance g in that potential range. The voltage sensitivity can therefore be described as a decrease in whole-cell conductance as the membrane potential becomes more positive. The extent of this voltage sensitivity can be quantitated by the ratio of any two whole-cell conductance values, for example, the ratio of g_{-90} (slope between -100mV and -80mV) and g_{+30} (slope between +20mV and +40mv) in our previous study (Yoshii *et al.*, 1987, and this thesis).

A consideration of kinetics

Such is the phenomenon of AChR voltage sensitivity. What is the underlying mechanism?

In a simple scheme for the AChR activation:

$$2A + R \underset{k_2}{\overset{k_1}{\rightleftharpoons}} A_2R \underset{\alpha}{\overset{\beta}{\rightleftharpoons}} A_2R^* \quad ; \qquad (1)$$

two acetylcholine molecules (A) bind to one receptor (R). The complex (A_2R) assumes the open-channel state (A_2R^*) with a finite probability, determined by the opening rate constant β. The open channel returns to the closed state with a closing rate constant α. In a voltage clamp experiment such as the one shown in

Fig. 3. Whole-cell I-V relationship.

The ACh-induced whole-cell currents are plotted against the corresponding membrane potentials. Each plot shows the typical results from a single oocyte.

A. I-V relationship of the *Torpedo* AChR.

B. I-V relationship of the mouse AChR.

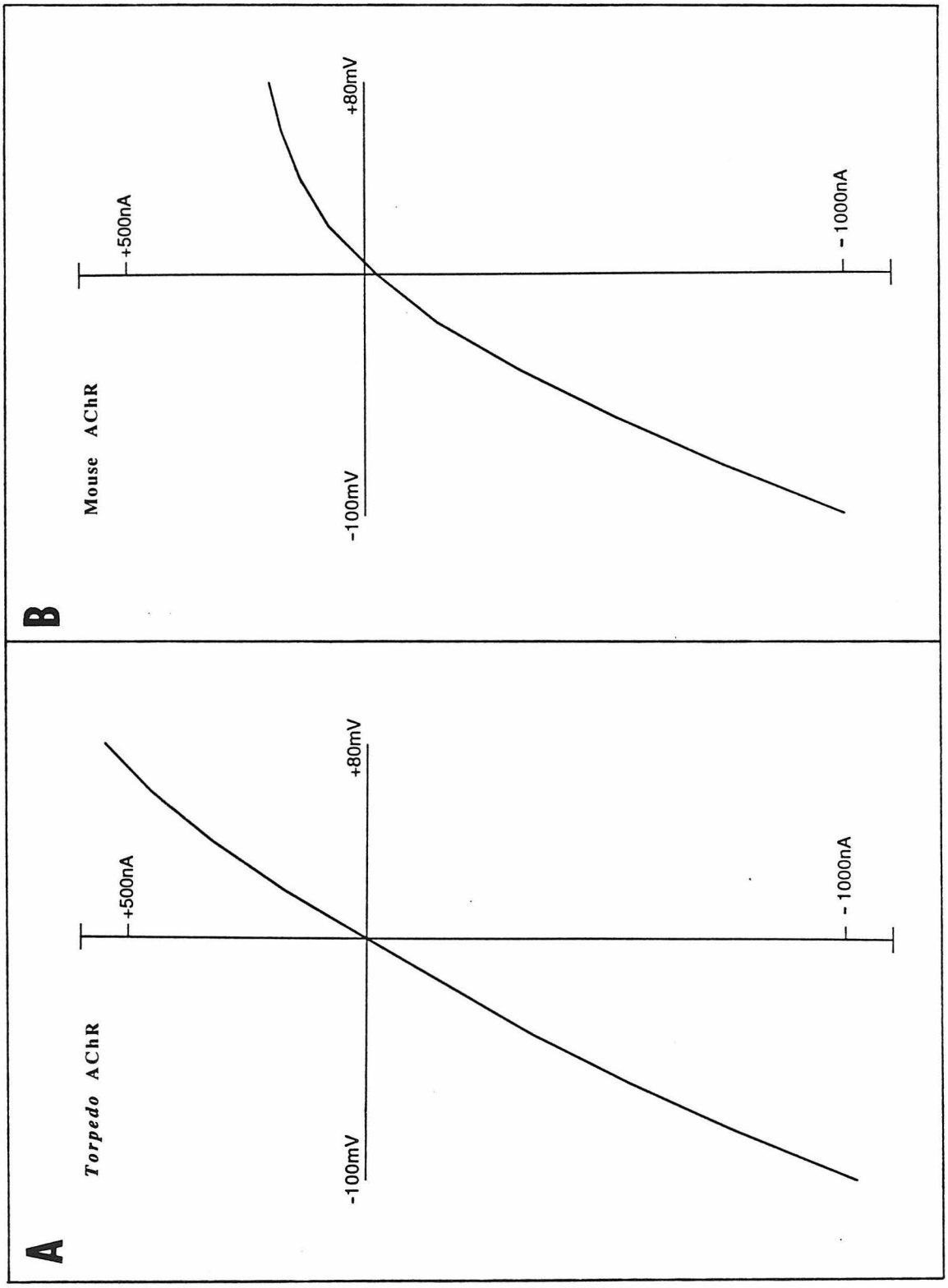
A
Torpedo AChR
+500nA
+80mV
-100mV
- 1000nA
B
Mouse AChR
+500nA
+80mV
-100mV
- 1000nA

Figure 2 where the agonist concentration and the number of the receptors on the cell surface do not change, the whole-cell current in response to acetylcholine stimulation is determined by three factors: how often the channel opens, how much current passes through the channel in unit time, and how long the channel stays open. β and α reflect the channel opening and closing probabilities, and the conductance is expressed as the single-channel conductance (the slope of a single-channel I-V curve). Voltage dependence of any of these three parameters can contribute to the voltage sensitivity in whole-cell response to ACh.

Single-channel recording

To study the single-channel properties of the mouse AChR, we chose to use the method of excised outside-out patch recording (see Figure 1). This mode of recording offers several advantages over the other alternatives, namely, the cell-attached mode and the excised inside-out mode.

Because of the high sensitivity of the electronic circuits for single-channel recording, the flow of bath solution during superfusion, which causes slight movements of the cell, increases the background noise in the cell-attached mode. Cell movements also increase the opening frequency of membrane stretch channels in *Xenopus* oocytes (Methfessel *et al.*, 1986), making the data analysis more difficult. The excised inside-out method does not have these problems, but it has a disadvantage that also exists in the cell-attached mode: Because the extracellular side of the membrane is now facing the inside of the microelectrode, the agonist ACh has to be in the pipette in order to induce the AChR channel opening. This not only eliminates the option of varying agonist concentration to obtain a favorable channel-opening frequency, but also renders it difficult to prove that the channel openings are indeed ACh-induced rather than being triggered by some other stimuli. With the excised outside-out configuration, the

extracellular side of the membrane faces the bath solution, and the superfusion can be switched among solutions of desired composition. The authenticity of the ACh-induced channels can be easily verified by changing the superfusion from agonist-free to agonist-containing solution, and an optimal frequency of channel opening can be obtained to minimize the effect of agonist-induced desensitization while maintaining a reasonable opening frequency.

Using the excised outside-out patch recording technique, we studied the single channel properties of the mouse AChR. Figure 4 shows examples of the single-channel current traces. Certain features are apparent from these traces. First of all, to the extent of recording resolution, the channel opening approximates an all-or-none event: The transitions between closed and open states are fast, and the amplitude of the single-channel current reaches a steady value once the channel is open. This makes it desirable and convenient to represent the single-channel currents as square waves. The last row in Figure 4 shows such a representation--- an idealized record. As can be seen, the idealized record is a fairly good approximation of the original current trace above it. Analysis of idealized records is, however, much easier than that of the real current traces, and is therefore a standard practice in single-channel studies (Sakmann and Neher, 1983).

Another feature of the single-channel currents is the variability of both the open and the closed duration from event to event. This is the case because the open and closed states of an ion channel are actually different conformations a receptor-agonist complex can assume. The movements of the atoms in the complex are the underlying cause for the transition between the two states, and the stochastic nature of the thermodynamic movements results in the randomness of individual transitions. However, the *probabilities* for the transitions are not random --- they are governed by the law of mass action. As can be shown from

Fig. 4. AChR single-channel current.

Examples of the ACh-induced single-channel currents from the mouse AChR are shown. The holding potential was -100mV. Inward current is downward. The bottom row shows the idealized records of the openings above it.

5 pA
10 ms

the kinetic equation (Equation 1), the times for individual events are stochastically distributed in accordance with these probabilities, like any statistical processes (Davidson, 1962). To obtain a good estimate of the probability of a stochastic process, a large number of events must be sampled. Therefore, statistical analysis is in order.

Analysis of single channel currents

As can be seen in Figure 4, the amplitude of single-channel currents at a given membrane potential appears to fluctuate around a constant value. This is confirmed by the scatter-plot analysis shown in Figure 5A. The amplitude values of all the openings from a patch held at -100mV were plotted against their channel open times. The plot appears as a single cloud of points, showing that the openings of various duration times all have the same unit conductance.

Since the amplitude values all center around a steady value, their distribution can be approximated by a Gaussian (normal) function. To obtain the mean amplitudes, the single channel currents were measured at various membrane potentials. The amplitude values from each potential were pooled together to construct a histogram for distribution curve fitting. Figure 5B is an example of the amplitude histogram histogram for the mouse AChR at the membrane potential of -100mV, containing the same data used in Figure 5A. The vertical steps represent the number of channel openings for the amplitude values in the corresponding amplitude range. The histogram was fitted to the normal distribution function:

$$Y = \frac{1}{\sqrt{2\pi}\sigma} e^{-\frac{1}{2}\left(\frac{x-\lambda}{\sigma}\right)^2} \quad ; \qquad (2)$$

where λ is the offset on the abscissa (therefore, the mean amplitude) and σ is the standard deviation, reflected graphically as the broadness of the data distribution. The fitting was aided by a subroutine in the computer program PSTAT (see Materials and Methods) using the Marquardt algorithm for least-squares fitting of nonlinear parameters (Marquardt, 1963). The smooth curve in Figure 5B shows the result of fitting. [It should be pointed out that because of the nature of normal distribution, a fairly good estimate can be made by simply calculating the numerical mean of the amplitude values. Function fitting improves the estimation to a certain extent, but more importantly, it serves to satisfy the drive for nonessential accuracy possessed by many scientists (N. Davidson, personal communication)].

Because the single channel conductance is defined as the slope of the current-voltage relationship (g=i/V), the mean amplitude values at different membrane potentials were plotted against the respective voltages to construct an I-V plot. As shown in Figure 5C, the data points from fitted Gaussian distribution are marked by the square symbols, and the straight line represents the result of linear regression of the data. It is clear that the amplitude is linearly related to the membrane potential. In other words, the single-channel conductance (the slope of the line) does not change with membrane potential.

Voltage effect on the duration of channel openings

Since the duration of channel opening is of a stochastic nature, a meaningful estimate can be obtained only with a large number of events, usually several hundred to a few thousand channel openings (Colquhoun and Sigworth, 1983). For a kinetic process such as the AChR channel opening postulated in Equation (1), once the channel is open, its duration is governed only by the closing

Fig. 5. Single-channel I-V relationship.

A. An example of scatter plot. The amplitude values of the single-channel currents at -100mV from a patch containing the mouse AChR are plotted against the corresponding duration times of these openings on a semilogarithmic scale.

B. An example of amplitude histogram. The data are from the same patch as those in A. Each vertical step represents the number of channel-opening events for the amplitude values on the horizontal axis. The smooth curve is the fitted Gaussian distribution.

C. I-V plot of the single-channel currents from the mouse AChR. Squares represent the mean amplitude values obtained from the Gaussian distributions fitted to the histograms at different voltages. The line represents the result of linear regression of the data.

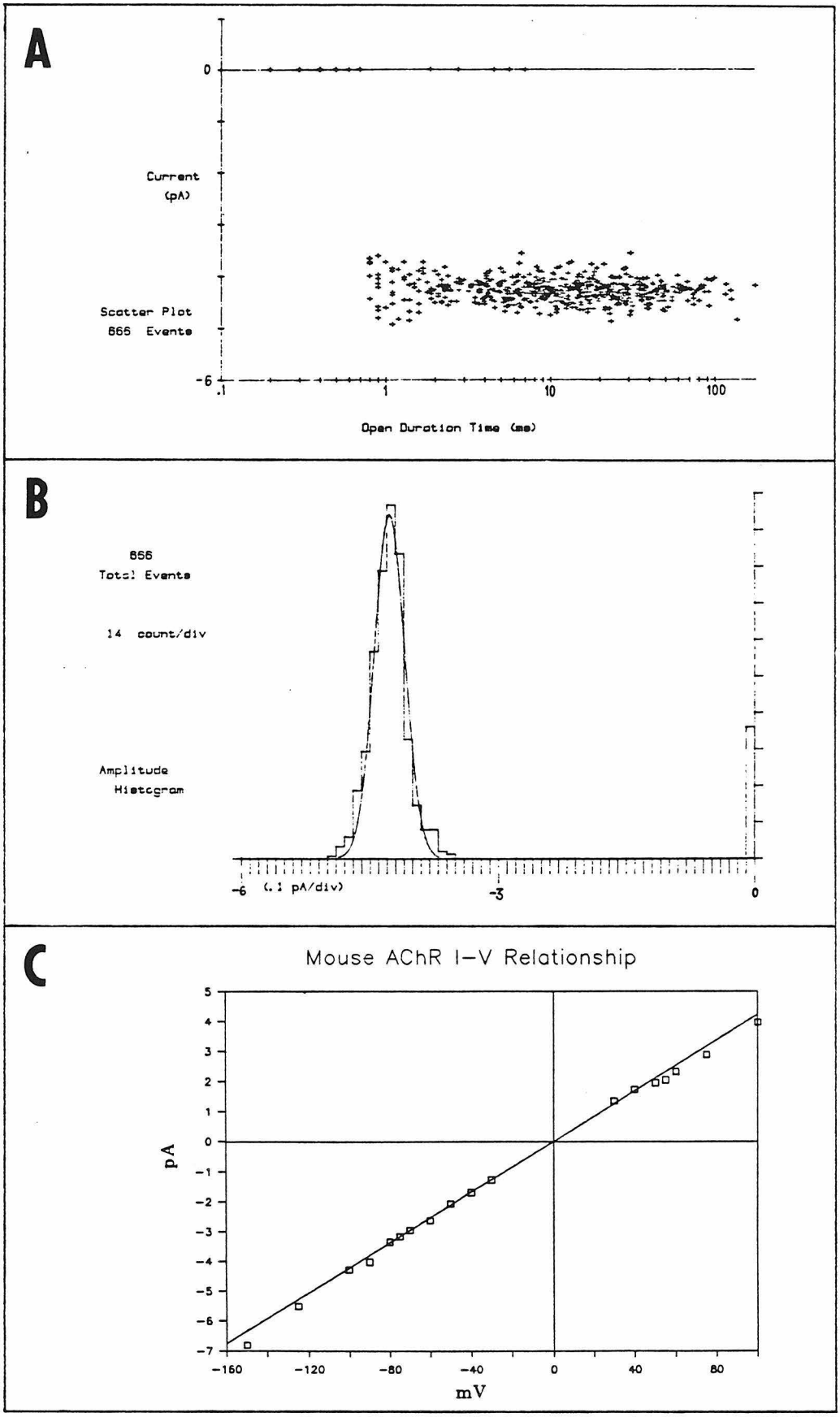
A
0
Current
(pA)
Scatter Plot
866 Events
-6
.1
1
10
100
Open Duration Time (ms)
B
866
Total Events
14 count/div
Amplitude
Histogram
-6 (.1 pA/div)
-3
0
C
Mouse AChR I-V Relationship
pA
mV
5
4
3
2
1
0
-1
-2
-3
-4
-5
-6
-7
-160
-120
-80
-40
0
40
80

probability that follows an exponential distribution. Using the data from the excised outside-out patch recording, the open durations of all the channel openings at a given membrane potential were measured, and histograms were constructed for each membrane potential. Figures 6A and 6B are examples of open-duration histograms at the membrane potentials of -60mV and +60mV, respectively. Each histogram was fitted to a double exponential function:

$$Y = C_0 + A_1 e^{-\frac{t}{\tau_1}} + A_2 e^{-\frac{t}{\tau_2}} \quad ; \qquad (3)$$

where C_0 is the offset on ordinate, A_1 and A_2 are the values at t=0 for the two exponential components, and τ_1 τ_2 are the time constants for the components. The two exponential components are a brief one and a long one, with the long one predominating. The brief component has been reported for AChRs from most preparations, but its significance is not clear, although it has been suggested to represent the monoliganded channel opening (see Chapter 1). The major exponential component with the long time constant contributes the most of the time-averaged current, and the standard practice is to base the interpretations on this component. We have followed this practice in the present study. The smooth curves in the histograms in Figures 6A and 6B are the fitted exponential functions, and the time constants of these exponentials give the mean duration of elementary currents with τ values of 8.65ms at -60mV and 3.21ms at +60mV. Evidently, the channel duration is strongly influenced by the membrane voltage. In order to estimate the degree of the voltage effect on channel duration, the τ values at various membrane potentials were calculated and plotted against the corresponding voltages on semilogarithmic coordinates, as shown in Figure 6C.

Fig. 6. Voltage effect on channel-closing rate.

The open durations of AChR ion channels at different voltages were analyzed to evaluate the voltage effect on the channel-closing rate of the mouse AChR.

A. Open duration histogram for the mouse AChR ion channels at -60mV. Each bar represents the number of events in that time range. The smooth curve represents the fitted exponential function for the distribution. The time constant is 8.65ms.

B. Open duration histogram for the mouse AChR ion channels at +60mV. The time constant is 3.21ms.

C. Relationship between the membrane voltage and the AChR open-channel duration. The time constants for the durations are plotted against the corresponding voltages. The line represents the result of linear regression of the data.

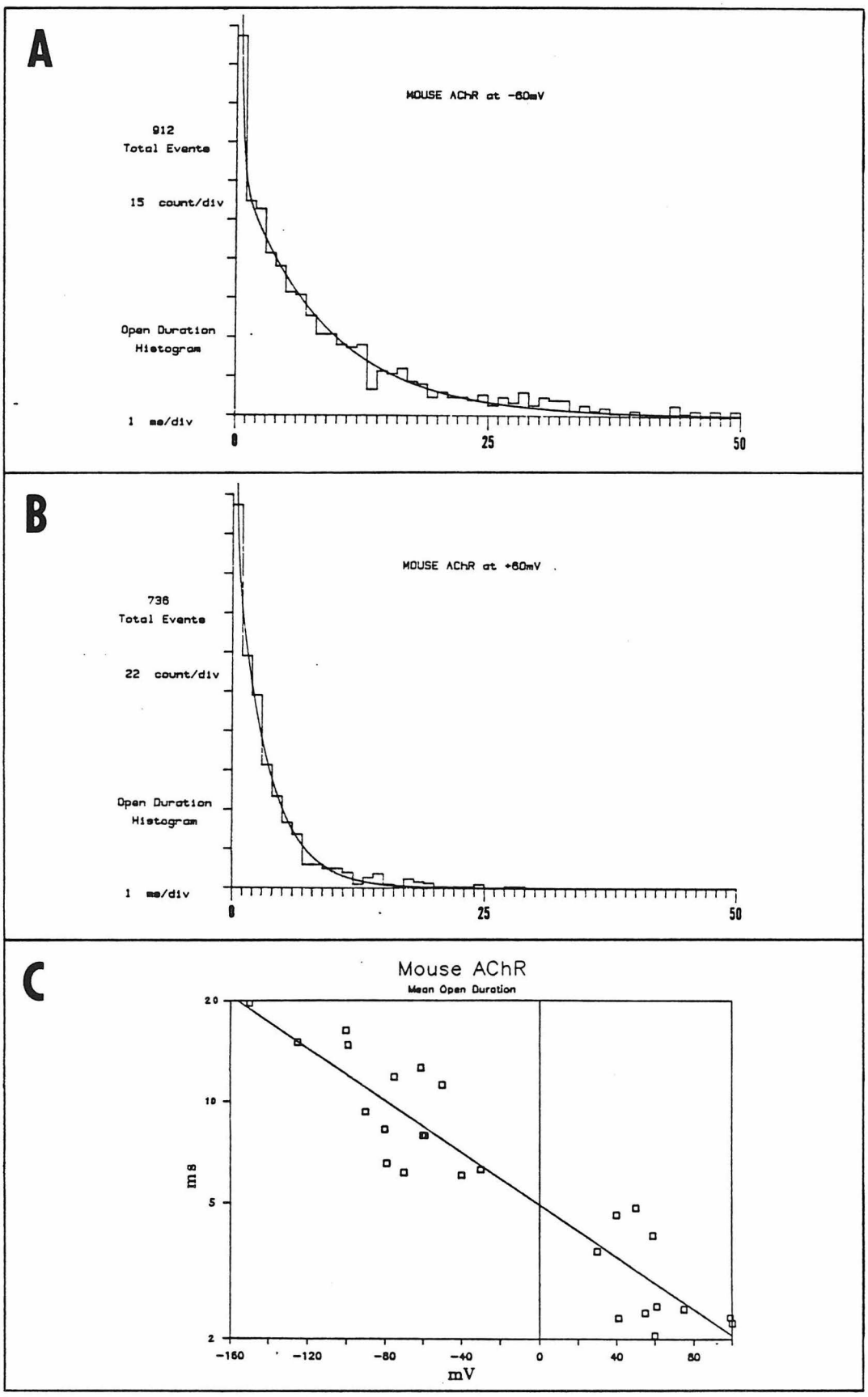
A
MOUSE AChR at -60mV
912
Total Events
15 count/div
Open Duration
Histogram
1 ms/div
0
25
50
B
MOUSE AChR at +60mV
736
Total Events
22 count/div
Open Duration
Histogram
1 ms/div
0
25
50
C
Mouse AChR
Mean Open Duration
20
10
5
2
ms
-160
-120
-80
-40
0
40
80
mV

The line represents the linear regression fit of the data points, and the slope has an absolute value of 3.86×10^{-3}ms/mV. The mean open duration τ increases *e*-fold per 113mV of hyperpolarization, indicating a strong correlation with the membrane potential. It is generally believed that the processes with rate constants β and α in Equation 1 are rate-limiting (Magleby and Stevens, 1972b; Adams, 1981; Auerbach and Sachs, 1984). Under these circumstances, the time constant for channel closing is equal to $1/\alpha$. The result then suggests that α is markedly voltage-dependent.

Voltage effect on the rate of channel openings

The effect of voltage on the channel-opening rate was also examined. Because the exact number of receptor molecules may vary from patch to patch during recording, only the data from the same patch at various holding potentials can be compared with one another. For the following analyses, we selected one patch that yielded the most unitary currents during recording and showed the least desensitization effect. Three different methods were employed to evaluate the voltage influence on the channel opening rate, as described below.

The first method concerns the channel-opening frequency, which is expressed as the number of channel-opening events in a given time at a given voltage. The values of such frequency were calculated and the results were plotted against the membrane potentials, as shown in Figure 7. While the actual values of opening frequency are dependent on the time unit used in calculation, their distribution with respect to the membrane potentials is not, thus allowing the evaluation of voltage influence on the AChR channel-opening rate. The line in Figure 7 represents the linear regression of the data, and the slope has an absolute value of $1.11 \times 10^{-3} ms^{-1} mV^{-1}$. From this, an *e*-fold change in voltage was

Fig. 7. Voltage effect on channel-opening frequency.

The channel-opening frequencies, defined as the number of openings per second, are plotted against the membrane potentials. The line represents the result of linear regression of the data.

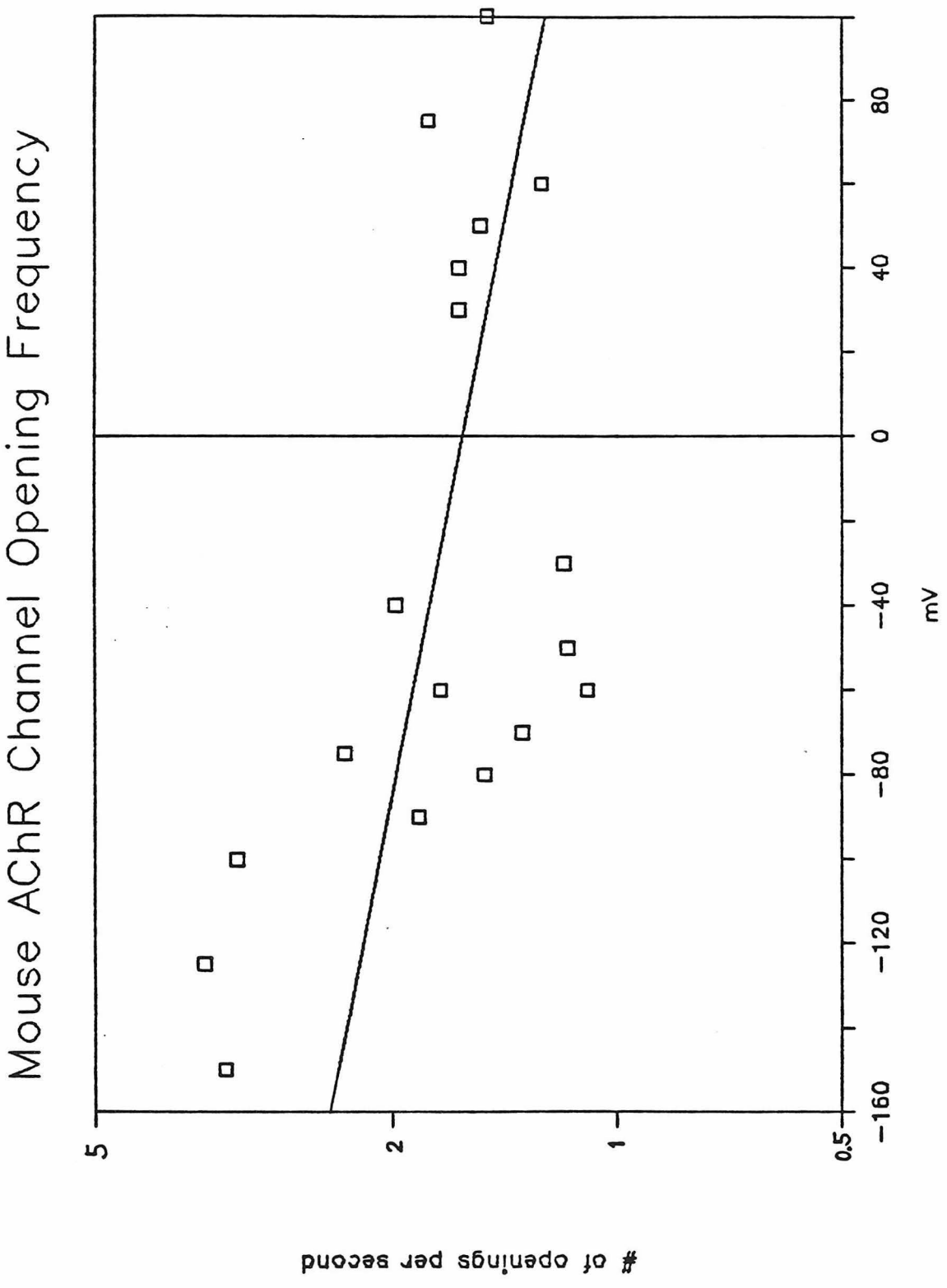
Mouse AChR Channel Opening Frequency
# of openings per second
5
2
1
0.5
−160
−120
−80
−40
0
40
80
mV

calculated to be 395mV. This represents a threefold lower voltage influence as compared with the *e*-fold potential shift of 113mV for the mean open duration.

Another way to evaluate the relationship between the channel-opening rate and the membrane potential is to study the time interval between the onset of successive openings. Figure 8 illustrates the analysis by this method. The interval time between openings was measured at -50mV and +50mV, and the histograms were constructed, as shown in Figures 8A and 8B. Like the channel open duration, the interval time also displays an exponential distribution and can be fitted in similar fashion. The smooth lines in Figures 8A and 8B are the fitted exponentials, their time constants being 607ms and 654ms for the membrane potentials at -50mV and +50mV, respectively. As in the channel-opening frequency analysis, the τ values here are meaningful only when they are compared with those from the same patch, because the actual value is influenced by factors such as the number of receptors in the patch, the agonist concentration, and the temperature in the experiment, in addition to the voltage effect we wanted to study. When the τ values are plotted against the membrane potentials, however, their relationship can be examined. Figure 8C shows the time interval vs. the membrane potential plot and the linear regression fit, which gives a slope of 0.83×10^{-3}ms/mV and an *e*-fold potential shift of 523mV. This outcome is in general agreement with the conclusion obtained by the channel-opening frequency method that the channel-opening rate is affected by the membrane potential, but to a lesser degree than that on the channel-closing rate. On the other hand, this method of analysis does give a smaller linear regression slope value and a larger membrane potential change to reach an *e*-fold shift than those derived from the opening-frequency analysis, implying a smaller degree of voltage dependence of the channel opening rate.

Fig. 8. Voltage effect on channel closed interval.

A. Closed interval histogram for the mouse AChR ion channels at -50mV. The interval is the time between the beginning of an opening and the beginning of the next one. The smooth curve represents the fitted exponential function. The time constant is 607ms.

B. Closed interval histogram for the mouse AChR ion channels at +50mv. The time constant is 654ms.

C. Closed interval vs. voltage plot. Symbols represent the time constants from the histogram curve fitting. The line represents the result of linear regression of the data.

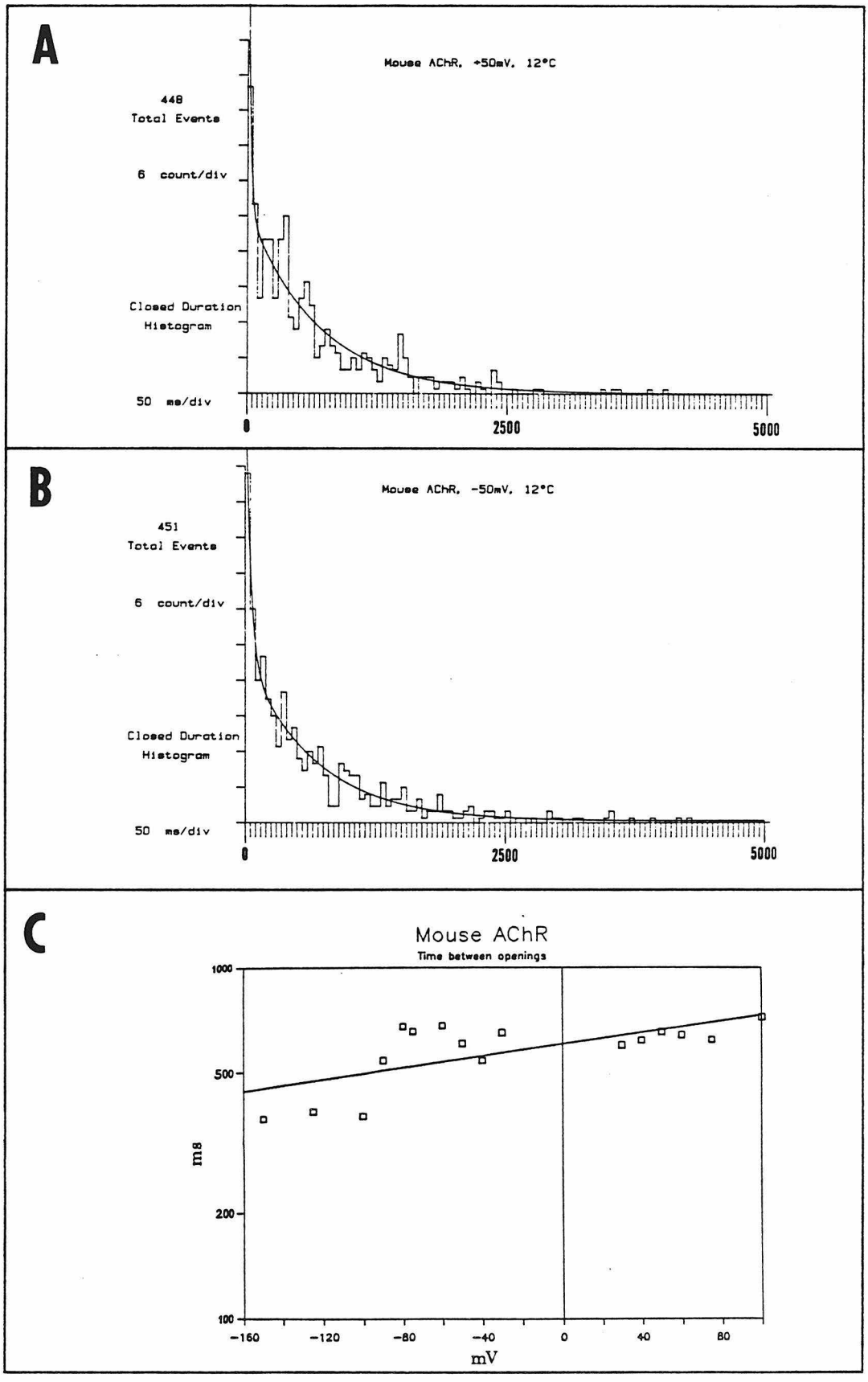
A
Mouse AChR, +50mV, 12°C
448
Total Events
6 count/div
Closed Duration
Histogram
50 ms/div
0
2500
5000
B
Mouse AChR, -50mV, 12°C
451
Total Events
6 count/div
Closed Duration
Histogram
50 ms/div
0
2500
5000
C
Mouse AChR
Time between openings
1000
500
200
100
ms
-160
-120
-80
-40
0
40
80
mV

The third method of analysis calculates the total time the receptors spend in the open state and derives the ratio of this "sum" open time vs. the whole record duration at a given potential. Because the total time in the open state is controlled by both the channel-opening rate and the channel-closing rate, the results have to be compared with those from the mean open-duration analysis in order to estimate the relative contributions from each component. Figure 9 shows the results of this analysis. The ratios of summed open time to the total record duration are plotted against the membrane potentials in semilogarithmic coordinates. The linear regression fitting is represented by the straight line in the plot, and the slope has an absolute value of $4.59 \times 10^{-3} mV^{-1}$ with an *e*-fold potential shift of 95mV. This strong dependence on the membrane potential is the combined effect of the voltage on the channel-opening and channel-closing rates. When the contribution of the channel-closing rate is subtracted, using the data from the analysis on the mean channel duration, a slope value of 0.73×10^{-3} and an *e*-fold change in membrane potential of 595mV are obtained. This again agrees with the results from the other two methods: The AChR channel-opening rate is influenced by the membrane potential, and its contribution to the whole-cell voltage sensitivity is smaller than that from the channel-closing rate.

Of the three methods we used, the third one --- calculating the effect of voltage on the opening rate by subtracting the voltage dependence of the closing rate from the combined effects on both the opening and closing rates --- seems to be more reliable for the following reasons. The method of channel-opening frequency analysis theoretically reflects the channel-opening rate, if all the openings are captured during patch-clamp recording. From the study on the channel-closing rates it is apparent that this latter parameter is heavily dependent on the membrane potential; specifically, the average channel duration becomes shorter as the voltage becomes more positive. Because the patch-clamp technique

Fig. 9. Voltage effect on percentage of channel open time.

Percentage of open time is defined as the total time channels are in the open state divided by the time of the entire record. The percentage values are plotted against the corresponding membrane potentials. The line represents the result of linear regression of the data.

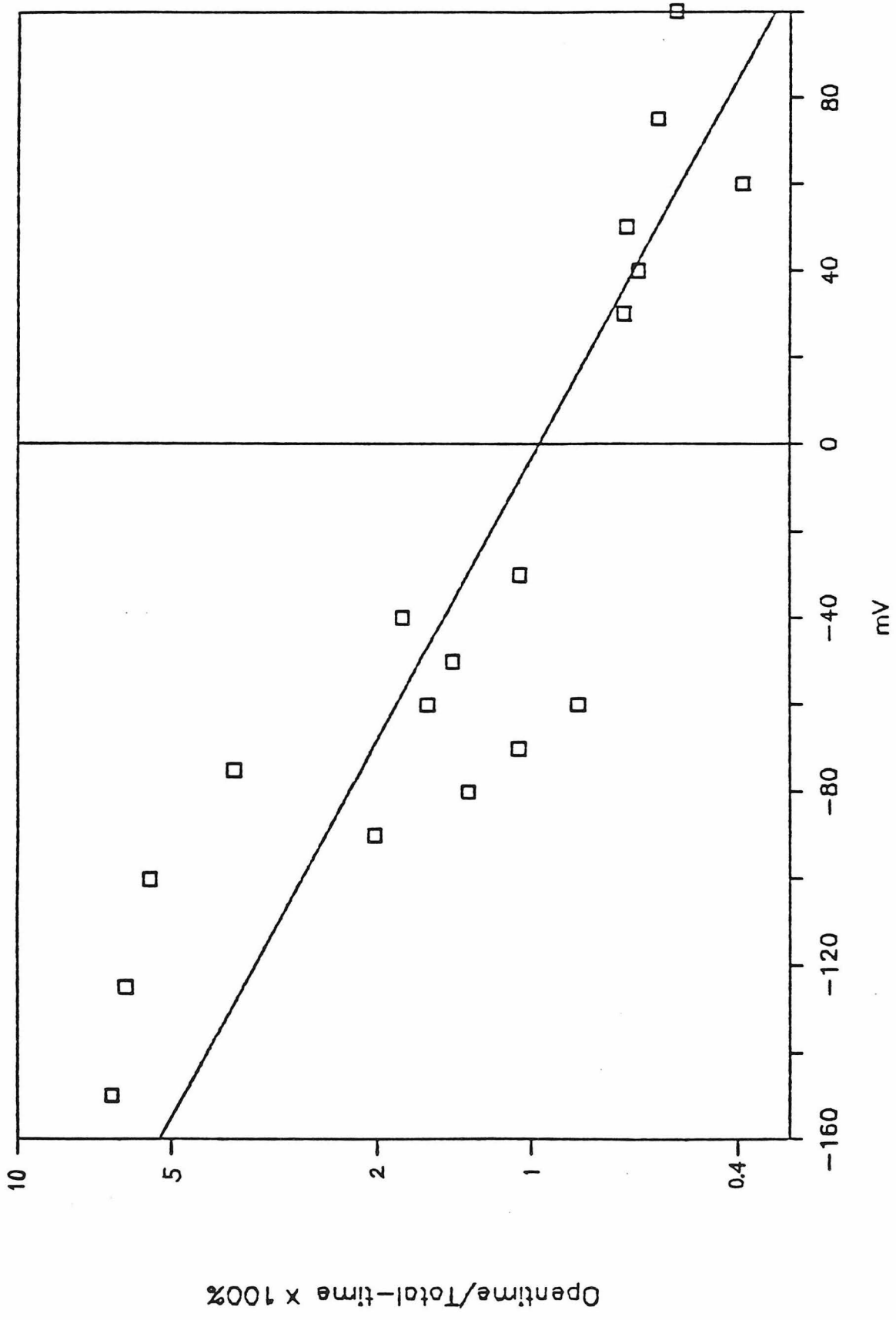
Opentime/Total-time x 100%
10
5
2
1
0.4
-160
-120
-80
-40
0
40
80
mV

has a finite time resolution, the number of openings of very brief duration that go undetected will increase with more positive holding potentials. Since the analysis relies on the number of recorded events within a time period, the outcome is bound to give a higher degree of voltage dependence of the channel-opening rate than actually exists. The second method analyzes the distribution of the time intervals between the neighboring events. While this method suffers from the same *type* of limitation as the first one, the *extent* of bias is presumably smaller, because the nature of the exponential distribution curve fitting is weighted more toward the majority of data points and therefore the outcome is affected less by the relative small percentage of the long intervals resulting from the missed brief events. Our results support this interpretation, as the second method suggested a smaller effect of voltage on the opening rate. The third method of analysis tabulates the total time the receptors spend in the open state and does not rely on the number of events recorded. While the missed brief openings still make the measurements underestimated, the effect is much less severe. This is because the missed events amount to an insignificant portion of the total open time, because of the very nature of their brevity which causes them to go undetected. This explanation is substantiated by our results that the third method gives the smallest value of voltage dependence of the open rate, suggesting that the voltage effect is the least overestimated by this method.

Conclusions

Our analysis of the single-channel data obtained by the technique of excised outside-out patch-clamp recording indicates that the voltage sensitivity observed at whole-cell level is not due to the voltage dependence of the single channel conductance: The current-voltage relationship is linear in the membrane potential range we examined. On the other hand, both the rate of channel opening

and the rate of channel closing are affected by the membrane potential. As the voltage becomes more positive, the opening rate β decreases and the closing rate α increases. These two parameters work in coordination to form the basis for the voltage sensitivity of the whole-cell response to agonist. Their contributions, however, are quite different. The three methods we used in estimating the relative contributions gave the contribution of 78%, 82%, and 84% for the channel-closing rate α. We believed that even the highest value is an underestimation. While more accurate measurements will make the issue more clear, it is reasonable to conclude that the ratio of relative contributions of the channel-closing rate vs. the channel-opening rate is higher than 3:1 for the AChR from mouse.

Subunit Role in Channel Properties

The rationale

Acetylcholine receptor (AChR) in vertebrate is a multisubunit protein, composed of α, β, γ, and δ subunits. These subunits share homology at both sequence and structural levels (Stroud and Finer-Moore, 1985). Why multisubunits? One explanation is that, for a multifunctional membrane receptor/ion channel such as AChR, different subunits may be responsible for different protein properties, therefore reducing the selective pressure on keeping the existing functions while developing new ones during evolution. This view is well exemplified by the fact that the α subunits carry the agonist and antagonist binding sites (Heidmann and Changeux, 1978; McCarthy *et al.*, 1986). The availability of the AChR cDNA clones from several species made it possible to construct hybrid receptors by substituting a subunit with its counterpart from another species and to build chimera receptors by shuffling certain fragments

between subunits. These experiments led to the discovery that the AChR from *Torpedo* has a quite different response profile from its counterparts in mammals and other vertebrates (White *et al.*, 1985; Sakmann *et al.*, 1985; Mayne *et al.*, 1987, and this thesis). Further studies by Sakmann, Numa, and colleagues on single-channel behavior revealed the importance of the δ subunit in determining the mean channel open duration (Sakmann *et al.*, 1985) and the single-channel conductance (Imoto *et al.*, 1986). Our earlier work on the whole-cell response to acetylcholine suggested that the β subunit plays an essential role in determining the receptor voltage sensitivity, while the δ subunit interacts with the β subunit in an additive and modulatory fashion (Yoshii *et al.*, 1987, and this volume). We wanted to study the receptor behavior at the single-channel level. Comparison of the single-channel data with that from the whole-cell recording may provide further clues to the subunit involvement in receptor functions.

Mean channel opening time

The AChRs from *Torpedo* and from mouse exhibit very different profiles of channel opening. As shown in Figures 10A and 10B, the *Torpedo* channels have predominantly brief openings, while the mouse receptors often open for a long time. The channel duration histograms for the *Torpedo* and mouse AChRs are shown in Figures 10C and 10D. The exponential curve fitting of the channel opening histograms gave the time constant τ values of 0.34ms for the *Torpedo* receptor and 8.65ms for the mouse receptor.

Two hybrid receptors, $\alpha_M\beta_M\gamma_T\delta_M$ and $\alpha_T\beta_T\gamma_T\delta_M$, were studied for their channel-gating behavior. Figures 11A and 11B show typical current traces of the two hybrid channels. It is apparent that both hybrid channels resemble their mouse parental receptor in that they both open for a long time. Statistical

Fig. 10. Open-channel duration of the *Torpedo* and mouse AChRs.

A. Examples of the AChR-induced single-channel currents at -60mV from the mouse AChR.

B. Examples of the AChR-induced single-channel currents at -60mV from the *Torpedo* AChR.

C. Open duration histogram for the *Torpedo* channels at -60mV. The fitted exponential has a time constant of 0.34ms.

D. Open duration histogram for the mouse channels at -60mV. The fitted exponential has a time constant of 8.65ms.

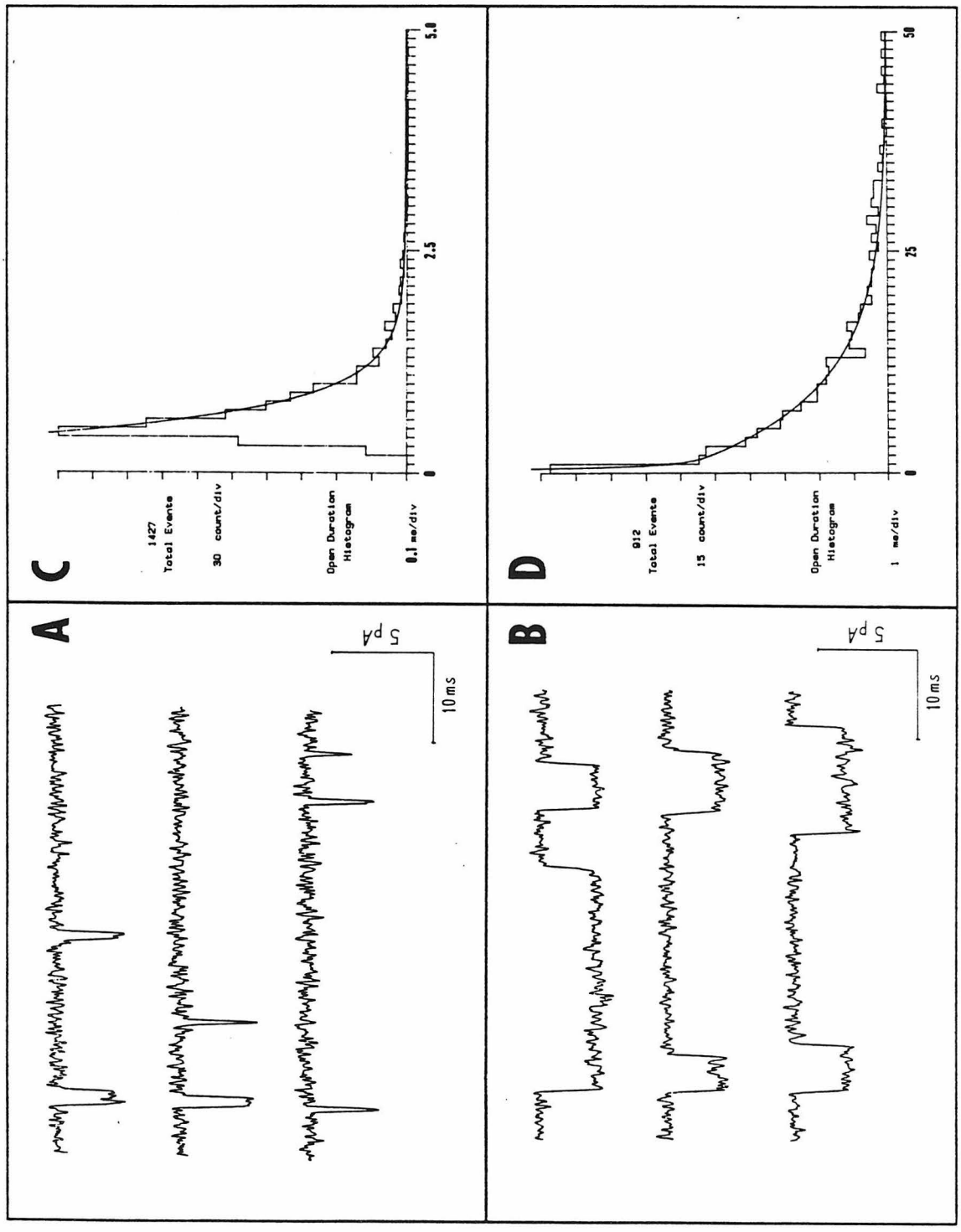
A
5 pA
10 ms
B
5 pA
10 ms
C
1427
Total Events
30 count/div
Open Duration
Histogram
0.1 ms/div
0
2.5
5.0
D
912
Total Events
15 count/div
Open Duration
Histogram
1 ms/div
0
25
50

Fig. 11. Open-channel duration of hybrid AChRs $\alpha_T\beta_T\gamma_T\delta_M$ and $\alpha_M\beta_M\gamma_T\delta_M$.

A. Examples of the AChR-induced single-channel currents at -60mV from the $\alpha_T\beta_T\gamma_T\delta_M$.

B. Examples of the AChR-induced single-channel currents at -60mV from the $\alpha_M\beta_M\gamma_T\delta_M$.

C. Open duration histogram for the hybrid $\alpha_T\beta_T\gamma_T\delta_M$ channels at -60mV. The fitted exponential has a time constant of 5.11ms.

D. Open duration histogram for the hybrid $\alpha_M\beta_M\gamma_T\delta_M$ channels at -60mV. The fitted exponential has a time constant of 4.29ms.

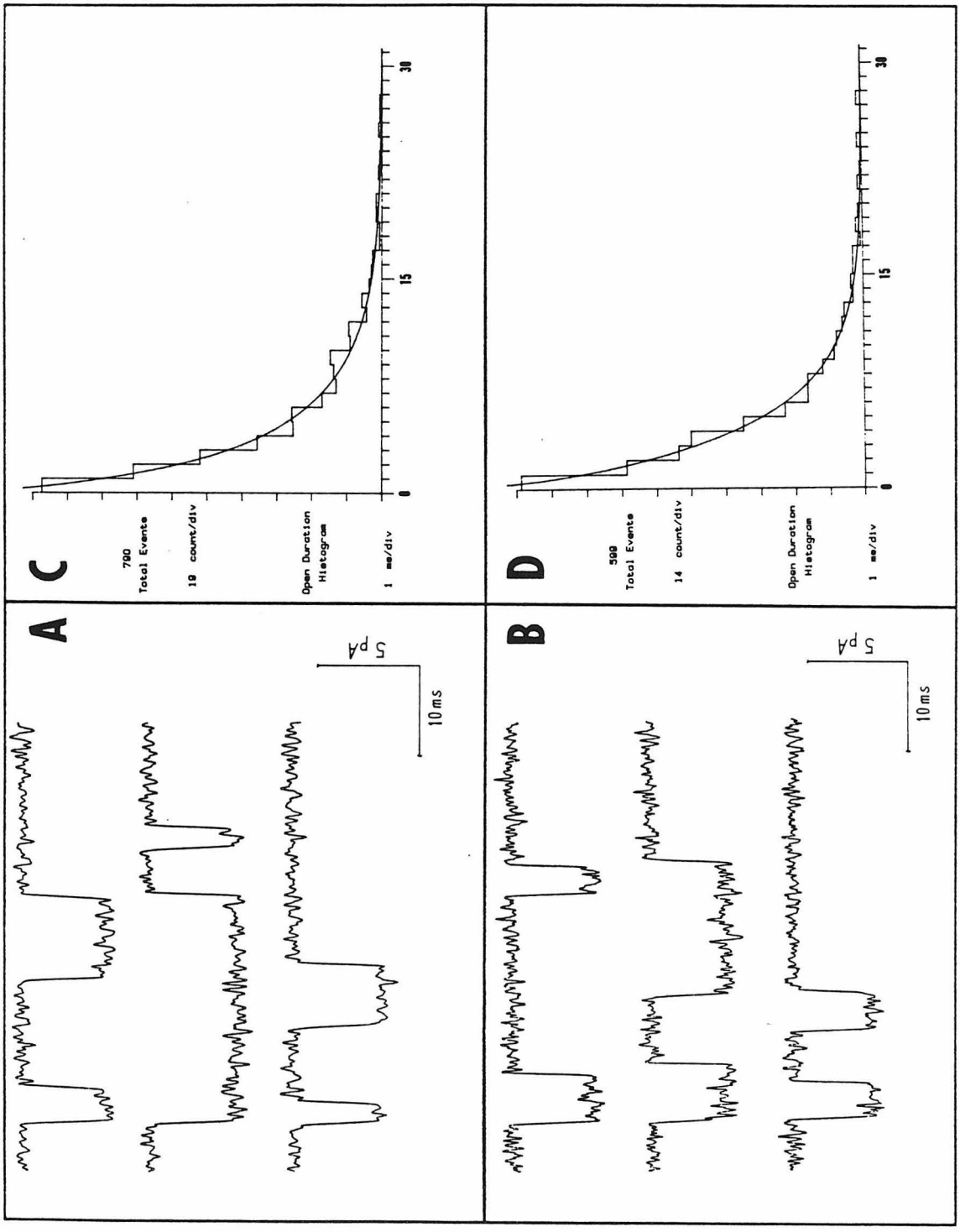
A
5 pA
10 ms
B
5 pA
10 ms
C
780
Total Events
10 count/div
Open Duration
Histogram
1 ms/div
0
15
30
D
590
Total Events
14 count/div
Open Duration
Histogram
1 ms/div
0
15
30

analysis confirmed this observation. Figures 11C and 11D show the corresponding histograms with fitted exponential curves. The time constant τ values are 4.29ms for the hybrid receptor $\alpha_M\beta_M\gamma_T\delta_M$ and 5.11ms for the hybrid receptor $\alpha_T\beta_T\gamma_T\delta_M$.

These results indicate that the open-channel durations of both hybrid receptors are similar to that of their mouse "parent." An inspection of the receptor compositions readily points out the existence of the δ_M subunit in all three long opening receptors. This is in agreement with the report by Sakmann *et al.* (1985), using the *Torpedo* and calf AChRs, that the mean open duration is short for the *Torpedo* receptors and long for the calf receptors and that the calf δ subunit confers the long channel open time.

Voltage sensitivity

Our previous work on the whole-cell response to agonist from mouse-*Torpedo* hybrid AChRs suggested the primary and secondary roles that β and δ subunits play in determining the degree of voltage sensitivity (Yoshii *et al.*, 1987, and this thesis). To confirm the results from whole-cell recording, a study was done with the homogeneous receptors $\alpha_M\beta_M\gamma_M\delta_M$ and $\alpha_T\beta_T\gamma_T\delta_T$ and with the hybrid receptors $\alpha_M\beta_M\gamma_T\delta_M$ and $\alpha_T\beta_T\gamma_T\delta_M$. Since the voltage sensitivity in the receptor is mainly determined by the open-channel duration (Figure 6C), the distributions of the open-channel duration from these receptors were analyzed. Openings with equal driving potentials but opposite directions (-60mV and +60mV) were measured, open duration histograms were constructed, and the time constant τ values were obtained from fitted exponential curves. The results are shown in Table 1. The ratio of the τ values at these potentials serves as an index to the extent of voltage dependence.

TABLE 1

Subunit role in voltage sensitivity exhibited by the ratio of mean channel open times

AChR composition	τ_{-60mV}	τ_{+60mV}	Voltage* dependence
$\alpha_T\beta_T\gamma_T\delta_T$	0.36+0.04ms	0.23+0.04ms	1.56
$\alpha_T\beta_T\gamma_T\delta_M$	5.35+0.16ms	2.19+0.29ms	2.44
$\alpha_M\beta_M\gamma_M\delta_M$	8.08+0.20ms	2.96+0.13ms	2.73
$\alpha_M\beta_M\gamma_T\delta_M$	3.72+0.09ms	1.19+0.16ms	3.13

* Voltage dependence is defined here as the ratio of the mean channel open times at -60mV and +60mV.

The homogeneous *Torpedo* receptor displays a weak, nonetheless detectable, voltage dependence. The receptors containing the β subunit from mouse ($\alpha_M\beta_M\gamma_M\delta_M$ and $\alpha_M\beta_M\gamma_T\delta_M$) show strong voltage dependence, and the hybrid receptor with *Torpedo* β subunit and mouse δ subunit ($\alpha_T\beta_T\gamma_T\delta_M$) displays intermediate dependence on voltage. These results are in good agreement with our results from the study on the whole-cell response to agonist and its sensitivity to membrane potential (Yoshii *et al.*, 1987, and this thesis), thus supporting our conclusions from that study that the β subunit plays an important role in determining the voltage sensitivity ($\alpha\beta_M\gamma\delta > \alpha\beta_T\gamma\delta$) and that the interaction between the β and the δ subunit has a modulatory effect ($\alpha\beta_M\gamma\delta_T > \alpha\beta_M\gamma\delta_M > \alpha\beta_T\gamma\delta_M > \alpha\beta_T\gamma\delta_T$). More hybrids should be tested to futher substantiate these conclusions.

ACKNOWLEDGMENTS

We thank F. Shon for his assistance in computer programming and M. Fearey for her management of equipment and supplies. We also thank Drs. D. Krafte and C. Labarca for their advice and encouragement. L.Y. is grateful to the associates of the J. Alfred Prufrock Society for their moral support.

This work was supported by research grants from the Muscular Dystrophy Association and the National Institutes of Health to N.D. and H.A.L., a California Foundation for Biochemical Research Fellowship to L.Y., and a Muscular Dystrophy Association Postdoctoral Fellowship to R.J.L.

REFERENCES

Auerbach, A., and C. J. Lingle. (1986) Heterogeneous kinetic properties of acetylcholine receptor channels in *Xenopus* myocytes. *J. Physiol. (London)* 378: 119-140.

Auerbach, A., and F. Sachs. (1984) Patch clamp studies of single ionic channels. *Ann. Rev. Biophys. Bioeng.* 13: 269-302.

Barnard, E., R. Miledi, and K. Sumikawa. (1982) Translation of exogenous messenger RNA coding for nicotinic acetylcholine receptors produces functional receptors in *Xenopus* oocytes. *Proc. R. Soc. Lond.* B215: 241-246.

Colquhoun, D., and F. J. Sigworth. (1983) Fitting and statistical analysis of single-channel records. In *Single-Channel Recording.* B. Sakmann and E. Neher eds., Plenum Press, New York.

Dascal, N., T. P. Snutch, H. Lubert, N. Davidson, and H. A. Lester. (1986) Expression and modulation of voltage-operated calcium channels after RNA injection in *Xenopus* oocytes. *Science* 231: 1147-1150.

Davidson, N. (1962) *Statistical Mechanics.* McGraw-Hill, New York.

Hamill, O. P., A. Marty, E. Neher, B. Sakmann, and F. J. Sigworth. (1981) Improved patch-clamp techniques for high-resolution current recording from cells and cell-free patches. *Pflugers Arch.* 391: 85-100.

Heidmann, T., and J.-P. Changeux. (1978) Structural and functional properties of the acetylcholine receptor protein in its purified and membrane-bound states. *Ann. Rev. Biochem.* 47: 317-357.

Hille, B. (1984) *Ionic Channels of excitable Membranes.* Sinauer Associates Inc. Publishers, Sunderland, Massachusetts.

Imoto, K., C. Methfessel, B. Sakmann, M. Mishina, Y. Mori, T. Konno, K. Fukuda, M. Kurasaki, H. Bujo, Y. Fujita, and S. Numa. (1986) Location of a δ-subunit

region determining ion transport through the acetylcholine receptor channel. *Nature* 324: 670-674.

Katz, B., and R. Miledi. (1972) The statistical nature of the acetylcholine potential and its molecular components. *J. Physiol. (London)* 224: 665-699.

Kegel, D. R., B. D. Wolf, R. E. Sheridan, and H. A. Lester. (1985) Software for electrophysiological experiments with a personal computer. *J. Neurosci. Meth.* 12: 317-330.

Kordas, M. (1969) The effect of membrane polarization on the time course of the end-plate current in frog sartorius muscle. *J. Physiol. (London)* 204: 493-502.

Lester, H. A. (1970) Transmitter release by presynaptic impulses in the squid stellate ganglion. *Nature* 227: 493-496.

Magleby, K. L., and C. F. Stevens. (1972a) The effect of voltage on the time course of end-plate currents. *J. Physiol. (London)* 223: 151-171.

Magleby, K. L., and C. F. Stevens. (1972b) A quantitative description of endplate currents. *J. Physiol. (London)* 223: 173-197.

Marquardt, D. W. (1963) An algorithm for least-squares estimation of nonlinear parameters. *J. Soc. Indus. Appl. Math.* 11: 431

Mayne, K. M., K. Yoshii, L. Yu, H. A. Lester, and N. Davidson. (1987) Expression of mouse-*Torpedo* acetylocholine receptor subunit chimeras and hybrids in *Xenopus* oocytes. *Molecular Brain Research*, in press.

McCarthy, M. P., J. P. Earnest, E. F. Young, S. Choe, and R. M. Stroud. (1986) The molecular neurobiology of the acetylcholine receptor. *Ann. Rev. Neurosci.* 9: 383-413.

Methfessel, C., V. Witzemann, T. Takahashi, M. Mishina, S. Numa, and B. Sakmann. (1986) Patch clamp measurements on *Xenopus laevis* oocytes: currents through endogenous channels and implanted acetylcholine receptor and sodium channels. *Pflugers Arch.* 407: 577-588.

Miledi, R., I. Parker, and K. Sumikawa. (1982) Synthesis of chick GABA receptors by frog oocytes. *Proc. R. Soc. Lond.* 216: 509-515.

Miledi, R., and K. Sumikawa. (1982) Synthesis of cat muscle acetylcholine receptors by *Xenopus* oocytes. *Biomed. Res.* 3: 390-399.

Mishina, M., T. Takai, K. Imoto, M. Noda, T. Takahashi, S. Numa, C. Methfessel, and B. Sakmann. (1986) Molecular distinction between fetal and adult forms of muscle acetylcholine receptor. *Nature* 321: 406-411.

Neher, E., and B. Sakmann. (1976) Single-channel currents recorded from membrane of denervated frog muscle fibres. *Nature* 260: 799-802.

Sakmann, B., C. Methfessel, M. Mishina, T. Takahashi, T. Takai, M. Kurasaki, K. Fukuda, and S. Numa. (1985) Role of acetylcholine receptor subunits in gating of the channel. *Nature* 318: 538-543.

Sakmann, B., and E. Neher., eds. (1983) *Single-Channel Recording*. Plenum Press, New York.

Schreiner, W., M. Kramer, S. Krischer, and Y. Langsam. (1985) Nonlinear least-squares fitting. *PC Tech. J.* 3: 170-181.

Stroud, R. M., and J. Finer-Moore. (1985) Acetylcholine receptor structure, function, and evolution. *Ann. Rev. Cell Biol.* 1: 317-351.

Takeuchi, A., and N. Takeuchi. (1959) Active phase of frog's end-plate potential. *J. Neurophysiol.* 22: 395-411.

White, M. M., K. M. Mayne, H. A. Lester, and N. Davidson. (1985) Mouse-*Torpedo* hybrid acetylcholine receptors: Functional homology does not equal sequence homology. *Proc. Natl. Acad. Sci. USA* 82: 4852-4856.

Yoshii, K., L. Yu, K. M. Mayne, N. Davidson, and H. A. Lester. (1987) Equilibrium properties of mouse-*Torpedo* acetylcholine receptor hybrids expressed in *Xenopus* oocytes. *J. Gen. Physiol.*, in press.